Investigations into the use of nano-based antimicrobial and osteoconductive coatings for bone implants.

Memarzadeh, Kaveh

Investigations into the use of nano-based antimicrobial and osteoconductive coatings for bone implants

Kaveh Memarzadeh

Thesis submitted to Queen Mary University of London
for the degree of Doctor of Philosophy

2014

Supervisors:
Prof. Robert P. Allaker
Dr. Jie Huang

I, Kaveh Memarzadeh, confirm that the research included within this thesis is my own work or that where it has been carried out in collaboration with, or supported by others, that this is duly acknowledged below and my contribution indicated. Previously published material is also acknowledged below.

I attest that I have exercised reasonable care to ensure that the work is original, and does not to the best of my knowledge break any UK law, infringe any third party's copyright or other Intellectual Property Right, or contain any confidential material.

I accept that the College has the right to use plagiarism detection software to check the electronic version of the thesis.

I confirm that this thesis has not been previously submitted for the award of a degree by this or any other university.

Signature: ***Kaveh Memarzadeh***
Date: 19/06/2014

Details of collaboration and publications:

Conferences

1) Turkey - Bioceramics 23 (2011)
   Form: Oral Presentation
   Title: *Antimicrobial effects of metallic nanoparticles for medical implant coatings*
2) Italy - 4th CESB Symposium on Biomaterials in Regenerative Medicine (2012)
   Form: Oral presentation
   Title: *Osteoconductive and antimicrobial nano-zinc oxide coatings for the next generation of prostheses*

Publications

Title	Antimicrobial activity of nanoparticulate metal oxides against peri-implantitis pathogens
Authors	M Vargas-Reus, **K Memarzadeh**, J Huang, G Ren, RP Allaker
Journal	International Journal of Antimicrobial Agents, 40(2):135-9
Year of publication	**2012**

Title	Nano metallic-oxides as antimicrobials for implant coatings
Authors	**K Memarzadeh**, M Vargas, J Huang, J Fan, RP Allaker
Journal	Key Engineering Materials, 493-494, 489
Year of publication	**2012**

Title	Nanoparticles and the control of oral infections
Authors	RP Allaker, **K Memarzadeh**
Journal	International Journal of Antimicrobial Agents, 43(2): 95-104
Year of publication	**2014**

Title	Nanoparticulate zinc oxide as a coating material for orthopaedic and dental implants
Authors	**K Memarzadeh**, AS Sharili, J Huang, S Rawlinson, RP. Allaker
Journal	Journal of Biomedical Materials Research: Part A, 103A:981–989
Year of publication	**2014**

Abstract

Objectives: Orthopaedic and dental implants are prone to frequent infections. This can lead to detrimental and often irreversible outcomes for many patients. The objective of this study was to develop a novel system using zinc oxide nanoparticles (nZnO) as a coating material that inhibits both bacterial adhesion / growth and promotes osteoblast growth.

Methods and Results: Initially bacteria (*S. aureus*, *E. coli*, *S. epidermidis* and *P. aeruginosa*) were exposed to different concentrations of zinc oxide nanoparticulate suspensions (250 µg/mL, 500 µg/mL, 1000 µg/mL and 2500 µg/mL); with the higher concentrations of the suspensions demonstrating significant bactericidal effects. A novel electrohydrodynamic atomization coating technique (EHDA) was used to deposit mixtures of nZnO and nano-hydroxyapatite (nHA) onto the surface of glass samples (1 cm^2). Exposure of the coated samples to phosphate buffered saline (PBS) and adult bovine serum (ABS) and measurement of bactericidal activity demonstrated superior antimicrobial activity for 100% and 75% nZnO composite coated samples. Lactate dehydrogenase (LDH) release from osteoblast-like cells (UMR-106 and MG-63) exposed to both nano-TiO_2 and nano-ZnO nanoparticulate suspension supernatants indicated minimal toxicity. Nano-ZnO coated samples did not elicit LDH release with an increase in proliferation and viability of cells was observed. Scanning electron microscopy (SEM) and optical microscopy indicated that all cell types used (mesenchymal stem cells and osteoblast-like cells) were able to maintain their normal morphological state when adhered to the surface of the nano-coated material. Further studies as regards to patterned coated samples showed an exclusive adhesion selection by osteoblast-like cells to nZnO patterned regions that needs to be further investigated.

Conclusion: ZnO NPs provide an antimicrobial and biocompatible coating material for medical and dental bone implants

Pictorial summary of the thesis

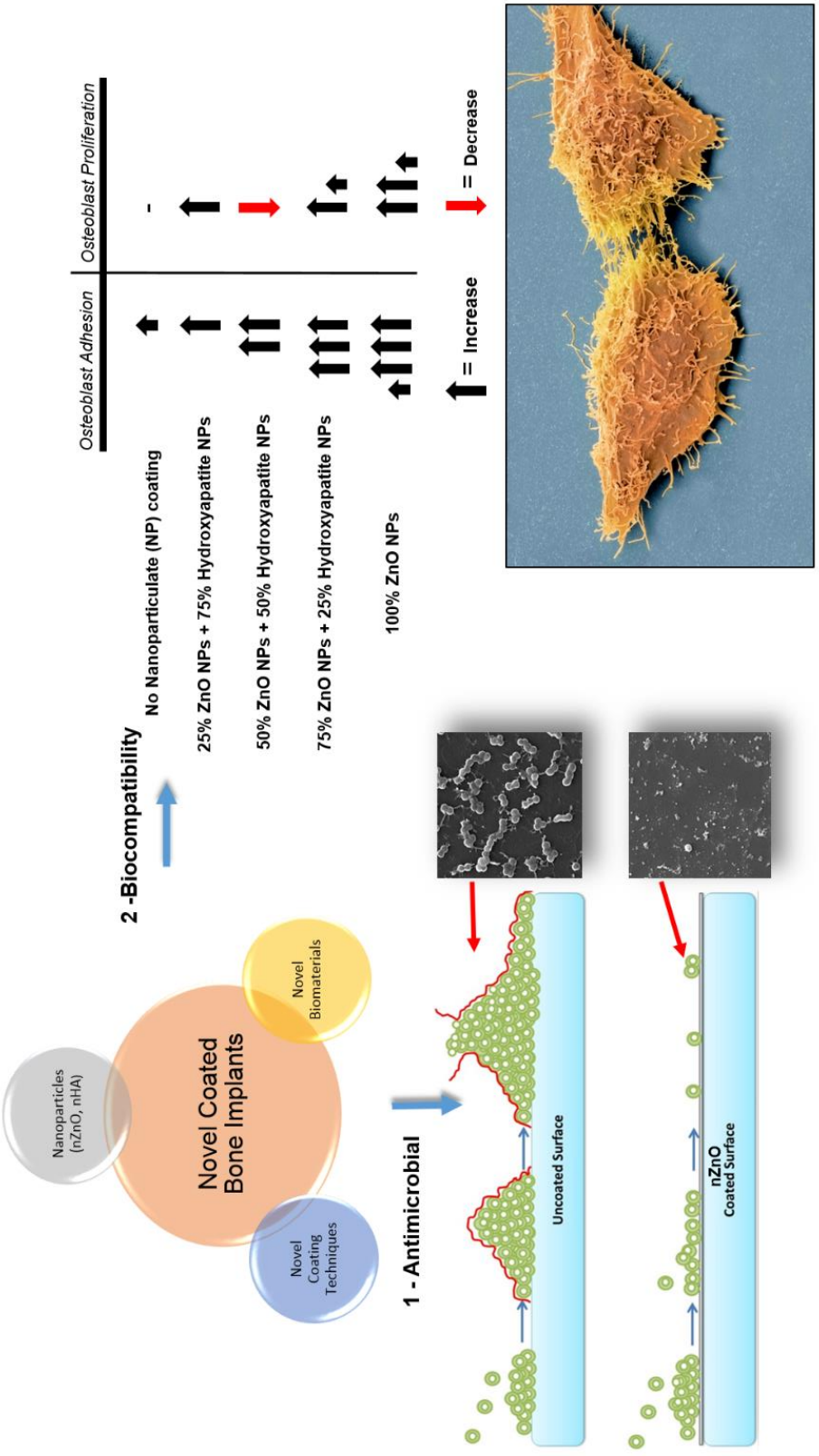

This illustration summarises the main findings of the present thesis – These findings are related to enhanced antimicrobial activity of the coatings and the nanoparticulates and also their biocompatibility and osteoconductive nature. The pictorail representaion is intended to showcase and breifly highlight the main findings to provide an overview of the work for the reader. The pseudo-coloured cells depict two healthy communicating cells on a nano-coated surface.

Thesis summary

Chapter 1 – Literature review

A literature review based upon the current and past research carried out on the subject of nanoparticles and their role in providing antimicrobial effects. This section covers topics on antibiotic resistance, biofilm formation together with the challenges that are often faced when dealing with these issues. Furthermore an overview of the application of different coating methodologies is provided and discussed.

Chapter 2 – Investigations into the antimicrobial activity of nano-metal oxides

The initial section of this chapter is based upon the introduction and optimisation of the utilised coating technique. The coating process is carried out by the novel technology of EHDA. In order to achieve the desired outcome, that is defined by a uniform nano-based coated surface, different parameters such as height of the nozzle from the substrate, voltage and the flow rate of the nanoparticulate suspension were investigated. The outcomes were then assessed using imaging systems. Furthermore, this section also deals with the antimicrobial activity of the nanoparticulates tested. The bactericidal effect of these nano-coated structures is qualitatively and quantitatively measured and a suitable particulate was chosen based upon careful deductive investigations, supported by experimental evidence.

Chapter 3 – Nano-ZnO as an implant coating material

This section provides background information on how bone forming cells (osteoblasts) respond to the selected nanoparticulate under altering conditions. The objective in this chapter is to demonstrate the non-toxic, biocompatible and osteoconductive nature of these coatings.

Chapter 4 – Future innovations

This section provides preliminary evidence for various novel applications of nZnO. It also explores the potential of testing coated surfaces in a novel setup where shear stress based on fluid movements will test for durability of NPs on treated surfaces. Additional initial investigations such as hydrogen peroxide and ion release capability, together with the role of patterned coated surfaces on cell behaviour are investigated. This chapter serves as a guide for a further coherent study research.

Chapter 5 - Discussion

General discussion on the outcome of the present research and how collectively all its components provide valuable insights for the development of an antimicrobial bone device that is potentially superior to products that are currently available in the fields of dentistry and medicine.

Table of contents

Chapter 1

Chapter 2

Investigations into the antimicrobial activity of nano-metal oxides

Chapter 3

nZnO as a biocompatible implant coating material

.

Chapter 4

Chapter 5

List of figures

Chapter 1 - Introduction

Chapter 2 - Investigations into the antimicrobial activity of nano-metal oxides

List of Tables

Abbreviations

ABS	Adult bovine serum
Ag	Silver
Al_2O_3	Aluminium Oxide
ALP	Alkaline phosphatase
CFU	Colony Forming Units
CO-Cr	Cobalt- Chromium
CuO	Copper Oxide (Cupric oxide)
dH_2O	De-ionised water
ECM	Extracellular matrix
EHDA	Electrohydrodynamic atomisation
ELISA	Enzyme-Linked Immunosorbent Assay
FCS	Fetal calf serum
HA	Hydroxyapatite
hMSC	Human Mesenchymal Stem Cells
IL-1	Interleukin -1
LDH	Lactate dehydrogenase
MBC	Minimum bactericidal concentration
MIC	Minimum inhibitory concentration
NCTC	National collection of type cultures
NHS	National health service
NP	Nanoparticles
O.D.	Optical density
PBS	Phosphate buffered saline
ROS	Reactive oxygen species
RPM	Rounds per minute
SEM	Scanning electron microscopy
TEM	Transmission electron microscopy
TiO_2	Titanium dioxide
TNF-α	Tumour necrosis factor- aplha
WHO	World health organisation
WO_3	Tungsten oxide
ZnO	Zinc oxide

Acknowledgements

It is only appropriate to initially thank my supervisors Prof. Rob Allaker and Dr. Jie Huang for supporting me throughout this rather challenging period. Your patience and guidance is profoundly appreciated.

To my parents: Thank you for providing me with the opportunity to better myself. Thank you for allowing me to freely express my thoughts and realise my potentials. Without your unconditional love I would not have been able to achieve the things that I have so far achieved... however small. Thank you for giving up on your dreams in order for your children to have a better future, a debt I could never repay. I dedicate everything I do to you.

To Sepideh: My one and only. I could not have achieved any of this without you. You are a constant source of inspiration and hope. You have taught me how not to give up. Your courage is like a candle, lighting the path that's yet unknown and undetermined. I know that together we can travel down any dark path and eventually make it. I love you dearly.

Many thanks to Orthopaedic Research UK for funding this project. Special thanks to Dr. Arash Angadji and Mr Brian Jones, your support has been invaluable.

Special thanks to Johnson Matthey plc for providing the nanoparticles for this investigation.

Many thanks to Archaeology (UCL) and Navision centre (QMUL) for providing their imaging services. Special thanks to Steve Gschmeissner, THE master of Electron Microscopy!!

Special thanks to all my friends and colleagues at the Blizard institute: Mojgan, Emma, Naseem, Navina, Steve, Ryan, Ahmed , Yoann, Amir, Kifaia, Eddie, Martha, Richard, Rob W, Minnie, Joe, Alice, Louise, Miguel and etc… too many to name!! Thank you for making it all worthwhile! I'm so grateful to have met you all. I have learned immensely form each one of you.

To my MSc students: Ying, Sadia and Hinesh thanks for your contribution to this work.

To Ola: I'll always remember you. You'll be missed. R.I.P

“A hair divides what is false and true.”

Omar Khayyam

Chapter 1

1. Literature review

1.1 Nanotechnology: a historical perspective

The general idea that small synthetic materials can be used for humans in order to provide health related benefits for humans is an odd idea. Many consider Richard Feynman, the celebrated physicist, as the father of nanotechnology (Peterson, 2004), an individual who proposed the use of such small scaled materials. During a 1959 lecture, Feynman stated that tiny robot like constructions can be used for a variety of medical conditions; these nano-machines will eventually interact at atomic scale and can have a potential positive impact on our health. In addition, he suggested that it is rather probable that in future mankind will be able to fit the entire Encyclopaedia of Britannica on top of a needle, referring to storage of information in nano-scale. This idea is widely known as the Feynman vision or thesis. In his lecture, Feynman hinted at several possibilities for these breakthroughs, such as "mechanical surgeons" and "small computers" (Feynman, 1960). These ideas were not thought of revolutionary at the time of the lecture and it wasn't until a decade later that scientists initiated their attempts at addressing the Feynman thesis. In fact the term "nanotechnology" was not devised by Feynman during his lecture and only 15 years post his famous lecture, a Japanese scientist named Norio Taniguchi suggested that technology "strives for precision" at the small scale of a nanometre. With the help of the advancing technology and subsequent innovative breakthroughs, the science of nanotechnology also thrived. A prime example of this is utilising the 1981 scanning tunnelling microscope (Binnig et al., 1985). This device allowed for a type of precision microscopy that permitted experts to detect the approximate height of

individual atoms, this then made a company like IBM to write the individual letters" I", "B" and "M" at atomic scale for the first time, beginning a new era for computing (Eigler and Schweizer, 1990).

1.2 Nanomaterials in medicine

Mainstream approaches to nanotechnology are now mostly focused on material sciences allowing for the application of nanomaterials to a vast number of products (Roco, 2004). Nanomaterials/Nanoparticles (NPs) are often divided into two distinct categories: organic and inorganic (Liong et al., 2008). Organic nanomaterials may include carbon NPs and liposomes whereas inorganic NPs include noble metals such as gold and silver and others which possess semi conductive properties, i.e. Titanium dioxide. These NPs maybe used for multiple applications such as diagnosis, therapeutics and drug delivery.

Organic NPs such as liposomes are known for their excellent biological properties, allowing them to diffuse and penetrate cells for drug delivery purposes (Torchilin, 2005). Carbon nanotubes on the other hand exhibit mechanical as well as electrical properties which makes them suitable for applications such as biosensors and anti-cancer (Logothetidis, 2006b). However, inorganic NPs are having a greater impact on diagnostic and medical sciences. They are being used as contrast agents for imaging techniques such as MRI and X-ray where used in low doses, tissue-specific targeting as well as imaging of the circulatory systems can be achieved (Na et al., 2009). They are also used as biological markers and as for probes for studying the structure of DNA among other complex and highly sophisticated molecules and experimental settings (Logothetidis, 2006a). Therefore, NPs can be used in line with other conventional methods for enhanced integration of bone to metal based prostheses. These devices can be designed in a way to enhance the interaction

between the existing surface and that of the living tissue (Singh and Manikandan, 2011).

Both orthopaedic and dental implants are also susceptible to failure due to a variety of causes with bacterial infection being of particular concern (Mack et al., 2006, Otto, 2013). This occurs despite extensive measures to reduce such infections. There are an increasing number of patients requiring medical devices, such as artificial joints to enable everyday activity. An improvement of current implants, i.e. infection-resistant prostheses, will offer tremendous benefits to countless patients. A common means by which these devices are exposed to infections is during surgical procedures. This is most probably due to the presence of nosocomial pathogens and although careful aseptic methods are usually followed by most hospital personnel and surgeons, these types of infections remain unchallenged. The official report (Surveillance of Surgical Site Infections in NHS hospitals in England 2013/14) for orthopaedic related infections suggests that in the UK alone there are various cases of patients whom acquire infections post-operatively. Although the incidents of contamination have decreased in orthopaedic related procedures between years 2008/09 and 2013/14, the challenge of total prevention still remains. This report suggests that patients who leave the hospitals and readmitted are at a greater risk of infection. The predominant species in orthopaedic related operations (hip, knee, repair of neck of femur and spinal related surgery) was *Staphylococcus aureus*, causing $\geq$ 40 % of all infections. Because of this the issue of orthopaedic related infections in nosocomial environments is still a major concern. Some medical devices incorporate antibiotics to help resist infection, however due to certain limitations for example, decreased release at the later stages of implantation,

resistance continues to rise (Aviv et al., 2007). Antibiotics have been used to combat these infections for many years but as a result of over-use and over-prescription, bacteria have evolved mechanisms to avoid their effects with microbial resistance rising significantly (Normark and Normark, 2002). Therefore development of innovative methods which deliver an alternative approach to antimicrobial function is therefore much in demand. In particular, the potential of antimicrobial NPs as future agents has received much attention (Rai et al., 2009). The antimicrobial activities of NPs vary depending on their structure and chemical composition. Their recent applications in tissue engineering and bone related research has gained considerable attention (Harrison and Atala, 2007, Corchero et al., 2010). Furthermore, these agents hold physiochemical properties that makes them unique among all antimicrobials (Albers et al., 2013). Their shape, increased surface area and size, combined with their toxic nature towards prokaryotic organisms make them extremely attractive as multifunctional agents (Salata, 2004).

Findings in the current study suggests that composites of hydroxyapatite (HA) and zinc oxide NPs (nZnO) are a possible choice as a prospective coating material for future orthopaedic implants (Zhao et al., 2013).

As coatings for medical bone implants gradually advance, a niche for products that outperform the previous generation of biomaterials is often created. Hydroxyapatite in its nano form (nHA) is a direct result of such evolution (Bryington et al., 2013). This material is understood to increase osteoblast function, proliferation, collagen production as well as osteoblast morphology (Shi et al., 2009b) Conventional coating methods such as plasma spraying utilise extreme heat that can change properties of NPs. However, such procedures often result in the production of a rough, thick (40-50 µm) and uneven surface (Sun et al., 2001). Therefore by applying a method that

allows for formation of a homogenised, micro-fabricated coating, it has been possible to produce layers of nano-coatings that are thin, homogenised and stable in nature. This unique quality allows for the exposure of groups of NPs to both bacteria and osteoblasts which may directly result in unique outcomes not achievable by conventional coatings. The combination of this novel approach with the advantage of zinc being an important trace element can be distinctively useful for bone related implants. More recently, it has been demonstrated that the addition of ZnO to bone-composites can enhance the proliferation, adhesion and differentiation of osteoblasts (Li et al., 2010) . Furthermore, zinc embedded calcium phosphate (CaP) ceramics have also been shown to promote the growth of bone cells when compared to non-embedded Zn CaP ceramics (Ito et al., 2002).

The antibacterial effects of metallic nanoparticles (MN) (silver (nAg) and nZnO) have so far proven to have a long lasting biocidal activity with high thermal stability and relatively low toxicity to human cells (Allaker, 2010). Recent studies suggest that nZnO is strongly bactericidal, making it suitable as a coating for medical implants (Seil and Webster, 2011). Preliminary observations suggest that this agent has a degree of selectivity towards *Staphylococcus aureus*, a species that is predominantly responsible for surgical site infections (Darouiche, 2004). The main proposed superiority of NPs compared to conventional antibiotics is their ability to instigate bactericidal effects via different routes, namely: ion release, direct contact and generation of reactive oxygen species (Padmavathy and Vijayaraghavan, 2008, Hernandez-Sierra et al., 2008). The present investigation is designed to help the current understanding of the relationship between coated nZnO and conventional nHA in relation to pathogenic bacteria and osteoblasts.

Orthopaedic related infections are mostly due to the presence of given species bacteria. The two main species of bacteria that have been shown to have a significant role in these infections are *Staphylococcus aureus* and *Staphylococcus epidermidis* (Stoodley et al., 2011, Olson et al., 2006). It is now accepted that S*taphylococcus* is the most frequently found genus of bacteria found on the surface of the skin and the mucous membranes (Chiller et al., 2001). Therefore their specific location may allow them to attach onto the surface of a specific material (Titanium or Glass) and with the right conditions, they initiate biofilm formation (Costerton, 2005). *Staphylococcus* communities have the ability to communicate to one another and this can increase their pathogenicity through quorum sensing (Yarwood et al., 2004). During the growth phase they release specific peptides to their extracellular environment that can result in enabling the release of unwanted invasive factors as well as reducing surface adhesion properties.

The intricacies of the biofilm system have in turn made it difficult for scientists to invent new viable strategies to coat medical devices (Meyer, 2003). Aside from specific infections such as the dental plaque, medical device related infections are not usually shared between species of bacteria or even different strains of the same bacteria. This phenomenon could be due to quorum sensing properties that bacteria use to maximise virulence capabilities. It is of interest that infections caused by different species of bacteria can have different surgical outcomes, for example, when infected with *S. aureus* these devices need to be replaced more frequently than when there is a *S. epidermidis* infection. Therefore a comprehensive knowledge is required when dealing with bacteria that form biofilms on medical devices.

1.3 Biofilm formation

Knowledge as regards the formation and properties of biofilms is growing and it has been established that this system plays an important role in protecting the integrity of a certain population of bacteria and essentially protects these populations from antimicrobial agents. The structures of biofilms are diverse and help bacterial population to withstand harsh conditions (Figure 1). These structures have specific properties that are essential for bacterial survival, and within them there is a sessile community of bacteria that are able to release certain proteins, macromolecules, exo-polymers, phenol soluble modulin surfactant peptides and more importantly DNA (Mann et al., 2009). Evidence suggests that DNA release plays an important role for communication between the bacteria (Whitchurch et al., 2002). Furthermore it has been observed that, in an effort to make a resistant population, the cells which are exposed to an antimicrobial agent don't normally die due to programmed cell death and instead undergo a " altruistic suicide" phase, whereby they are lysed and their contents are released to the surrounding environment (Nedelcu et al., 2011). This phenomenon is hypothesised not to be due of the actions of the antimicrobial agents per se, it is likely due to an effort to provide a communal resistance as a result of the inflicted "stress". The cells that have survived the intrusion (persistors) are then able to use the materials and nutrients released form the dead cells and promote the growth of the community. This action allows bacteria to release vesicles that contain their genetic information, thereby communicating the presence of danger or the presence of an unrecognisable object to the rest of the population. However there is much debate about the relationship of genes and antimicrobial resistance in the scientific community that suggests that genes might play less of a role in this process than it was previously believed (Stewart and Costerton, 2001). The more exposed a

population to an antimicrobial agent, the more resistant it becomes. It is therefore essential to have an antimicrobial agent that has the potential to challenge these intricacies for prolonged periods of time.

Pictorial description of biofilm formation

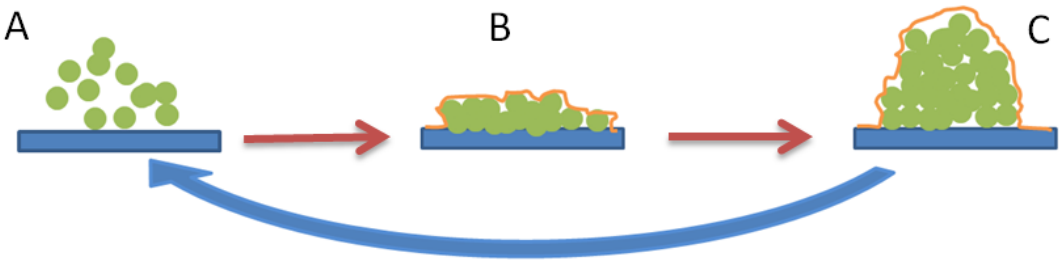

Figure 1 - A) Planktonic bacteria attach to a desirable surface, B) Biofilm formation takes place, cells begin to communicate and quorum sensing is initialised, C) A mature biofilm is formed and there is potential for bacteria to further disperse into their surrounding environment.

Staphylococcus species are responsible for most orthopaedic infections and hence most biofilm formation. A recent study looking at both *Staphylococcus aureus* and *Staphylococcus epidermidis* suggest increased resilience to the newest form of antibiotics (Campoccia et al., 2006). Findings suggests that, bacteria in planktonic stage (Figure 1-A) can be eradicated, however after a period of 24 h, biofilm formation takes place and most antibiotics are not effective. Despite the fact that recently used substances such as silver nitrate are shown to have detrimental effects against persistent infection with *E.coli* (Morones-Ramirez et al., 2013) It is inevitable that bacteria, given a short period of time, will develop resistance (Percival et al., 2005). Therefore a plan for prevention rather than direct destruction of the biofilm is more desirable (Nishimura et al., 2006). This will be most beneficial, since most bacteria can reside on implant coatings during invasive surgical procedures (Campoccia et al., 2006). However before tackling the issue of biofilm formation, it is of utmost importance to have a thorough knowledge as regards to bone biology,

the various factors which contribute to bone formation and its loss. When a specific site of bone infection is examined, it immediately becomes evident that an acute inflammation site is where most bacteria reside. In addition, other inflammatory factors (including leukocytes) contribute to bone destruction. Furthermore, the blood supply to bone is disrupted by compression of vascular channels which in turn contribute to direct bone necrosis. A region of bone without blood supply can detach from its main body and potentially lead to microbial contamination despite various antibiotic treatments (Lew and Waldvogel, 2004). Therefore knowing the intricate structure of bone allows researchers to devise a system that is suitable for bone implants that are antimicrobial. While generally a multidisciplinary approach is required for tackling this issue, the following will elaborate on some of these important factors.

1.4 Bone biology

The structure of bone is complex (Figure 2). Crucial information about bone biology can help to devise improved and more efficient implants, both mechanically and biologically. Therefore a brief but inclusive look at its relevant structures is presented in the following.

Bone anatomy: bone's interior structure

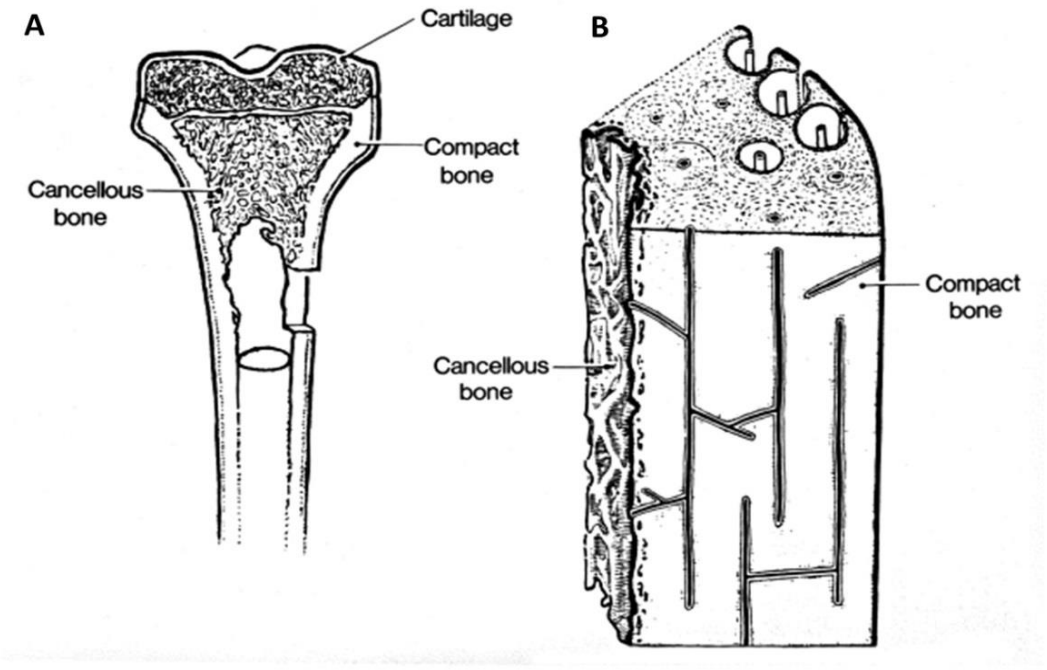

Figure 2 - The interior structure of the bone. A) A cross section highlighting the positions of both cancellous and compact bone. B) A comparison of the cancellous bone and compact bone. Longitudinal tubes like structures embedded within the structure of compact bone are Haversian canals that overtime have evolved to carry blood vessels and nerves. In an infection scenario, these canals could collapse as a result of bone destruction and lead to further complications. Image obtained from: http://goo.gl/SIUv2A (Titled: interior bone structure).

The macrostructure of bone consists of cortical and cancellous or trabecular bone. For implant purposes these two types of bone structures are important. An implant or a medical device that is positioned within the structure of the bone is mostly in contact with cancellous bone. Whereas external implants are initially introduced to external tissues (i.e skin) and cortical bone. The main difference between cortical and trabecular bone can be seen in their structure, strength and function. Cancellous bone is thought to be the more metabolically active of the two. This type of bone is easily remodelled and contains marrow filled pores, nerves and blood vessels. This remodelling and modelling is due to the involvement of different factors such as

aging, activity, and different loading properties of bone. Bone implants with the aid of calcium phosphates are designed to help preserve this inner structure of the bone by encouraging the growth of osteoblasts and creating an environment which is "biologically friendly" (Giannoudis et al., 2005). Devices coated with calcium phosphates are capable of promoting bone growth by coming into close contact with both of these bone types. For extreme surgical cases such as hip replacements or dental related procedures, hydroxyapatite or bio-glass coated metallic implants are commonly utilised in order to promote bone growth with the aid of modified metal surfaces. Three types of eukaryotic cells are responsible for integration between the implant's surface to bone as well as early and late bone formation and resorption, (Figure 3).

Commitment and terminal differentiation of mesenchymal stem

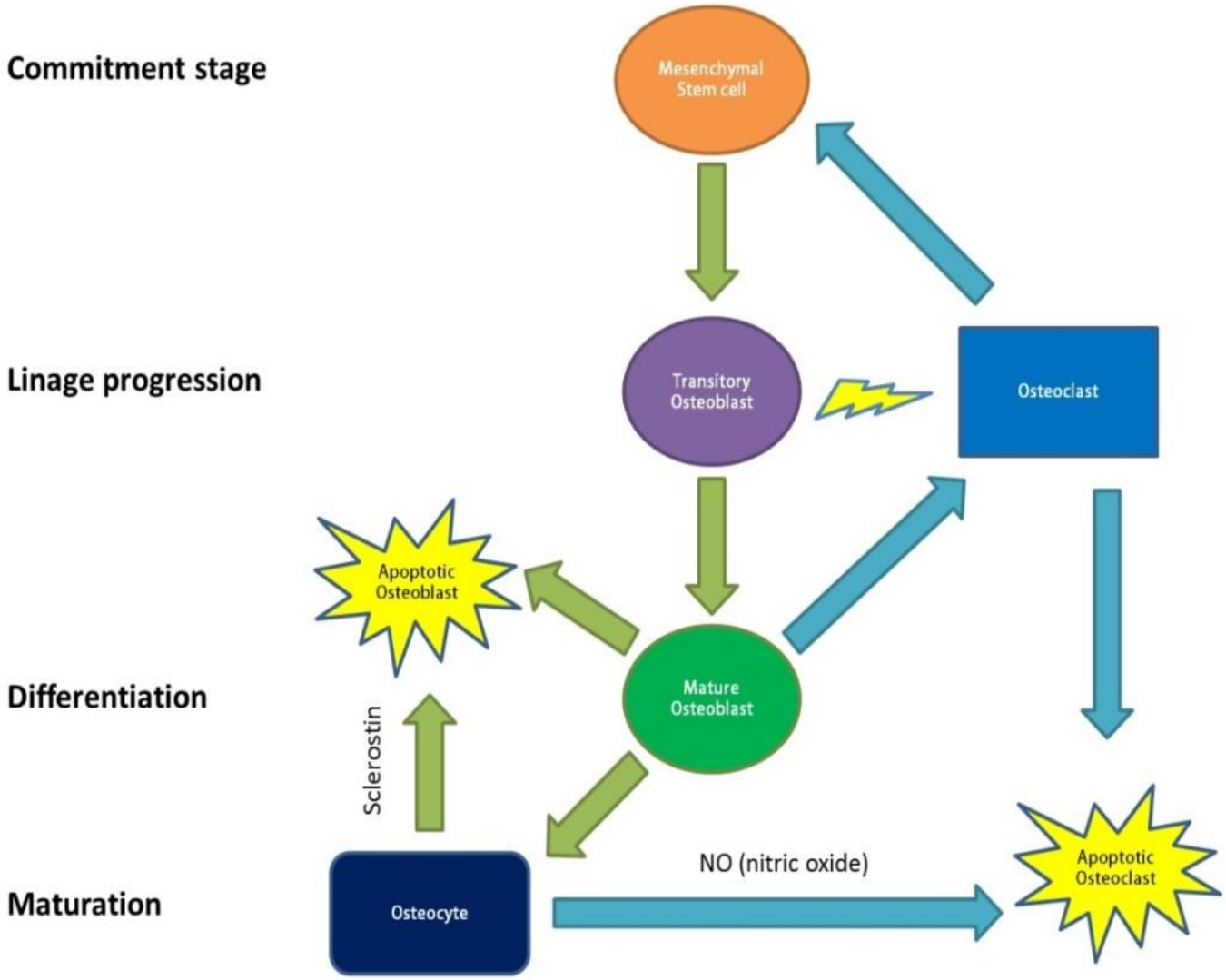

Figure 3 - The intricate relationship between cells responsible for bone formation and resorption. Interaction between osteoblasts, osteoclasts and osteocytes is essential for bone formation, its remodelling and development. The balance in activity of each stage allows for a healthy bone to form. Image adopted and from: http://goo.gl/ygYv0A (The university of Chicago medical centre).

These cells are Osteoblasts (as tested in the present study), osteoclasts and osteocytes. Osteoblasts derive from mesenchyme and their main role is to produce a rich matrix that is subsequently mineralised (Harada and Rodan, 2003). Cells that remain deep within the mineralised structure of bone are referred to as osteocytes. These cells are solely responsible for bone remodelling as they are able to control the activity of both osteoblast and osteoclasts (Aarden et al., 1994). This is achieved by making connections with these (osteoblasts and osteoclasts) cells via dendritic structures that can be elongated for relatively short distances of approximately 100 nm. Upon direct physical contact, regulators are released that either inhibit or promote the activity of the above cells that ultimately will lead to bone resorption or formation. Finally osteoclasts are cells that control bone resorption, which can secrete chemicals such as hydrochloric acid and hydrolases that destroy calcium phosphates and the collagen fibres respectively, this leads to the loss of bone mass that could result in either damage or bone remodelling (Miyamoto and Suda, 2003). This remodelling of bone is carried out throughout an individual's life; therefore the presence of cells which respond to the different environmental, as well as structural cues, is essential for a healthy skeleton. Healthy bone is also prone to serious damage, be it environmental or genetic. One of the prominent challenges faced both fields of dentistry and orthopaedics is bacterial infection, which eventually may lead to the lack of proper bone mineralisation and eventually bone destruction.

1.5 Orthopaedic infections

Orthopaedic implants (devices) are predominantly assisting the general population with maintaining their quality of life. However in some cases complications can

occur. Among all complications, infections are thought to be the hardest to deal with. Orthopaedic related infections comprise of 1 to 13% of these complications, while the percentage is rather low, the outcome can lead to serious health risks in patients and cause major consequences, such as: immobility, reoccurring acute pain, chronic pain and implant failure. Additionally, the National Joint Registry (NJR) for England and Wales (2010) reports that in 2009 alone there were 72,432 hip replacements of this, 65,229 were first time surgeries and the remaining 7203 were revision surgeries, of which more than 3% were infection related. The underlying mechanisms that leads to these consequences also disrupt the normal balance between bone formation and resorption and in turn the process of remodelling is halted. It is well documented that exposure of bacteria, especially *Staphylococcus aureus* to osteoblasts results in manifestation of markers that are recognised as essential for osteoblast growth and division (Widaa et al., 2012). Bacterial adhesion to bone prosthesis can be divided into two segments: 1) loose attachment and 2) fixed attachment. The initial stage comprises of bacteria adhering to the surface of an implant by utilising weak physical forces, such as Van der Waals and gravity. These forces allow the loose attachment of bacteria, which in turn allows the initial interaction of bacteria and the material surface. The fixed attachment comprises of a series of complex processes that collectively depend upon the environment, the material surface and the bacterial species/genus involved. At this stage a firmer connection is made that can result in biofilm formation. However various essential factors are known to be involved in *Staphylococcus aureus* attachment. These include molecules that are involved in immune evasion, bacterial adhesion, anti-inflammatory interactions, biofilm formation and cell invasions. Collectively these factors are either released or reside on the surface of the microorganism and in *S. aureus*, approximately 50 genes are

involved in encoding for all these factors that lead to pathogenesis (Sittka and Vogel, 2008). If spread from the surface of the material to bone, the outcome will likely cause a reduction in alkaline phosphatase production as well as an abrupt end in production of type I collagen, which in turn could indicate both reduced activity for both bone formation and resorption. Furthermore, the escape of bacteria from the immune system or multiple antibiotic treatments might lead to implant removal and ultimately extensive bone removal.

1.6 Dental infections

Classification of failure in dental implants is categorised into failing and failed implants. The failing implants are treatable and the implant can be saved, whereas failed implants need to be removed completely. Infection is one of the factors involved that is often related to late failing implants that ultimately lead to total failure. The initial bacterial flora involved in early stages of a failing implant is often gram-positive, non-motile and facultative in nature. However there is a transition from these populations towards one that contains more gram-negative, motile and anaerobic bacteria (Alcoforado et al., 1991, Leonhardt et al., 1999). At this stage, an inflammatory process that affects the surrounding tissue, peri-implantitis, may occur which leads to the loss of the surrounding bone that serves as a support for the implant (Pye et al., 2009). Some of the most common bacteria isolated from these regions are highlighted in Table 1.

Predominant bacterial species involved in peri-implantitis

Table 1 - A series of bacterial species involved in dental related infections. Bacterial population percentages compare infection occurrences when healthy implants are compared to failing implants. The population of most species increase significantly during peri-implantitis. Data obtained from Persson et al (Persson and Renvert, 2014).

Bacterial Species	Healthy implants (> $1*10^4$ Cells %)	Peri-implantitis (> $1*10^4$ Cells %)
Fusobacterium nucleatum sp.nucleatum	40.4	64.5
Prevotella intermedia	21.3	45.8
Pseudomonas aeruginosa	21.3	44.0
Porphyrmonas gingivalis	27.7	56.0
Staphylococcus aureus	19.1	43.4
Tannerella forsythia	25.5	61.4

In general the process of bone destruction also applies for dental implant infections but with a heightened risk of having many more species of bacteria (mostly anaerobic bacteria) involved in the process.

1.7 Medical implant coatings

Coatings have been utilised since ancient times for various purposes. The interest of the author is directed towards the field of orthopaedics and bone implants in general. The use for orthopaedic device coatings was initiated by an ever increasing problem of failing bone implants. The main purpose for an invasive surgery and employment of a device is to restore and improve a potentially morbid function of bone which in turn would allow fast rehabilitation and bone healing. However, while an appropriate mechanical and biological function is ideal, acute and chronic infections provide complications that might lead to further invasive surgery (Moriarty et al., 2010, Darouiche, 2004). Coatings for bone prosthesis are predominantly designed to enhance osseointegration; however there is always a competition between host cells and microorganisms to adhere onto the surface, a phrase named “race for the surface”(Gristina, 1987). These coatings can be categorised into two distinct groups:

passive or active. Passive coatings are referred to as coatings that are not able to release any bactericidal agents into their immediate surroundings; an example of this is hydroxyapatite coated materials. Active coatings on the other hand are coatings that mitigate bacterial adhesion or are actively releasing bactericidal agents (Goodman et al., 2013). Aside from understanding the biology and structure of the bone, it is required to understand and study other bone-related factors involved in developing relevant bone prosthesis. These involve the coating materials used, design of the implant, its various methods of fixation and ultimately its shape. The following is a brief outline of two coating materials utilised in the current study and their relative advantage and disadvantages.

1.7.1 Hydroxyapatite as a coating material

Natural hydroxyapatite (HA) constitutes nearly 65% of the bone. Its relatively simple chemical composition $Ca_{10}(PO_4)_6(OH)_{2,}$ has allowed scientists to successfully reproduce it under laboratory conditions. Investigators have since used numerous ways to incorporate this ceramic into bone studies, often by using it as filler for bone (Sotome et al., 2004). In the fields of medicine and dentistry, calcium phosphates have gained substantial attention and most of the medical devices that are in contact with bone are coated with a layer of calcium phosphate. This is because of its innate ability to allow bone growth, in other words, hydroxyapatite is a biocompatible osteoconductive material (Chu et al., 2002). Osteoblasts found in the structure of trabecular bone interact well with it and can proliferate inside its porous structure. There are however disadvantages. One of the most important factors is its brittleness. Using HA on medical implants that require intense surface torsion or impact pressure can prove difficult. Other problems include an incompatible Young's modulus to that of the bone and not being able to resist tension or shear (Mahan and Carey, 1999).

These properties however do not take away the fact that, today, nearly all titanium based orthopaedic related devices use HA as a coating that acts as a bone substitute to promote bone growth and oseoinduction. Titanium metal has been frequently used for medical purposes (Figure 4).

Human femoral bone implant

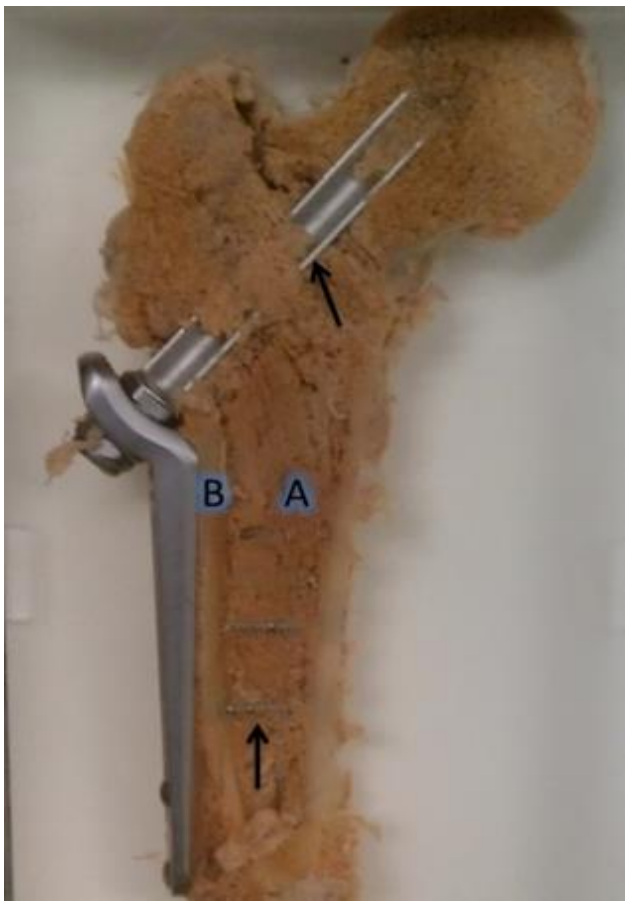

Figure 4 – Human femoral titanium prosthesis. A) Cancellous bone, the metabolically part of femur B) Cortical bone has a strong and dense structure that is in full contact with the external site of the prosthesis. The black arrows represent the sites where the implant is in full contact with bone. This particular implant is not coated and is semi-external.

Its applications in the field of orthopaedics are many; this is because of the unique set of properties that this metal offers. Early animal experiments in the 1940s indicated its biocompatibility and its use in the medical field has continued since (Wang, 1996). In general, a bone implant should have the same mechanical properties as the bone itself. Finding this property in inorganic materials can be a challenge and scientists have not been able to achieve this ideal. Titanium also does not does not have the "required" properties as a bone implant. It has a higher modulus compared to that of the bone, meaning it is not as elastic.

This causes the bone to lose its mass due to the stress shielding and load imbalance. Due to these factors and various other complications, the introduction of HA to the surface of titanium implants is a necessary addition. It is has to be stressed that that surface structure of such implants also present a profound effect on how these implants behave mechanically. In order to address this issue scientists have utilised a rough titanium surface that possesses porous structures so that bone ingrowth at the later stages of implantations is as mechanically stable and secure as possible (Morscher, 1991, Giordano et al., 2004).

1.7.2 Nanoparticles as coating materials

NPs generally refer to materials that are smaller than 100 nm. Their importance and usage in the field of biology and medicine are widespread (Salata, 2004). Their small size makes them particularly notable to science and modern medicine. This property has allowed innovative methods to be devised by scientists in the field of nano-medicine. A notable example of this is the usage of silver NPs for antimicrobial purposes (Morones et al., 2005). Many more materials such as polymers (encapsulated with drugs) can also be turned into NPs via different methods. These nanoparticulates can travel almost "freely" within a biological system and have been found to be useful in the fields of cancer therapy (Yang et al., 1999, Ferrari, 2005). Some NPs are able to target cancer cells and others can be traced *in vivo* using modern medical imaging techniques. Scientists have been able to use these particles as "magic bullets" to target a specific tumour (Jordan et al., 1999, Jain et al., 2007).

The concept of magic bullet refers to "selectivity" in drugs. This can mutually apply to the field of NPs. Some nanoparticulates may be coated with different materials so that their surface is recognised by the cells of interest, thereby attaching to the surface of the microorganism and causing damage, while in other NPs, coating is not necessary and the same type of behaviour can be achieved using particulates that are able to show selectivity towards different bacterial species (without being manipulated chemically) as well as diverse type of cancer cell lines (Reddy et al., 2007, Ostrovsky et al., 2009). Furthermore, it has been observed that as the size of NPs decrease, their antimicrobial activity increases, therefore relating the bactericidal effects to shape, most nanoparticles have different shapes based on the different methods with which they were synthesised (Choi and Hu, 2008, Azam et al., 2012). This is an important feature that could prove useful in future investigations of this field and is also explored in our present study. NPs are however not without their side effects and can accumulate in certain organs or tissues in order possibly cause biological toxicity (Tang et al., 2009). Therefore if nano-sized particles are to be implemented as coating materials for medical devices, they need to be secured onto a surface, this could be achieved both mechanically as well as chemically, using various innovative methods (i.e plasma spray or EHDA).

1.8 Coating systems

The last generation of orthopaedic implants did not have the capacity to be bioactive or introduce bone growth around the device. This is because the prosthesis was surrounded by cement that was not bioactive. This provides an interface between bone and the implant, preventing any direct contact between the two, leading to an end-result that seems to be satisfactory (Huo and Osier, 2008). However, because of catastrophic events of post-operative failure in cemented implants such a huge bone

loss and free debris of cement in the structure of the bone (Hungerford and Jones, 1988, Navarro et al., 2008), scientists have been searching for more bioactive and biocompatible methods that could be applied to both orthopaedic and dental implants. Uncemented implants are the product of this pursuit. These are products that with the help of modern technology have been coated with osteoconductive (i.e being able to attract bone material such as hydroxyapatite to provide the needed stability). Some post-operative results indicate that these uncemented implants could prove as effective as their cemented counterparts (Hofmann et al., 2002). Most uncemented implants in the field of orthopaedics use thermal coating methods such as plasma spraying that allow the attachment of deposited materials by using very high temperatures of around 20,000 ºC (Zaat, 1983). The use of such temperatures can lead to rapid deterioration of the plasma gun and prove very expensive. Other methods such as ultrasonic nozzle and electrohydrodynamic atomisation (EHDA) provides a novel method for coating medical devices that cost much less than the thermal methods and provide an equally uniform and efficient coating (Huang et al., 2011). Finally, regardless of coated and uncoated devices, there is an urgent need for major reform in the field of biomaterials and antimicrobials. Multiple examples for such novel coatings are the incorporation biomolecules, such as antimicrobial peptides which might lead to bone/implant integration by having desirable effects on cell function and differentiation (Goodman et al., 2013). Furthermore, layer-based coatings, whereby between each layer of a multi-layered coating there are active molecules that are released in a controlled manner, the sustained release of active agents could prove beneficial for long term maintenance of the implant-bone interface (Sun and Lynn, 2010). Technologies and scientific discoveries are an ever evolving phenomena, this evolution also applies to living beings such as bacteria. As

a species, humans need to comprehend and expand their relevant knowledge in order to tackle the ever increasing challenge of antimicrobial resistance and colonisation. This requires innovative new approaches which allow benefits and challenges these ever adapting threats.

Hypothesis

A nano-based coating system will offer enhanced antimicrobial activity for future bone-related implants. This coating will also allow for efficient, bio-functional and stronger bone integration.

Aims and Objectives

- To understand, compare and analyse the antimicrobial capability of a number of novel nanomaterials for potential future medical use.
- To provide mechanistic evidence as to how nZnO is able to instigate its antimicrobial effect.
- To optimise a novel nano-based coating system in order to create a thin but functional surface that is both biocompatible and potentially osteoconductive.
- To compare and contrast novel coatings with conventional dental/orthopaedic coatings.
- To innovate and bring new ideas as to how manipulation of coating surfaces can maximise implant stability and performance.

Chapter 2

Investigations into the antimicrobial activity of nano-metal oxides.

1. Introduction

1.1 Emergence of antibiotic resistance

Exploited by humans since the discovery of penicillin, the resistance to antibiotics is the major factor behind the ultimate failure of an ever continuing struggle against bacterial pathogens (Davies and Davies, 2010).

The human body is colonised by approximately 10^{14} bacteria, this is despite the fact that our bodies are roughly comprised of 10^{13} eukaryotic cells (Clemente et al., 2012). Our microbiome is at the centre of major scientific research efforts and as a result we are getting ever closer to an understanding of the important role that bacteria play in our everyday lives. It is therefore vital to understand that these microorganisms live in symbiosis within and on our bodies and also are an important part of human evolution (Xu et al., 2007). Since there is no single species of bacteria within our bodies, there is a struggle and symbiont relationships between the pre-existing bacterial species in this dynamic environment (Dethlefsen et al., 2007). This interspecies mutualism can be disrupted if a small population of antibiotic resistant bacteria are introduced to a region where no pre-existing host population is present.

Despite exposure to antibiotics, the newly introduced bacteria are likely to thrive, proliferate and eventually become established elsewhere in the body.

Some bacteria are naturally resistant to antibiotics and as the newly introduced population increase in numbers, mutations occur leading to the development of bacteria with lower susceptibility to applied drugs (Wang et al., 1998). There are multiple ways in which resistance can occur, namely, mutation, protection, replacement and alteration of the drug target or mechanisms that involve inactivation or removal of the drug (Canton, 2009). The unsupervised global experiment in bacterial evolution (Figure 5) is therefore a direct link to the accelerated process of antimicrobial resistance. This is an ill-fated situation since not only do bacteria possess the strongest total number of species on our planet but they are vastly diverse. Not much is known about fundamental bases for antimicrobial resistance. The ecology and role of resistance genes are still new to science, our limited knowledge as to how bacteria thrive in its natural environment is still in its infancy and despite this limited knowledge, some species of bacteria contain antibiotic resistance genes despite human intervention (Allen et al., 2010). In fact, Alexander Fleming who discovered penicillin in 1928, had warned that bacteria could evolve to beat antibiotics and a recent report by the World Health Organisation (WHO) published on April 30th, 2014 confirms this prediction. Therefore we are fighting a losing battle. However a strategy of prevention, rather than total obliteration is the most appropriate solution.

Figure 5 - Evolution through the process of natural selection is the major drive behind the phenomena of bacterial resistance. Image adopted from www.Science.com and http://academy.asm.org.

1.2 Infections and a new generation of antimicrobials

The following section will focus on important and relevant pathogens to the current study and subsequently introduce novel ways that can be applied in order to decrease the probability of infections or contaminations.

Gram positive infections make up the majority of bone and joint infections (Darley and MacGowan, 2004). With regard to bone and specifically joint related procedures, conventional antibiotics are thought to only penetrate into the peripheral regions and fail to gain access to deeper regions of bone. As a result, treatment of osteomyelitis and joint related infections requires prolonged periods of time to take effect (Del Pozo and Patel, 2009). Consideration of such factors and the role of bacteria in the more common bone related infections has placed an emphasis on the following species:

- *E. coli*
- *P. aeruginosa*
- *S. epidermidis*
- *S. aureus*

1.2.1 *Escherichia coli (E. coli)*

E. coli, a gram-negative species, and a facultative organism, is one of the species of bacteria that humans are exposed to early in life. *E. coli* can colonise the gut and is one the main members of the faecal bacteria (Edberg et al., 2000). Any object touched or in direct contact with our skin would almost certainly be contaminated with faecal bacterial populations that include *E. coli.* When presented into and on tissues that are not normally inhabited by such bacteria, pathogenesis can occur. *E. coli* contamination that may lead to bone loss is rare but can occur in multiple ways such as an open fracture or contamination via soil faecal material. Moreover, *E. coli* related osteomyelitis can similarly occur in the very young and elderly patients and often occurs in their long bones. A case reporting a rare maxillofacial *E. coli* infection indicates that, after consumption of contaminated water, bacteria had found their way into the bone tissue, causing serious bone loss (Padhiary et al., 2013). It has also been observed that conventional antibiotics utilised by dentists are often impractical and further care and of multiple antibiotics courses are required in order to deal with these types of infections. Researchers reporting these findings stress that while rare, most surgeons would benefit if *E. coli* was always considered as a potential candidate for aggressive osteomyelitis (Padhiary et al., 2013).

1.2.2 *Pseudomonas aeruginosa (P. aeruginosa)*

This species is involved mainly with contamination that occurs within catheters and various foreign body implants. *P. aeruginosa* is gram negative and not commonly associated with bone related diseases. However, *P. aeruginosa* is the predominant species removed from contaminated bone implants. A recent study also suggests that biofilm formation by this species can have detrimental effects as initial antibiotic

treatment decreases the population by 44%, however the remaining resistant cells are no longer treatable by conventional antibiotics anymore (Daniëlle et al., 2005). Furthermore orthopaedic prosthesis that are contaminated by this species of bacteria are often required to be subjected to multiple medical revisions, solely for the nature of the infection, often needing the application of multiple antibiotics at the same instant (Bernard et al., 2004).

1.2.3 *Staphylococcus epidermidis (S. epidermidis)*

S. epidermidis is a gram positive species found on the surface of the body, mostly skin (Grice and Segre, 2011). It is predominantly related to nosocomial infections and therefore is a high risk to patients who undergo invasive surgical procedures. With respect to bone and medical devices, the implants presented by surgeons are sterilised but contamination can occur if there is minimal contact between the patient's skin and the medical device. Therefore, *S. epidermidis* can be transferred to bone and produce a rather thick multi-layered biofilm. Similar to most bacteria, biofilms are thought to protect *S. epidermidis* from the host's defence system and potential antibiotics applied to the infected area (Lima et al., 2013). Furthermore, *S. epidermidis* can release lantibiotics, a group of antimicrobial peptides which serve as a deterrent for other gram-positive species in addition to providing exclusivity for this species to grow on a surface without competition (Harris and Richards, 2006), leading to biofilm formation.

1.2.4 *Staphylococcus aureus (S. aureus)*

S. aureus is responsible for most biofilms formed by a single species of bacteria in bone related diseases. Studies investigating this bacteria indicate that contamination and biofilm formation are the main reason behind chronic osteomyelitis (Marrie and Costerton, 1985). This chronic disease destroys bone and in parallel osteogenesis markers dramatically decline over time. An *in vitro* study, over a period of 7, 14 and 21 days measured the production of one of these markers to see if there is a direct relationship between *S. aureus* infection and bone-marker reduction. Comparison between infected and uninfected osteoblast cultures incubated for more than 21 days indicated a significant reduction in bone marker production in infected cells (Widaa et al., 2012). *S. aureus* also has other properties such as the heightened ability to adhere to the surfaces of biomaterials that are exposed to plasma proteins. When introduced into the bone via the route of an implant, by utilising adhesins that are termed microbial surface components recognizing adhesive matrix molecules (MSCRAMMs), bacteria can adhere to regions (Patti et al., 1994) that are essential for bone formation and will inhibit their function.

1.3 An alternative to traditional antibiotics

Because of the continued failure of antibiotics and the rise of resistant strains of bacteria mentioned in the previous sections (Section 1.1), NPs offer new opportunities as potential precautionary antimicrobial agents. Unlike conventional antibiotics, they are believed to instigate their effects via multiple mechanisms that are discussed further in this chapter. Their varied and yet almost homogenous size coupled with their heterogeneous structures gives them the ability to show enhanced antimicrobial activity against most pathogenic bacteria. These synthesised NPs are

also multifunctional. They are utilised as coating materials on clothes, food storage, cosmetics and sometimes for diagnostic and medical applications that are directly invasive (Park et al., 2009, del Campo et al., 2005). Understanding the full scope of their potential within different disciplines of the sciences, especially that of medical science, can result in novel innovations that will potentially lead to an increase in the longevity of human life. In the present study, nanoparticulates in suspension as well as on coated substrates are exposed to different environmental circumstances hypothesised to influence their antimicrobial behaviour. The resulting activity should provide a great deal of insight into how bacteria react when exposed to environments dominated by these small scaled particulates.

2 .Materials and Methods

Flame pyrolysis method

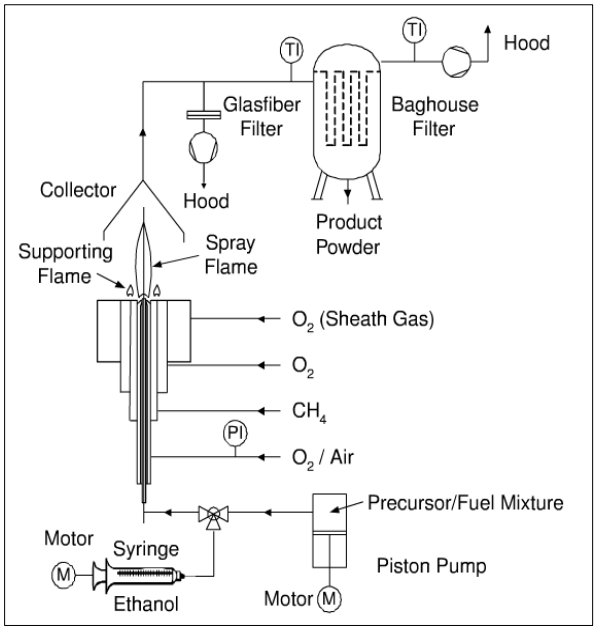

Figure 6 - An outline of the specific setup for the flame pyrolysis method. The fuel and the precursor for the NPs are fed through the nozzle. The mixture is then synthesised using spray flame which is controlled by the intensity of fuel injection and hence directly affecting the NP production. Image obtained from Mueller et al, (2003) with permission.

2.1 Nanoparticles

All NPs except nHA were synthesised using the unique method of flame pyrolysis (Figure 6). The basic method is initialised when the precursor of the NPs is mixed with fuel (usually ethanol) and passed through a nozzle that leads to a spray flame which in turn aids synthesising these particulates based upon its height and intensity. The synthesised particulates are then collected in a

collector and processed. The advantage of this system is in its relative simplicity as well as the broad spectrum of nanoparticulate precursors that can result in various functional NPs upon successful synthesis (Mueller et al., 2003).

The metal oxide NPs are therefore well characterised with an increased surface area to weight ratio and a size range of between 50 and100 nm. Handling and storage of these NPs was carried out according to industrial safe-working practices to avoid biological and environmental harm. The NPs were not discarded into the sewage system; they were instead filtered and incinerated. The NPs tested included: Zinc Oxide (nZnO), Titanium Dioxide ($nTiO_2$), Tungsten Oxide (nWO_3), Cupric Oxide (nCuO), 70% Silver + Zinc Oxide (70% wt nAg + 30% nZnO), 70% Silver + Cupric oxide (70% wt nAg + 30% nCuO) and Hydroxyapatite (nHA). Hydroxyapatite NPs were made by the process of wet precipitation between calcium hydroxide ($Ca(OH)_2$) and orthophosphoric (H_3PO_4) acid.

Collectively, most NPs were suspended in 100% ethanol and were sonicated for a period of 5 min thoroughly in order to maintain particulate stability. The exact mechanism with which the mixed NPs were created was not disclosed by the Johnson Matthey plc. Selection of these NPs depended upon their availability, scientific relevance, novelty and their potential applications based upon previous findings.

2.2 Bacteria

Both gram negative and gram positive species of bacteria were used in the present investigation. These included: *Staphylococcus aureus* (Oxford, NCTC 6571), *Escherichia coli* (NCTC 9001), *Staphylococcus epidermidis* (Lab Isolate) and

Pseudomonas aeruginosa (PAO1). All of these species are known to be involved in orthopaedic and bone related infections.

2.3 Minimum bactericidal concentration (MBC)

Minimum bactericidal concentration determination indicates the lowest concentration of an antimicrobial agent / antibiotic that can kill all bacteria in a given setting. Bacteria obtained from frozen stocks were grown on TSA (Tryptone Soya Agar – Oxoid, UK) plates for a period of 24 h at 37ºC in a 10% CO_2 Incubator. 3 to 4 colonies were removed from the plate and mixed in 5 mL of TSB (Tryptone Soya Broth - Oxoid, UK) in a 20 mL universal tube (sterile conditions).

Bacterial suspensions were placed in a shaking incubator at 200 rpm for a period of 24 h under at 37°C. The optical density (O.D.) of the turbid suspension was adjusted to 0.1 at a wavelength of 540 nm (this corresponds to a population of ~10^6 bacteria). A volume of 1 mL from NP concentrations tested (250, 500, 1000 and 2500 µg/mL) was added to a series of 1.5 mL centrifuge tubes and subsequently inoculated with 12.5 µL of bacterial culture with the inclusion of positive and negative controls. The positive control consisted of 1 mL of TSB inoculated with 12.5 µL of the bacteria, while the negative control was 1 mL of TSB. A volume of 5 µL from each of these mixtures was taken and inoculated onto a plate immediately and left in an incubator overnight at 37ºC, 10% CO_2.

2.3.1 Comparative agar based MBC determinations

Multiple concentrations of nanoparticulate suspensions mixed in 1.5 mL tubes were left in a shaking incubator at 200 rpm, 37ºC and 10% CO_2. The NPs used were comprised of nWO_3, nZnO, and nAg 70% wt + 30% nZnO. The tubes were removed from the incubator and left in room temperature for 10 min. This allowed for precipitation of nanoparticulates and therefore the total removal of bacteria. An aliquot of 50 µL was removed from each bacterial/NP suspensions and placed on a TSA plate and placed at 37ºC, 10% CO_2 overnight. Bacterial growth was qualitatively analysed and compared for each suspension (Figure 10).

2.4 Minimum inhibitory concentration (MIC)

Bacteria were obtained from frozen stocks, thawed and plated onto TSA plates for a period of 24 h to allow sufficient growth. The freshly grown bacteria were removed from the plate and were mixed in 5 mL of TSB in a universal tube. The bacterial suspension along with 5 mL of broth (control) was placed in a shaking incubator for a period of 24 h. The O.D. of the turbid suspension was adjusted to 0.1 at the wavelength of 540 nm using a light spectrometer. Furthermore 1 mL of each NP concentrations was added to a series of 1.5 mL tubes and subsequently inoculated with 12.5 µL of the bacterial suspension. A 200 µL sample from each of these mixtures was obtained and placed in a 96 well plate and the initial O.D. was measured using a plate reader. The tubes were then placed in a shaking incubator (100 rpm) for a period of 24 h and a 200 µL sample removed and the final O.D. measured.

2.5 Time based bactericidal studies

Concentrations of NPs were suspended in PBS and ABS. Concentrations from 250 µg/mL to 2500 µg/mL were used to observe their bactericidal properties. The suspensions were sonicated for 5 min. Subsequently 450 µL of each suspension was re-suspended into 1.5 mL micro-centrifuge tubes. In addition, 50 µL of the O.D. adjusted bacterial suspension (only *S. aureus* and *E. coli*) were introduced into these tubes and a 1:10 serial dilution was performed for each nanoparticulate suspension. Furthermore 20 µL of each mixture was plated on TSA plates and incubated overnight at 37°C, 10% CO_2. Colony forming units (CFU/mL) were then counted and the number of bacteria present in each mixture was quantified and calculated. *S. aureus* and *E. coli* were chosen as representatives of gram positive and gram negative bacteria.

2.6 Coating with NPs

2.6.1 EHDA deposition of NP coating

EHDA was used to coat all samples (Figure 7). This is a relatively novel and cheap method that allows for the formation of a uniform coating onto the surface of samples with high productivity and versatility. Briefly, EHDA consists of an epoxy resin embedded nozzle connected to both a power supply (Glassman High Voltage, Inc) and a 10 cc syringe pump (Harvard Apparatus, PHD 4400 Programmable) containing suspended NPs. The applied voltage (3.2 - 4.2 kV) creates an electrical field between the nozzle and the substrate, which allows for the formation of a uniquely shaped stable cone jet. Such a jet, together with a steady flow rate of 5 µL/min, is required to create a uniform spray which forms nano sized droplets that encapsulate the NPs. The spraying is carried out for 2 min with a 30 mm distance

between the tip of the nozzle and the substrate. Subsequently, the coated samples were heat treated at 500ºC for 1 h and allowed to cool gradually to help ensure the stability of the coating, allowing for mechanical integrity of the adhered NPs. The spraying time was defined based upon crack-formation on these surfaces. This was tested by looking for potential surface coating cracks using electron microscopy. The 2 min coating period produced a thin layer of coated NPs with no cracks.

The setup for electrohydrodynamic atomisation

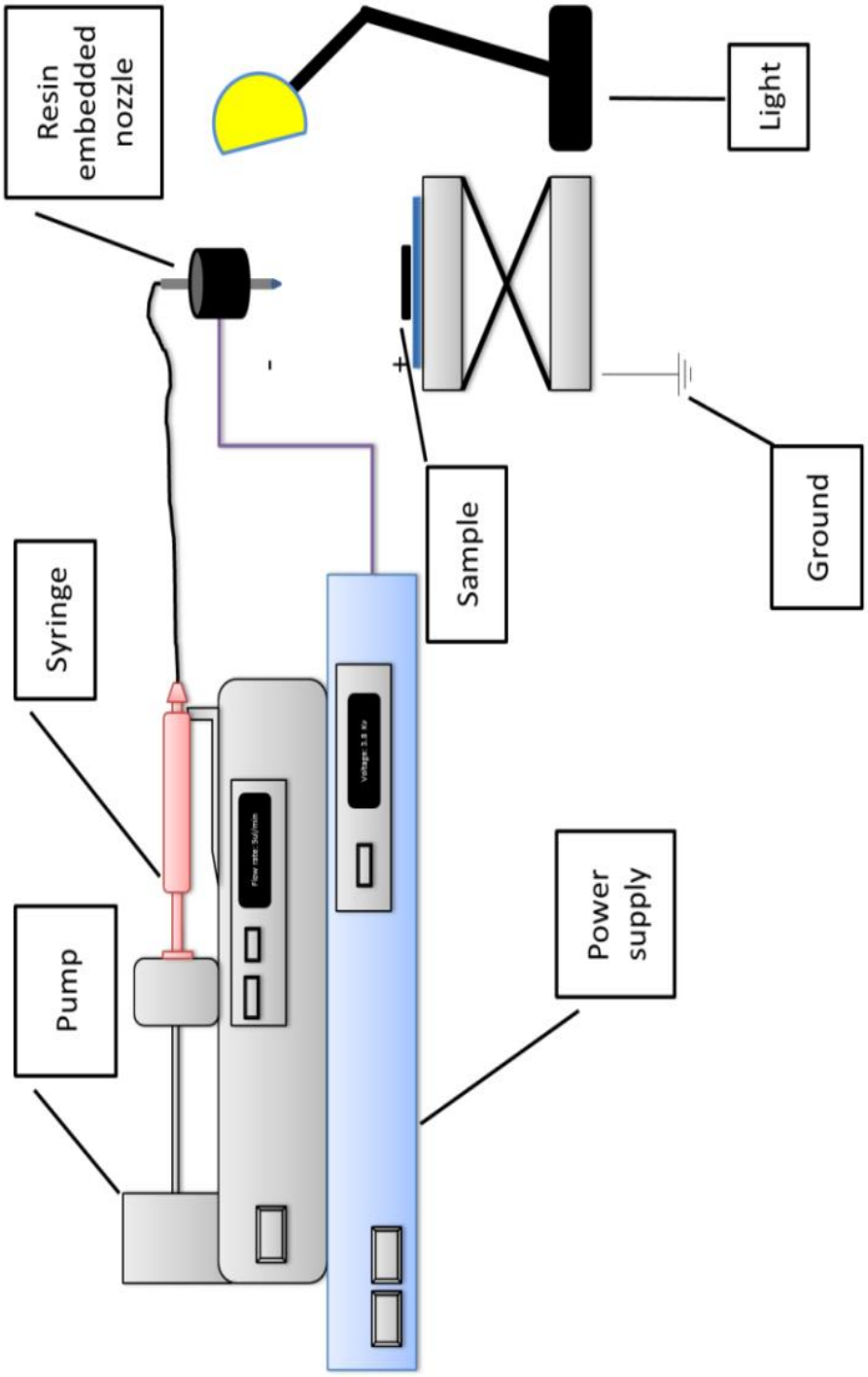

Figure 7 - Electrohydrodynamic deposition schematic illustration. From left to right: Syringe Pump, power supply to generate the electrical field between the needle and the Syringe filled with nanoparticles suspended in ethanol, ground connection for avoiding an electrical shock, the glass/metal sample (situated on top) and the substrate, nozzle and spraying process, Light source is also incorporated to provide a better visualisation of the spray.

2.6.2 Glass substrates

Glass slides and 13 mm coverslips were used in this study (VWR international). These slides were utilised for most studies whereas 13 mm circular glass coverslips (agar scientific, UK) were used for studies involving immunostaining. A diamond cutter pen was used to separate 1 cm^2 samples from each glass slide. In order to create sterilised substrates, each sample was dipped in 70% ethanol for a period of 1 min and air dried for 5 min before EHDA spraying. Various concentrations of nanoparticulate suspensions and nHA (in 100% ethanol) were made by calculating the nHA/NP ratio (1:1) and sonication before spraying. These concentrations ranged from 500 – 10,000 µg/mL for both NPs.

2.7 Nano-coated bactericidal samples

The spraying was carried out for 2 min with a fixed 30 mm distance between the tip of the nozzle and the substrate. Subsequently, the coated glass samples were heat treated at 500ºC (250ºC was used for 13 mm samples as they have a brittle nature and cannot survive higher temperatures) for 1 h and subsequently cooled in a gradual manner in order to ensure the mechanical integrity of the coating.

2.7.1 Bactericidal testing: samples in bacterial suspensions

The glass samples were coated with both nZnO and nWO_3 for periods of 2, 4, 6 and 8 min at 10,000 µg/mL. These were then sterilised using 70% ethanol placed in 3 mL volumes of PBS together with 37.5 µL of O.D. adjusted (0.1 at 54 nm, which equates to 10^6 CFU/mL) bacterial suspension (*S. aureus*). Samples were placed in a shaking

incubator at 37°C for 24 h. Dilutions of the suspensions (1:10) were performed, agar plates inoculated and colonies counted after overnight incubation at 37ºC in 10% CO_2.

2.7.2 Bactericidal testing: Bacterial suspensions on samples

The coated samples were dipped in 70% ethanol for 1 min and flamed to ensure sterility. Test species of bacteria were grown overnight in TSB at 37°C and 200 rpm. The O.D. of the bacterial suspension was adjusted to 0.1 at 540 nm in PBS or ABS (10^6 CFU/mL). A volume of 30 µL of the O.D. adjusted bacteria suspension was transferred onto the surface of the coated samples. As 30 µL is an extremely small volume of liquid, initial experiments displayed that once placed in an incubator; the liquid evaporates after only a few hours of incubation. Therefore a method was devised whereby a dampened cloth was placed next to the samples in order to create a humidified chamber. The samples were then placed in an incubator at 37ºC with 10% CO_2 for a period of 24 h. Subsequently each sample was carefully removed and placed in 3 mL of PBS. Approximately 5 glass beads were added to each tube to aid the detachment of the bacteria while vortexing (non-detrimental to bacteria) the tubes for a period of 30s at 2500 rpm. A volume 50 µL of the suspension was then removed and a 1:10 serial dilution performed. Neat (not diluted) and dilutions (1:10) were plated onto TSA plates and incubated for 24 h at 37ºC, 10% CO_2, after which colonies were counted.

2.7.3 Bactericidal testing: patterned coated samples

Custom made grids (agar scientific – 3.0 mm) with various internal patterned shapes were used in order to create diverse structural patterns. These patterns can be made on any surface and their thickness controlled by the timing and height of the coating process. The coating times for the present coatings were 2 and 5 min respectively. The 2 min coating time was used for antimicrobial tests and because visualising NPs is challenging under an optical microscope, the 5 min coating time was chosen. Each grid was carefully attached to a square shaped paper plate (1 cm^2) with four girds positioned at each of it extremities. The paper plate was positioned on top of the glass substrates. The regions covered by the grids would be coated and the rest remain uncoated.

2.8 NP characterisation

ZnO NPs were placed in 5 mL of distilled water and sonicated (Diagenode, Bioruptor) for 30s intervals at a high frequency setting in order to provide an even suspension. Carbon film grids (400 Mesh Cu, Agar Scientific) were briefly dipped into the nanoparticulate suspension and left at room temperature to air dry. This process allows for the NPs to be trapped within these grids and remain there for extended periods of time. The prepared grids were transferred into the Transmission Electron Microscope (TEM) through a vacuum chamber and each sample viewed and analysed.

2.9 Statistical analysis

One way ANOVA and student's t-Test (GraphPad Prism 5) were used to analyse all data and time-point comparisons. When $p < 0.05$, the analysis was considered statistically significant.

3. Results

3.1 Nanoparticulate characterisation

Synthesised NPs have various shapes and structures. Figure 8 highlights these unique structural characteristics for multiple NPs that were tested for their potential antimicrobial activity in the present study. Because NP size and shape are believed to be an important factor in instigating their antimicrobial activity (Sotiriou and Pratsinis, 2010), it is likely that these characteristics could also lead to their multifunctionality as antimicrobials targeting multiple microbial sites.

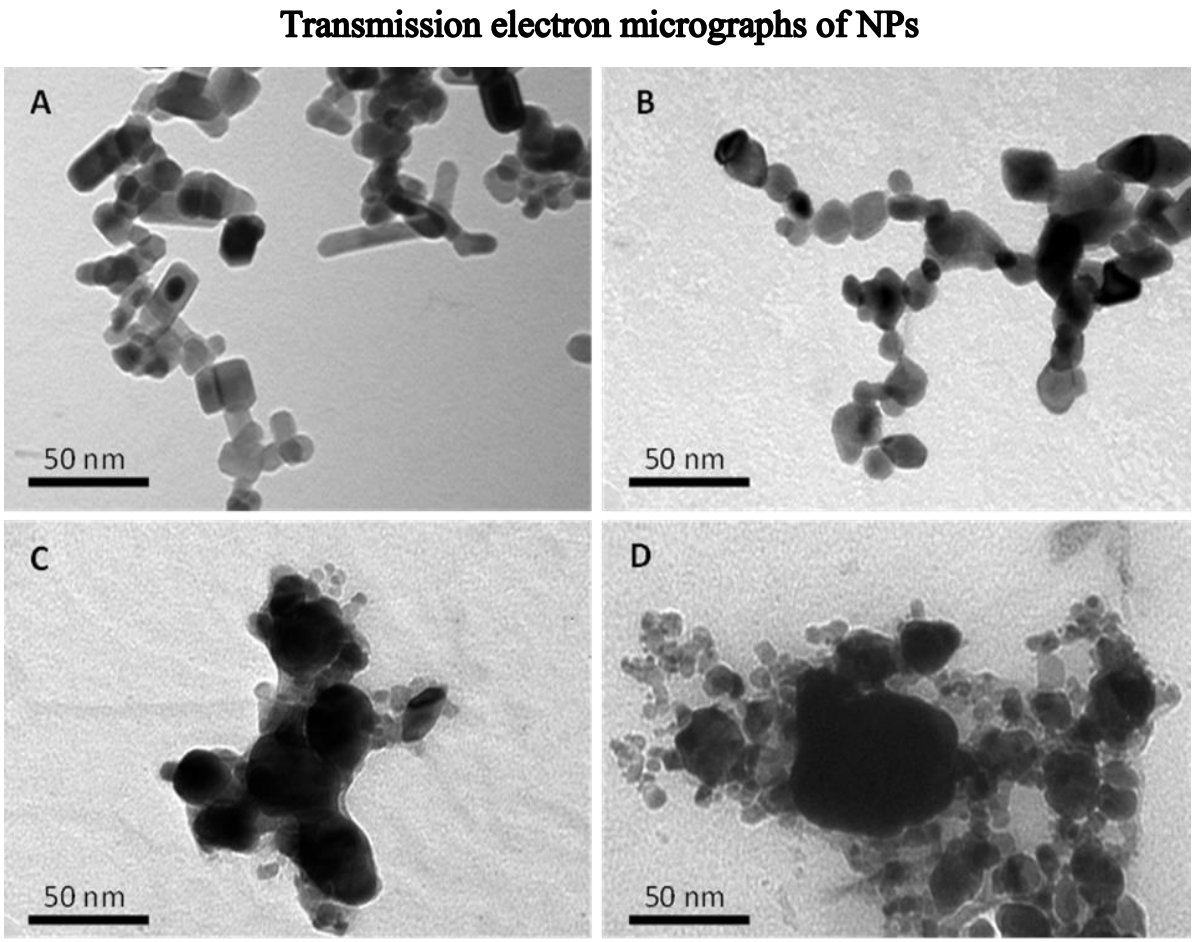

Figure 8 - Electron micrograph of numerous NPs. A)) Zinc Oxide (nZnO), B) tungsten oxide (nWO_3), C) nAg conjugated nZnO particulates and D) nAg conjugated nCuO particulates. The average sizes for all nanoparticulates are between 20 – 100 nm.

Initial observations indicate that the two mixtures of 70% nAg + 30% nZnO and 70% nAg + 30% nCuO were collectively comprised of bulky circular structures that were surrounded with smaller particles that are chemically attached to the larger particles. The sizes of the larger agglomerated regions were approximately equal to one another, whereas the smaller particles varied in size. For the 70% nAg + 30% nZnO particulates, the average size for the nAg agglomerations was 75 nm and the nZnO particles were between 10 and 50 nm. The second mixture that comprised of 70% nAg + 30% nCuO demonstrated altered features with agglomerated regions varying greatly in size (between 50 - 100 nm) and smaller copper oxide NPs measuring between 10-50 nm. The physical contrast between NPs is more transparent when both nZnO and nWO_3 are compared to one another.

While similarities exist between their sizes (on average between 20 – 100 nm), their structures are different. Whereas nWO_3 comprises of particles that possess a round shape, nZnO particles have rod-like and elongated structures that have sharp edges. This is further highlighted in Figure 9, where a comparison between nZnO and $nTiO_2$ is showcased. The $nTiO_2$ possess round shapes, similar in size to nZnO but lack sharp edged confirmations. Red triangles indicate round shaped TiO_2 particulates.

Comparison of electron micrographs of nZnO and $nTiO_2$

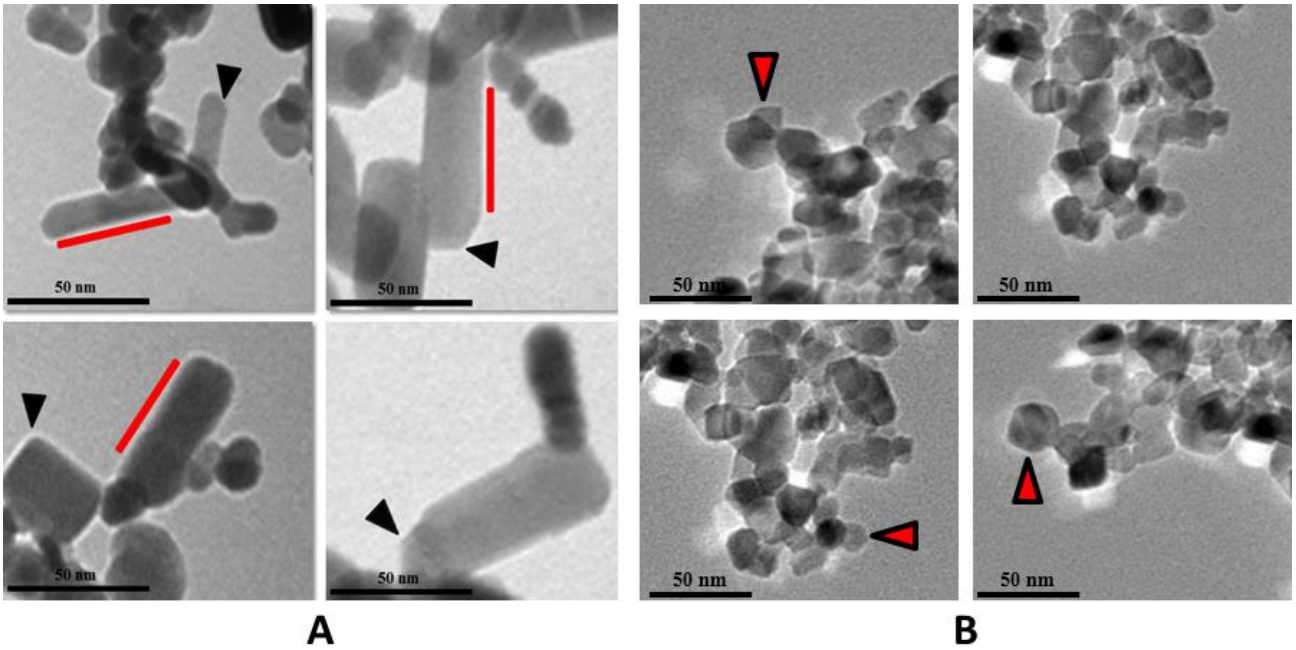

Figure 9 - Transmission electron micrograph of both ZnO (A) and TiO_2 (B) nanoparticles. A) Red lines indicate rod shaped structures of the NPs whereas the black triangles showcase the sharp edged particles. B) TiO_2 NPs are similar in size but lack sharp edged confirmations. Red triangles indicate round shaped TiO_2 particulates (Memarzadeh et al, 2014).

3.2 Antimicrobial studies

3.2.1 Minimum inhibitory (MIC) studies

Inhibitory concentrations of NPs indicate an overall antimicrobial superiority of the conjugated nanoparticulates. MIC values against all species of bacteria were comparatively high (> 500 µg/mL) with the exception of the chemically modified mixtures of nAg and nCuO. Cupric oxide NPs demonstrated an increased inhibitory activity towards most bacterial species closely followed by the zinc oxide NPs (Table 2). The tungsten oxide NPs demonstrated their bactericidal effects at 2500 µg/mL, the highest concentration of NPs used in this experiment.

3.2.2 Minimum bactericidal (MBC) studies

Similar patterns were observed when the MBC for each NP was determined with the composites having the greatest bactericidal effect. As with other antimicrobial agents the concentration required to kill is generally found to be greater than that required to inhibit growth (Table 2).

These findings indicate that there was no underlying specific selectivity towards any of the two gram-negative (*E. coli* & *P. aeruginosa*) and gram-positive (*S. aureus* & *S. epidermidis*) by any of the NPs presented in this study.

Minimum inhibitory and bactericidal concentrations of NPs

MIC µg/mL	nZnO	70% wt Ag + nZnO	70% wt Ag + CuO	CuO	WO_3
Staphylococcus aureus	>2500	1000	500	500	2500
Staphylococcus epidermidis	2500	1000	250	500	2500
Escherichia coli	2500	1000	250	500	2500
Pseudomonas aeruginosa	1000	500	<100	500	2500

MBC µg/mL	nZnO	70% wt Ag + nZnO	70% wt Ag + CuO	CuO	WO_3
Staphylococcus aureus	2500	1000	2500	500	2500
Staphylococcus epidermidis	>2500	1000	1000	>2500	2500
Escherichia coli	>2500	1000	1000	1000	2500
Pseudomonas aeruginosa	2500	>2500	500	>2500	2500

Table 2 - Minimum inhibitory concentration (MIC) and minimum bactericidal concentration (MBC) values (µg/mL) for nZnO, nCuO, nWO_3, as well as novel mixtures of nAg with nCuO and nZnO against four different species of bacteria. Nano-TiO_2 is thought to be antimicrobial when exposed to ultraviolet light and therefore not used in this experiment.

3.2.3 Agar-based bactericidal study

For comparative purposes, *S. aureus* and *E. coli* were used in this experiment. Qualitative assessments of the drop-based bactericidal studies indicate that all positive controls exhibited full growth and all negative controls exhibited no growth. Results for both nZnO and the nAg, nZnO composite indicated bactericidal activity for all applied concentrations (250, 500, 1000 and 2500 µg/mL) against both tested species of bacteria. Contrary to these findings, nWO_3 did not show any bactericidal activity against *E. coli* and *S. aureus*. It is important to note that despite this total growth, when exposed to 2500 µg/mL, the bacterial growth was not as prominent as compared to preceding concentrations and instead of forming regions of growth that are approximately 0.5 cm in diameter, there were clusters of individual colonies forming on the plate (Figure 10).

3.2.4 Optimisation of time based bactericidal assays

An initial test to observe the bactericidal efficiency of specific nanoparticulates within a given time period and a given environment was devised. 70%nAg + 30 % nZnO was tested against both *S. aureus* and *E. coli* (Figure 11 and 12) respectively. Apart from the significant ($p < 0.01$) antimicrobial activity of this nanoparticulate against both species, these findings allowed for further investigation of the current method. As regards to the antimicrobial activity of this novel mixture, there was a strong antimicrobial activity against both bacteria after the second hour of incubation. This was more evident for the bactericidal effect of this mixture against *S. aureus* (Figure 11).

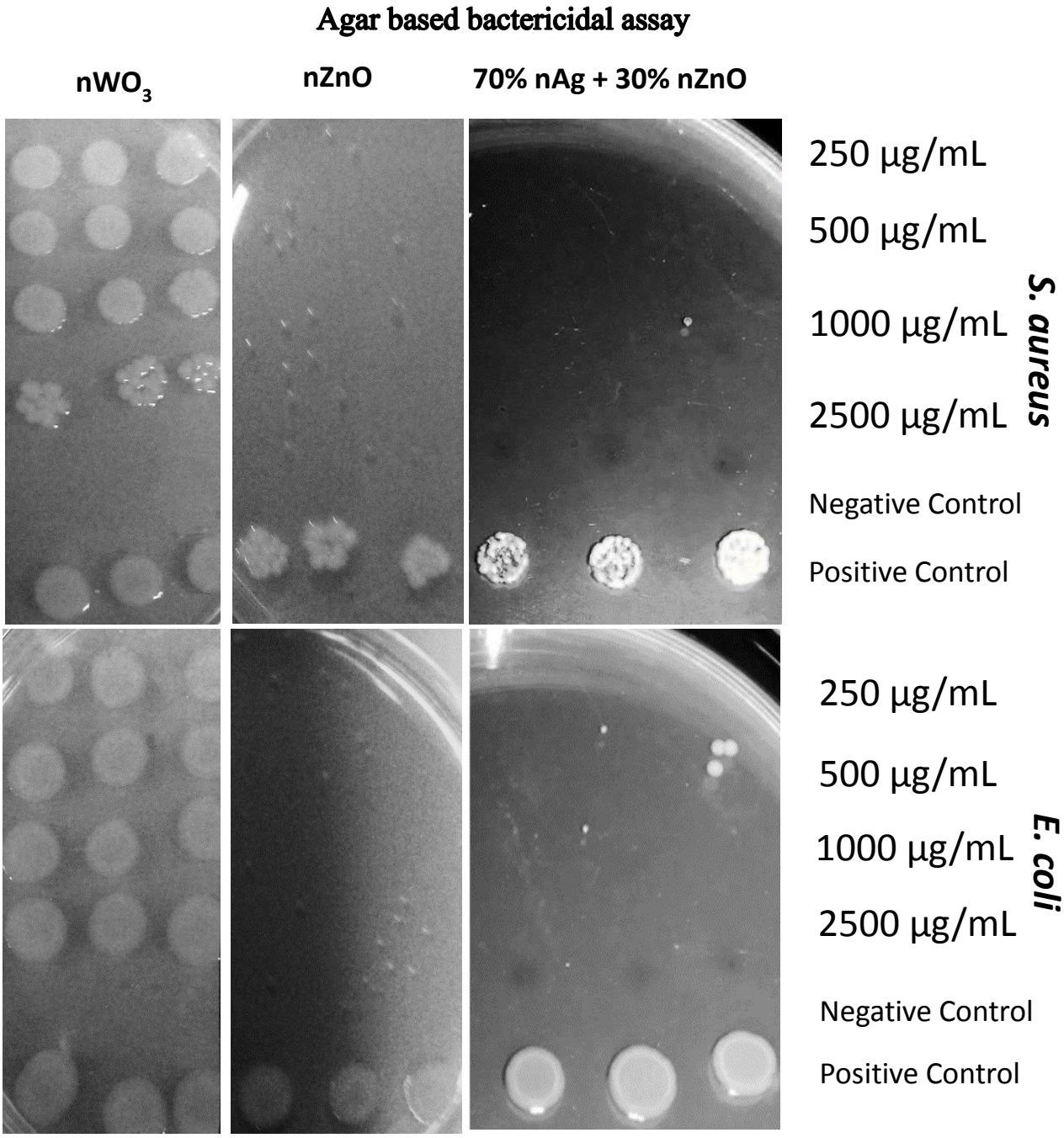

Figure 10 - Comparison of the bactericidal activity of tungsten oxide (nWO_3), Zinc oxide (nZnO) and nZnO mixed with nAg (70% nAg + 30% nZnO). Various concentrations of NPs were exposed to an O.D adjusted suspension of bacteria (*S. aureus* or *E. coli*) and cultured on TSA plates for comparative purposes. Bacteria containing supernatants for all concentrations of NPs (250 µg/mL, 500 µg/mL, 1000 µg/mL and 2500 µg/mL) were placed on TSA plates. Their growth was compared to the negative (no bacterial growth) and positive (total bacterial growth) control. TSA plates were placed at 37°C with 10% CO_2.

Bactericidal activity of 70% nAg + 30% nZnO against *S. aureus* and *E. coli*

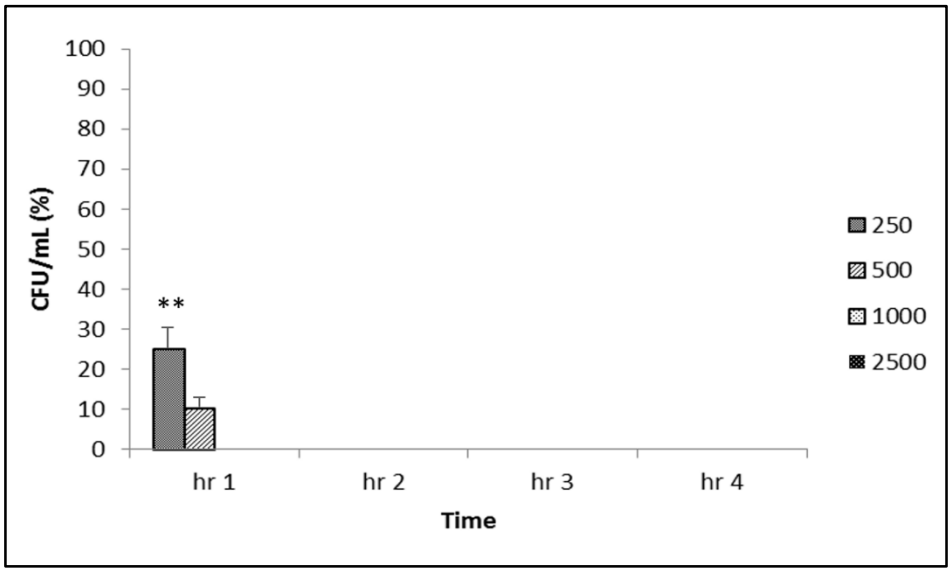

Figure 11 - The bactericidal activity of 70% nAg + 30% nZnO in PBS against *S. aureus*. The concentrations of NPs were exposed to suspended bacteria in PBS for 1, 2, 3 and 4 hours. All percentages are compared to the control. n = 3, ±SEM, ** = $p < 0.01$

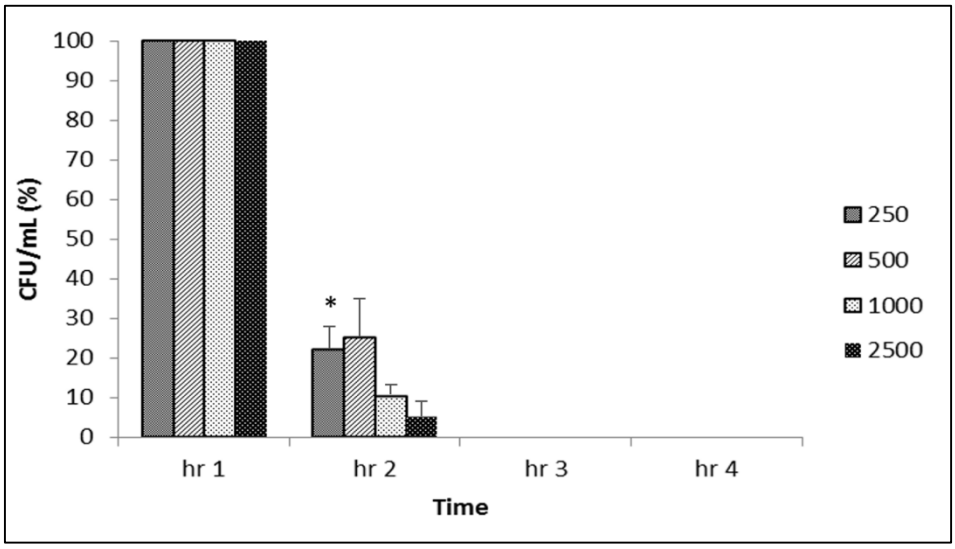

Figure 12 - The antimicrobial activity of 70% nAg + 30 %nZnO in PBS against *E.coli*. There is a significant reduction in bacterial survival after exposure to all concentrations of NPs. n =3, ±SEM, * = $p < 0.05$.

Because of an observed bactericidal effect of nWO_3 (MIC = 2500 µg/mL) in the initial MIC and MBC investigations, the need to further investigate the antimicrobial potential of nWO_3 was investigated. The rationale behind carrying out a time based antimicrobial study was to further investigate selected nanoparticulates for their antimicrobial activity, before selection and their application onto a coated substrate. At the time of writing this work, of all tested NPs, both nWO_3 and nZnO were significantly less studied as compared with other commercially available NPs such as silver and copper. Further investigations into the bactericidal of nWO_3 showed that all concentrations of this nanoparticulate tested were seldom bactericidal in timed-based killing assays, over a period of 4 h, confirming the previous finding and contradicting the initial results obtained in the MIC and MBC investigations which showed antimicrobial activity at 2500 µg/mL. As the NPs in suspension were exposed to both *S. aureus* and *E. coli*, no significant change was observed at each hour (Figures 13 and 14). ZnO NPs were selected as the most effective antimicrobial agent in the current setting of experiments. Nano-Ag has been used for multiple purposes in many fields and so was not investigated further, the over-use of silver can lead to future antimicrobial resistance (Silver, 2003, Percival et al., 2005). Furthermore, CuO is widely known to be toxic to human cells (Karlsson et al., 2008, Hanagata et al., 2011) and $nTiO_2$ is not a strong antimicrobial agent (Figure 15) and only antimicrobial under certain conditions(Brunet et al., 2009). After validating the physical characteristics and elemental composition of nZnO powder (Figure 16), both *E. coli* and *S. aureus* were exposed to suspension of nZnO particles under different nutritional environments. These species were chosen because of their ever increasing importance as the main emerging pathogens with respect to health-related infections.

Bactericidal activity of nWO_3 against *S. aureus* and *E. coli*

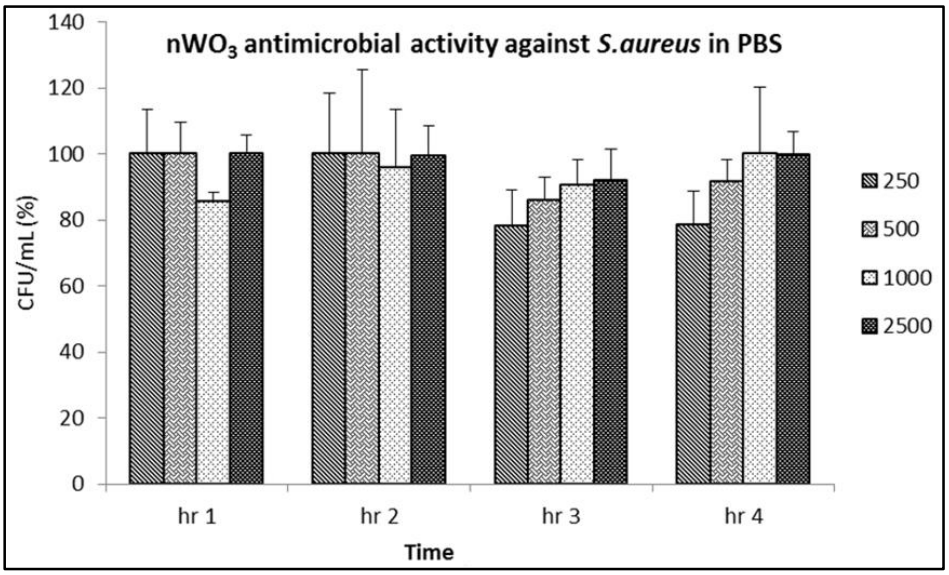

Figure 13 - The effect of different concentrations (µg/mL) of nWO_3 against *S. aureus* suspended in phosphate buffered saline. The antimicrobial activity was observed at each successive hour for a period of 4 hours. n =3, ±SEM

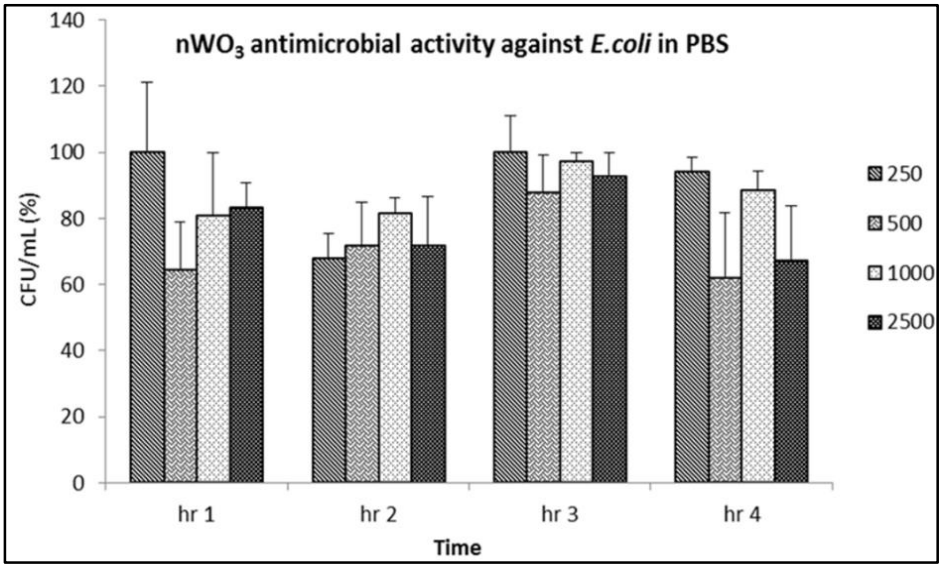

Figure 14 - The effect of different concentrations (µg/mL) of nWO_3 against *E. coli* suspended in phosphate buffered saline. Limited antimicrobial activity was observed at each successive hour for a period of 4 hours. n = 3, ±SEM

Bactericidal activity of $nTiO_2$ against *S. aureus* and *E. coli*

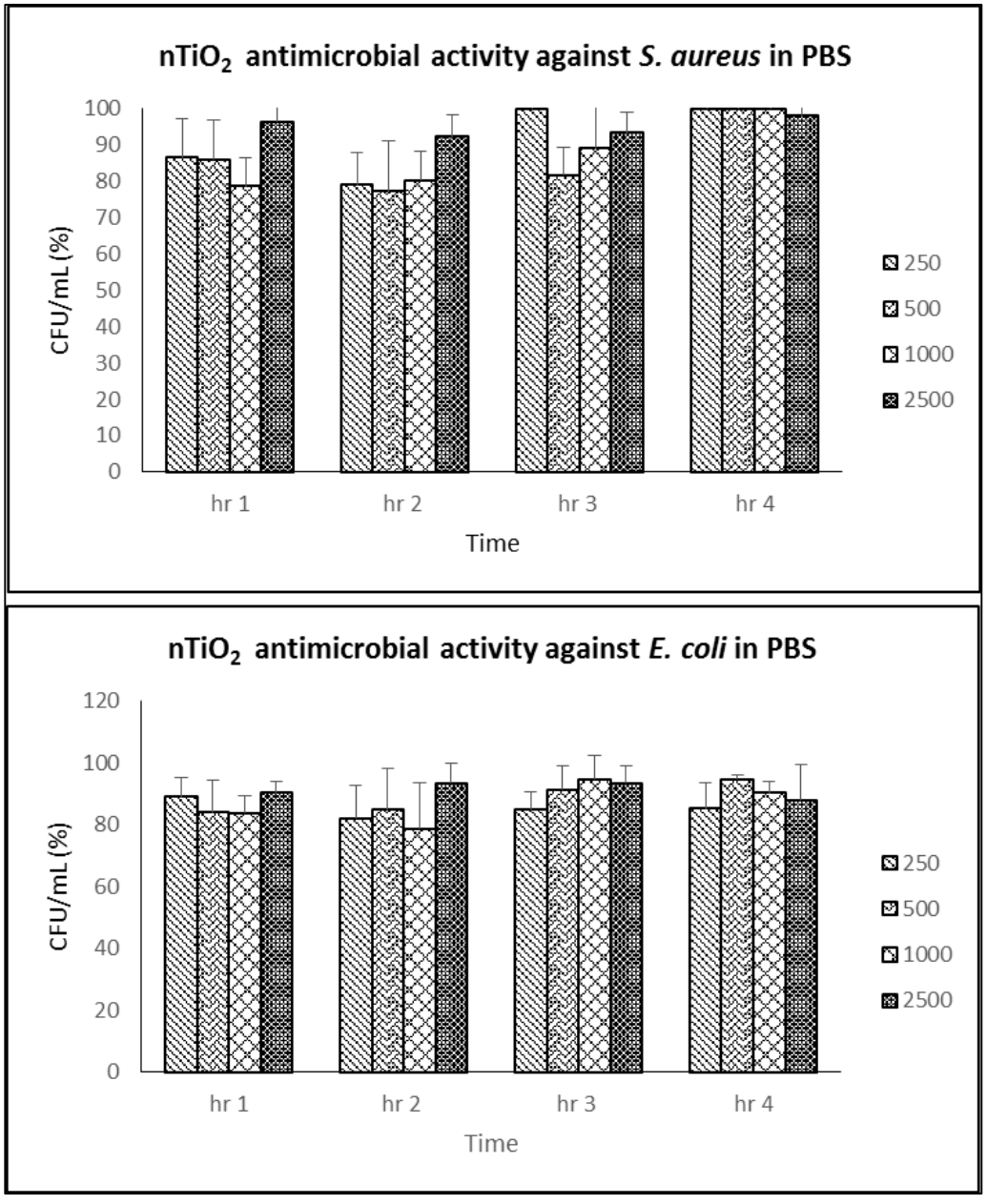

Figure 15 - The effect of different concentrations (µg/mL) of $nTiO_2$ against *S. aureus* and *E. coli* suspended in PBS. Limited or no antimicrobial activity was observed at each successive time period for a period of 4 hours. n = 3, ±SEM

Energy-dispersive x-ray spectroscopy of nZnO powder

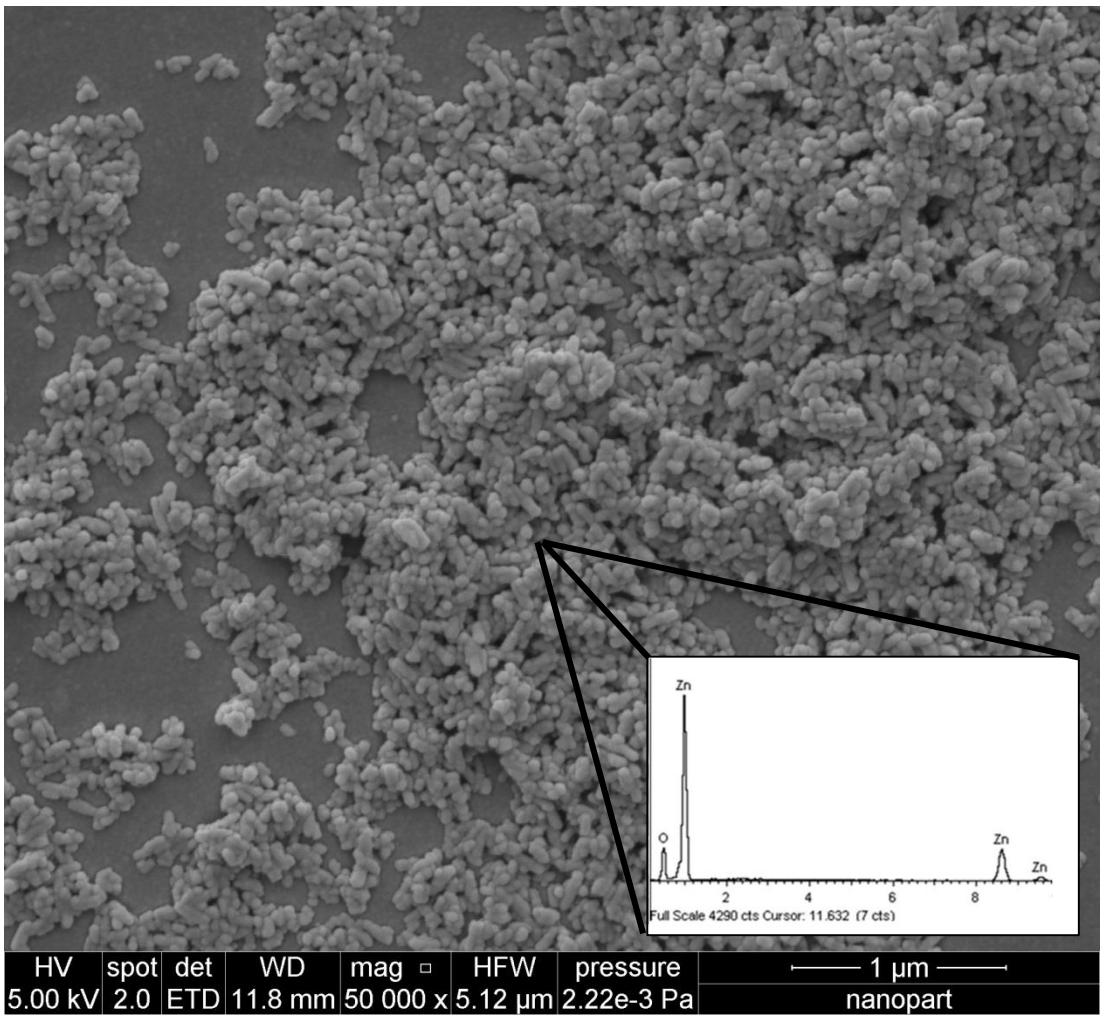

Figure 16 - The nZnO powder was tested for its purity by utilising EDX (Energy-dispersive X-ray spectroscopy) via scanning electron microscopy. The spectrum indicates the purity, with no other element present except that of Zn and O.

3.2.4 (a) Time based bactericidal activity: nZnO + *S. aureus* and *E. coli* (PBS)

Nano-ZnO particles were used under two different nutritional environments (PBS or ABS) and their bactericidal activity was quantified over time. When PBS suspended nZnO was exposed to *S. aureus*, there was a steady reduction in its survival (Figure 17 & 18). Testing under different environmental factors allows for analysis of bacterial growth under multiple nutritional conditions, providing insight on how they thrive depending on environmental conditions. Figure 17 describes the antimicrobial activity of the suspended nanoparticles as a percentage of the control, while figure 18 depicts the change in population of NP-bacteria as compared to the control. The control in all the following time-based studies consists of bacterial suspensions (in any medium) without the presence of NPs.

Time-based bactericidal effect of nZnO

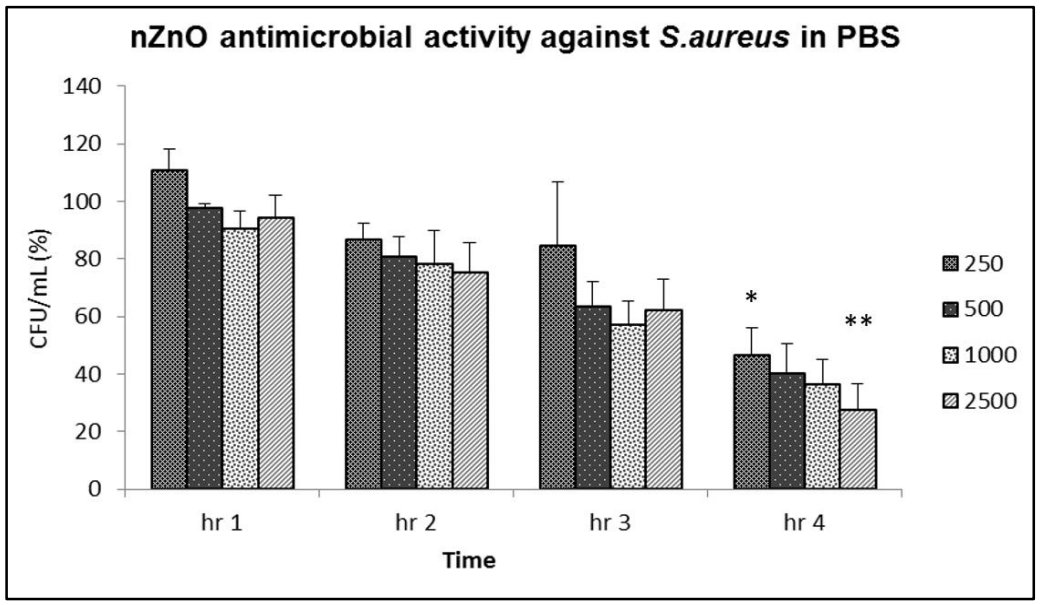

Figure 17 - The effect of nZnO particles against *S. aureus* suspended in phosphate buffered saline. The different concentrations of NPs (µg/mL) were in suspension with bacteria for a period of 4 hours. The population of bacteria has been calculated (each hour) as a percentage of control (CFU/mL), n=3, ±SEM, * = $p < 0.05$, ** = $p < 0.01$.

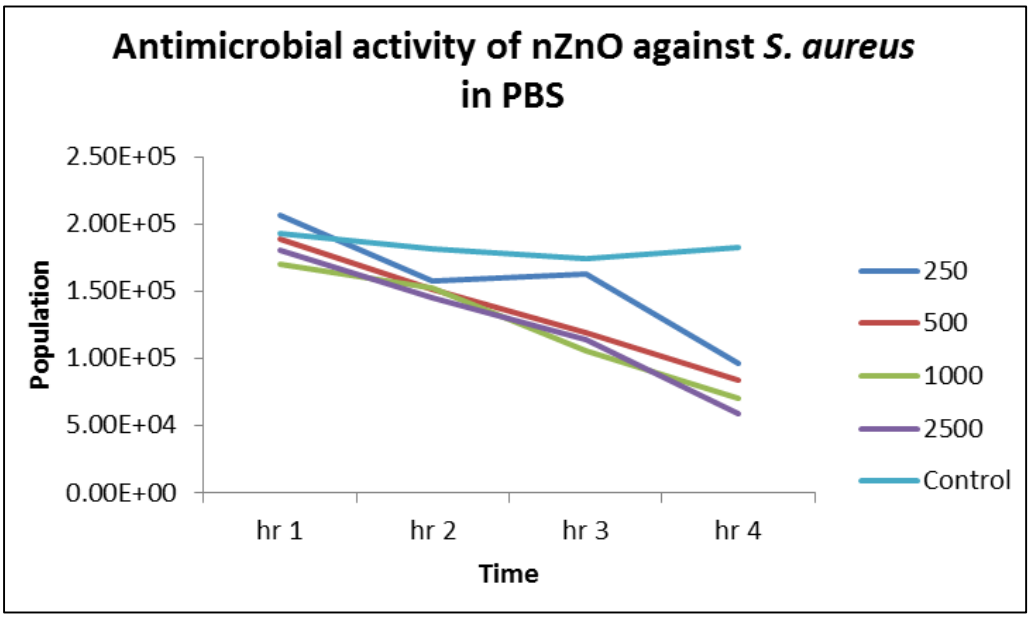

Figure 18 - The bacterial population (in PBS) declines for all nanoparticulate suspensions tested; the control remains almost constant during the 4 hour period, n=3.

Furthermore it was observed that in general as the concentration of nZnO increases, bacterial survival decreases (Figure 17). The control kept relatively constant throughout the four hours, so allowing an accurate insight into how nZnO is able to reduce the population of bacteria. Nano-ZnO particulates were less active against *E. coli*, as evident from an undefined bactericidal structure of its activity (Figure 19 and 20). While there was a general trend of decline in the *E. coli* population with an almost constant control, the lower concentrations of nZnO appeared to elicit a greater effect compared to the higher concentrations, indicating no dose dependent behaviour when compared to nZnO. Furthermore, it is important to state that multiple concentrations of NPs (250 µg/mL and 1000 µg/mL) lose their antimicrobial activity after four hours of incubation. All studies were performed for over 4 hours to provide bacteria with relatively sufficient time to grow and also for NPs to have a time window within which observations can be made as regards to their nature of antimicrobial activity.

Time-based bactericidal effect of nZnO

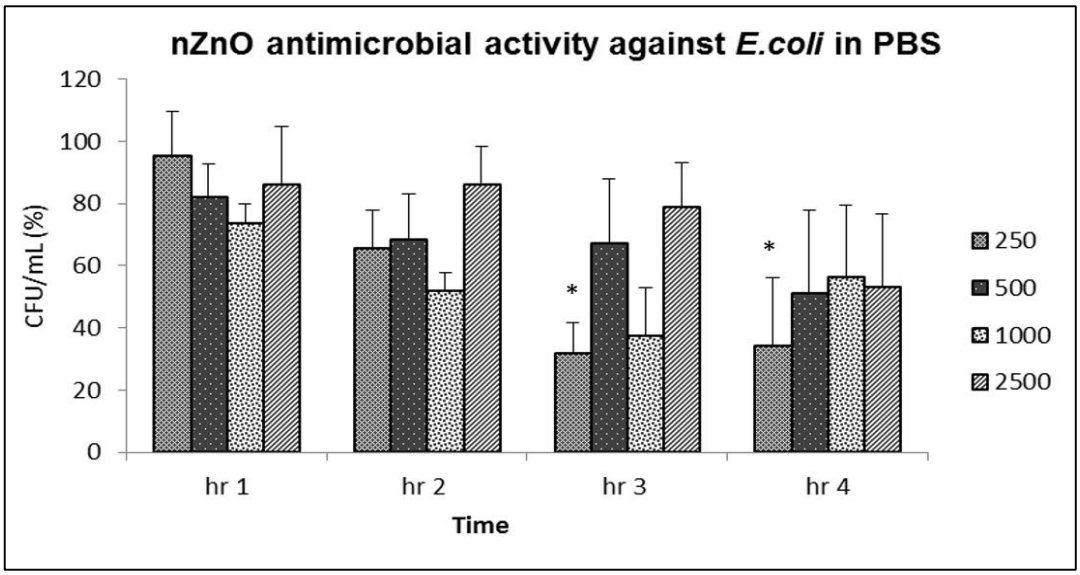

Figure 19 - The effect of nZnO particles against *E. coli* suspended in phosphate buffered saline. The different concentrations of NPs (µg/mL) are in suspension with bacteria for a period of 4 hours. The population of bacteria has been calculated (each hour) as a percentage of control (CFU/mL), n=3, ±SEM, * = $p < 0.05$.

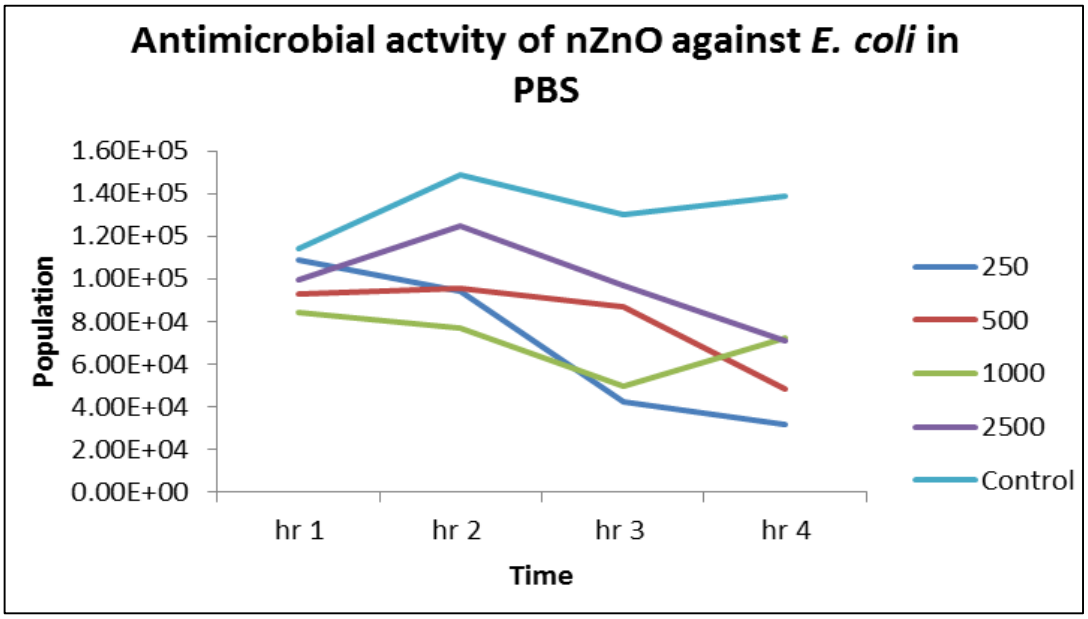

Figure 20 - Plot of microbial populations. Control is unaltered and with increasing concentrations as the population of bacteria decrease over time, with the lowest concentration showing the largest decline. n =3.

3.2.4 (b) Time based bactericidal activity: nZnO + *S. aureus* and *E. coli* (ABS)

Nutritionally rich environments provide an opportunity to allow sufficient bacterial growth, this in turn allows for a better measurement of bactericidal activity of NPs in an environment where bacteria thrive and grow. Studies based upon these concepts indicate a significant increase level of bacterial growth for the provided controls (Figures 21 and 22). As the control culture grows the population of *S. aureus* remains relatively unchanged. However when the bacterial population is observed as a percentage of control at each stage of the experiment (Figure 22), it becomes evident that these NPs greatly reduce the bacterial population ($p < 0.05$).

Time-based bactericidal effect of nZnO

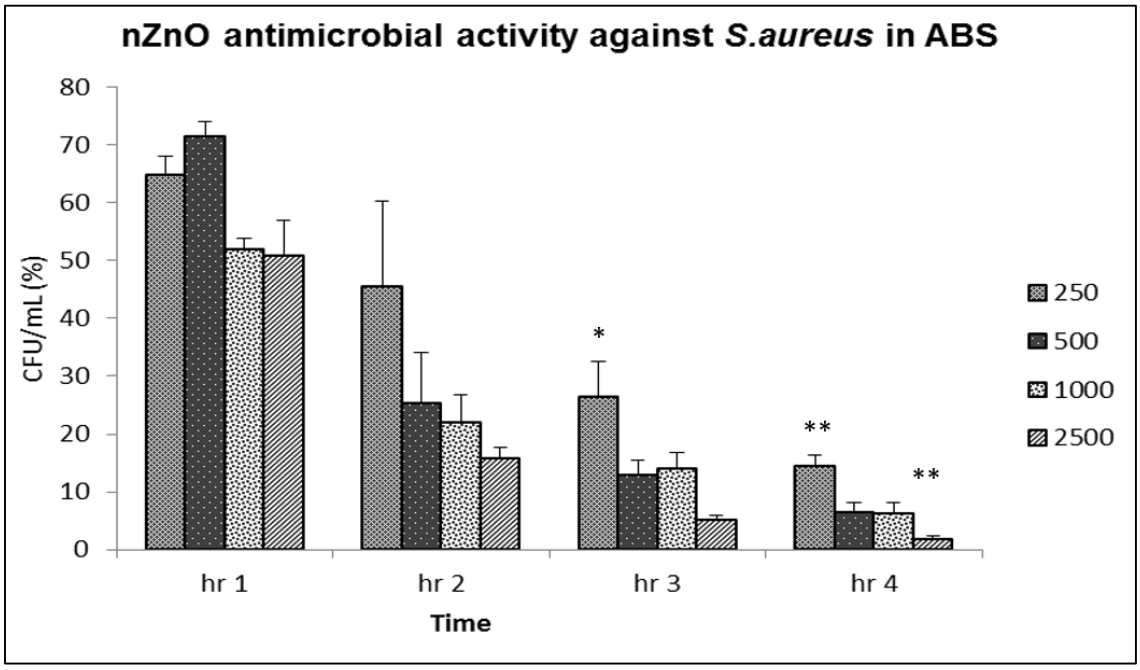

Figure 21 - Antimicrobial properties of different concentrations of nZnO against *S. aureus* over a fixed period of time. Histograms represent the gradual decline of the population of ABS-suspended bacteria. n=3, ±SEM, * = $p < 0.05$, ** = $p < 0.01$, *** = $p < 0.001$.

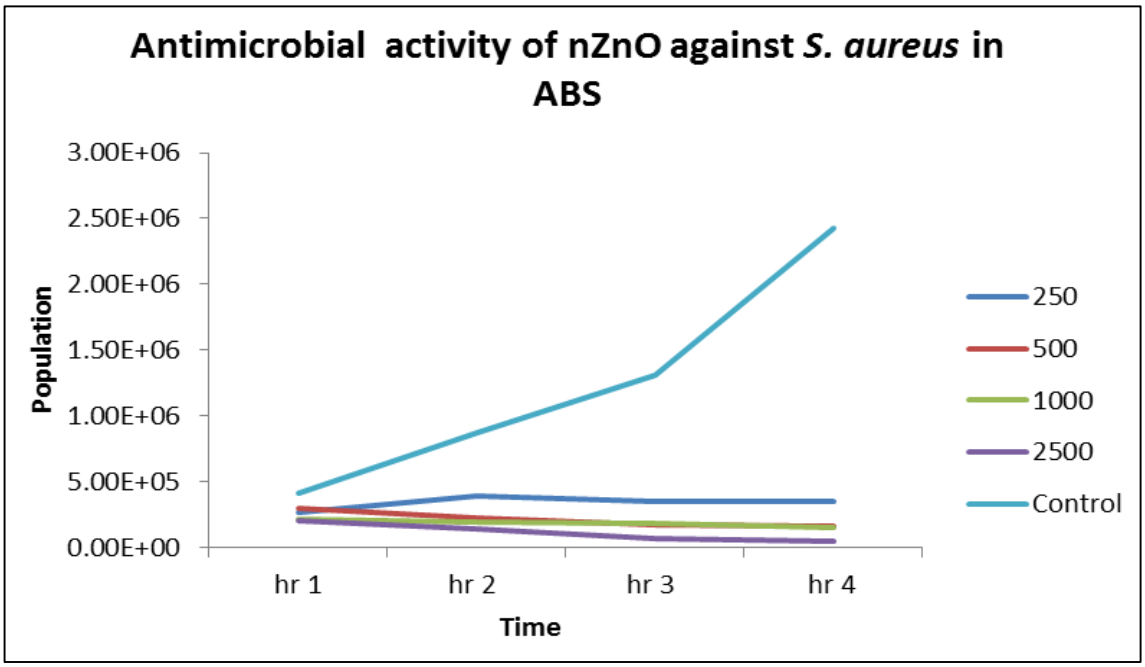

Figure 22 - Comparison of the bacterial populations in each nanoparticulate suspension against time. The bacterial population control rises as the NP-suspended bacteria remain dormant or decrease in population, n =3.

Time-based bactericidal effect of nZnO

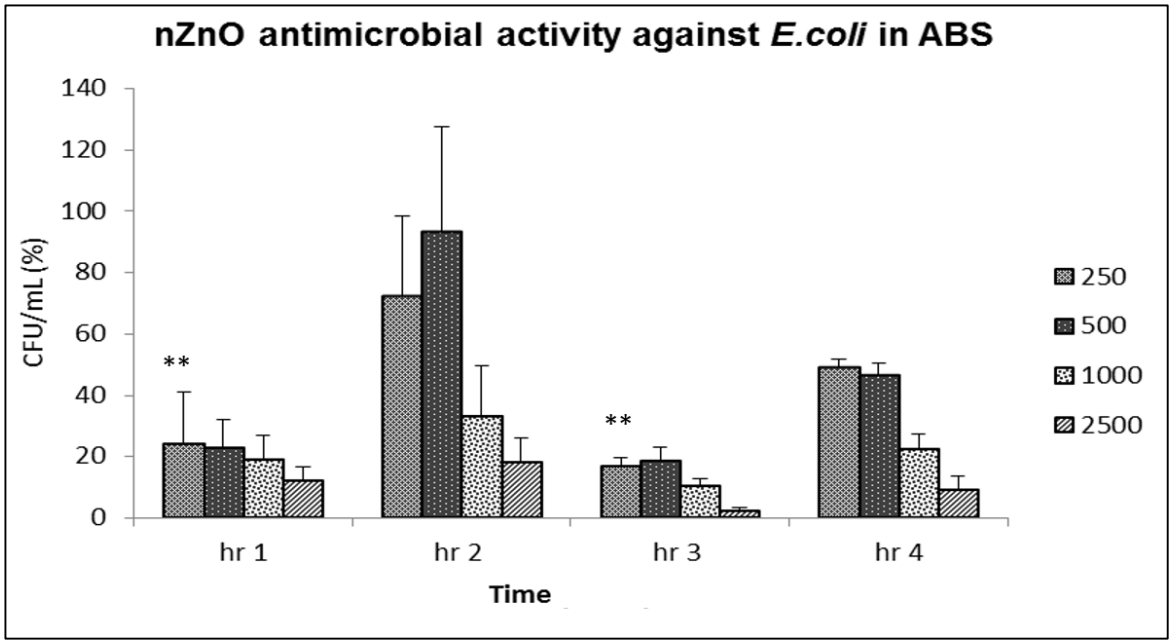

Figure 23 - The antimicrobial activity of nZnO against *E. coli* suspended in adult bovine serum. The activity of different concentrations of ZnO nanoparticles in a period of 4 hours (CFU/ml (%)), n =3, ±SEM, ** = $p < 0.01$.

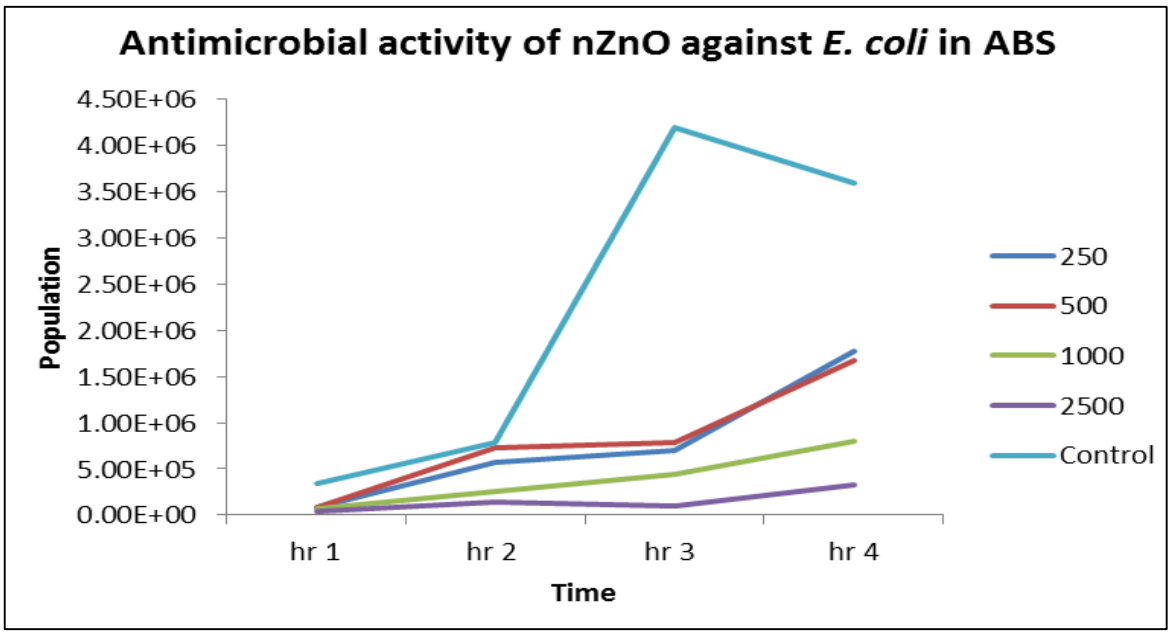

Figure 24 - The control has grown rapidly following 3 hour incubation. nZnO particles appear to have an inhibitory effect under these conditions. However increasing growth can be observed after 4 hours of incubation, n=3.

While similar growth patterns were observed in this experiment as compared to the effect of nZnO on *S. aureus*, the bactericidal effects against *E.coli* (Figure 23) indicates that there was a gradual increase in bacterial population that became prominent ($p < 0.05$) after 2 h of incubation and then significantly declined as bacterial growth in the control declined (Figure 24). While growth for both species of bacteria is less than that of control, results indicate that in both studies, there is a clear nZnO is more effective against *S. aureus*.

3.3 Coating

3.3.1 Optimisation of the EHDA spraying process

As highlighted previously, the initial step in order to create a suitable coating was to observe the relevant parameters and choose a suitable a scenario where an appropriate setting for the desired outcome is achieved. By varying different parameters such as the voltage applied to the nozzle, the distance between the nozzle and the substrate and the flow rate of the nanoparticulate suspensions, the deposition area change. Figure 25 highlight the experimental stages that lead to an understanding of the relationship between voltage, distance and the relative size of the "circular like" deposition regions.

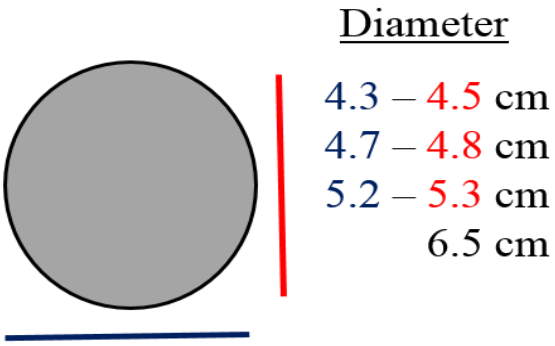

Figure 25 – Measurements taken of the diameter of the almost circular nature of the nZnO coated surface. Most measurements are approximately equivalent and therefore it can be assumed that the coated region created by spray is circular-like in shape. The two numbers in each row represent measurements taken from each side of the coating area (depicted in different colours) and the last measurement (6.5 cm) represent the diameter of fully circular coating region.

These variables (height and voltage) are also highlighted in Table 3 and their direct effect on the coating area diameter is shown in Figure 25 as a linear relationship. Furthermore findings suggest that (assuming the nozzle diameter is constant), as the distance of the nozzle from the sample increases, the diameter and dispersion of the NP suspensions also increase. Indeed further findings show that voltage applied to three different NP suspensions (nHA, nZnO and $nTiO_2$) at different heights can slightly differ, however this difference was not found to be significant.

Coating surface parameters

Table 3 – The distance between the substrate and the nozzle, as well as the voltage applied to the suspension determines the different rounded shapes produced upon the silicon wafer.

Coating Diameter (cm)	Height (mm)	Voltage (kV)
2.35	10	2.9 - 3.5
4.7	20	3.5 - 4.1
7.2	30	4.1 - 5.1
9.6	40	5.1

For the purpose of the current study a distance of 30 mm and a voltage of 3.8 - 4.1 kV (A uniform cone-jet spray is formed at this voltage range) was chosen as the standard for all coatings. This 30 mm distance allows for a full coverage of a thin NP based coating on multiple samples (Figure 27). Furthermore, this coating process also allows for multiple samples to be placed underneath the deposition area and therefore the relative thickness of the coating can be deduced (Figure 26).

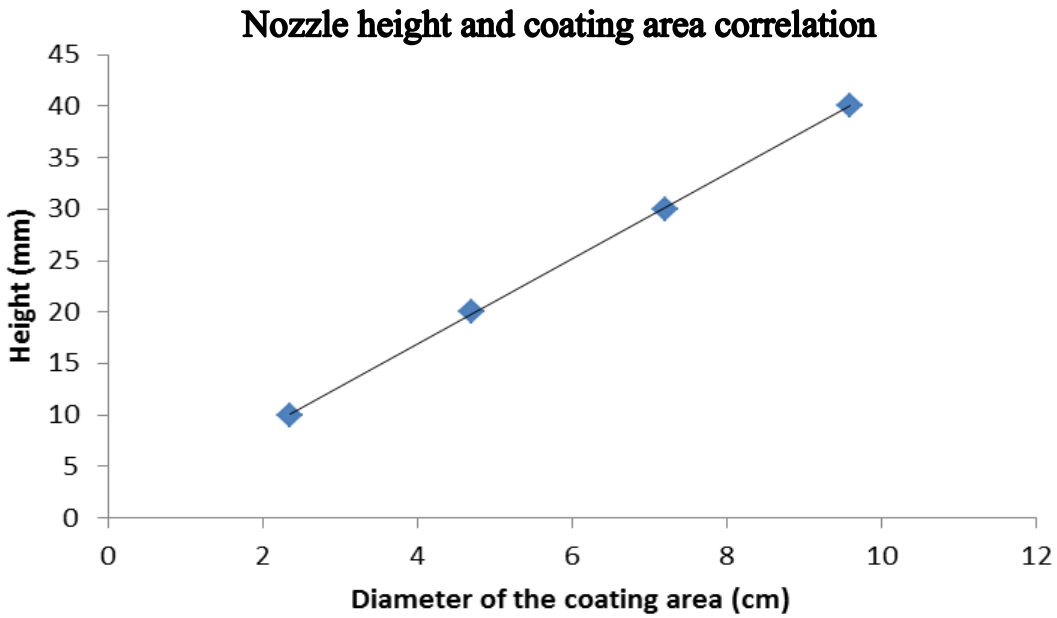

Figure 26 - The linear relationship between height of the nozzle from the substrate and the diameter of the coated area. As the height increases, the diameter of the coated area also increases. This property can be used to control the coating area as well as determining the maximum number of samples that are ought to be coated.

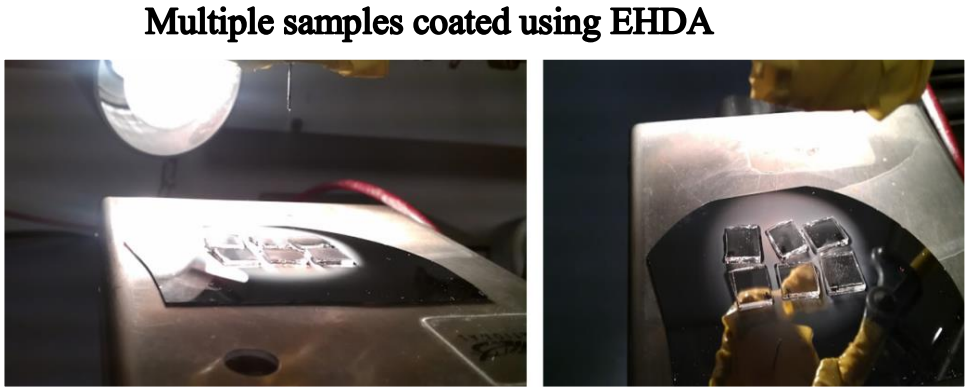

Figure 27 - The above images show 1 cm^2 glass samples being coated. The coating area is visible below the samples. This area can vary based upon different parameters utilised during the process.

3.3.2 Mechanical integrity

In order to determine the thickness of the film coated on substrates, initially, titanium samples were coated with nZnO using different lengths of time (2, 4, 6 and 8 min).

Upon investigation using scanning electron microscopy, samples coated for 2 min at a flow rate of 5 µL/min, with a concentration of 10,000 µg/mL, formed a rather thin layer of film on the Ti samples. This coating film did not demonstrate major physical fissures (cracked structures) on its surface; this is in contrast with samples that were coated for 4 and 6 min, respectively, where cracks were appearing. The formation of cracks was identified as major irregularities that appeared on the surface of the coating samples, identified as red marks in figure 28. The agglomerations present on the surface of Ti samples increased as the coating time increased and therefore the cracks were not so apparent on surface analysis of samples that were coated for more than 6 min (Figure 28).

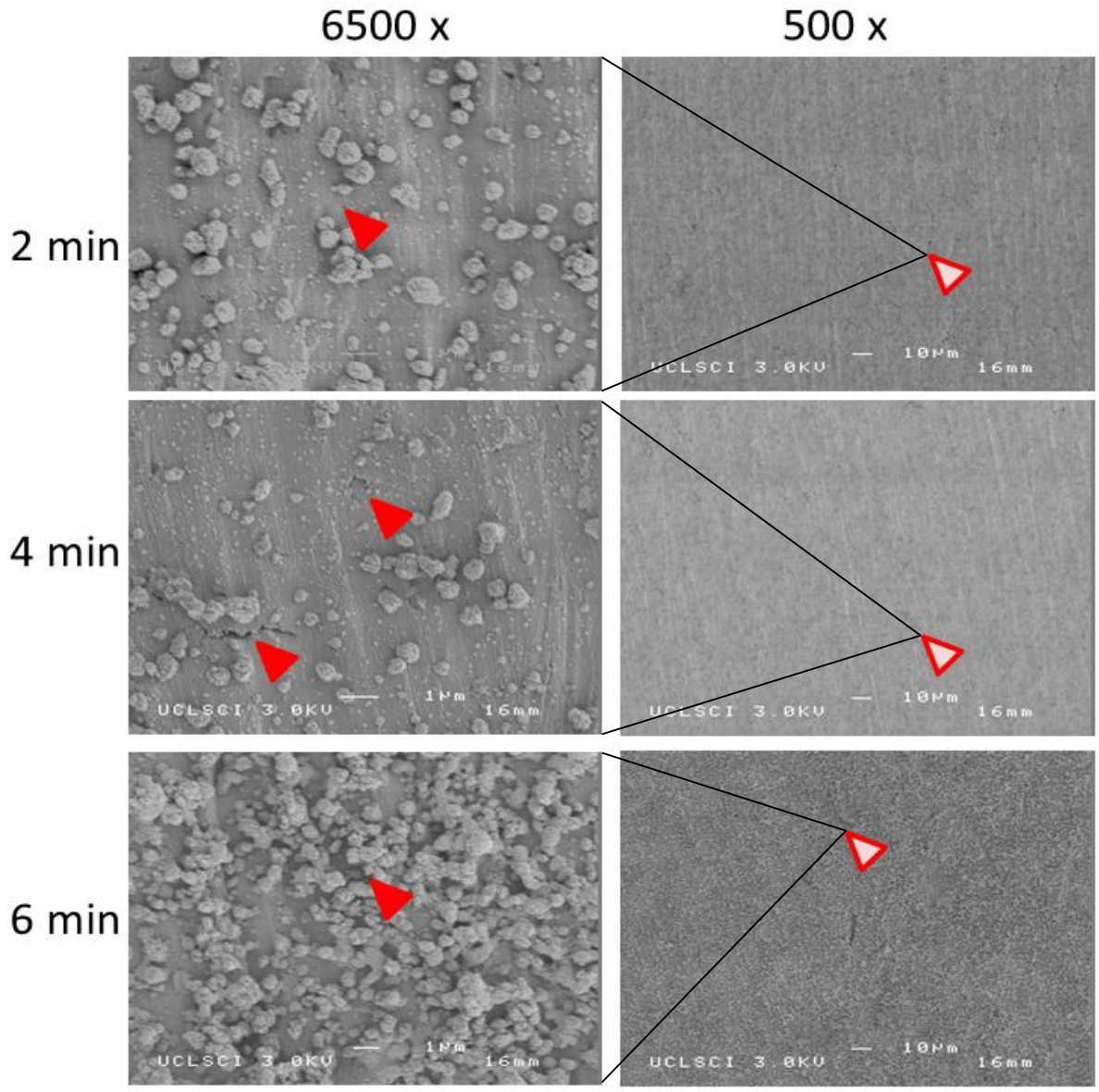

Figure 28 - nano-ZnO coated Ti surface. Highlighting the physical change between different coating times. The red arrows (on the left) indicate the regions where cracks have formed and arrows with outlined red lines indicate regions with lower magnifications. Cracks are not visible when observed at low magnifications (Black lines represent magnified areas).

3.3.3 Antimicrobial activity of coated samples: immersed in bacterial suspension

To further validate findings as regards to the length of the coating procedure and in order to further test the antimicrobial potential of coated samples, a study was devised where glass samples, (both nWO_3 and nZnO) coated for different time periods were tested against *S. aureus*. The findings confirm previous results, showing that nWO_3 is highly unlikely to be antimicrobial. In terms of the antimicrobial activity of nZnO, there is a significant ($p < 0.05$) difference between the non-coated and the coated samples. It has to be stressed that while this antimicrobial effect is valid and the coating is bactericidal, it does not represent what occurs on the surface, meaning that there is no possible direct contact with suspended bacteria. Additionally, this antimicrobial activity provides evidence for prolonged coating of NPs and hints that a thicker coating may slowly compromise the antimicrobial potential of the coated substrates, as samples coated for 8 min were less antimicrobial as compared to samples coated for a shorter time period (Figure 29 and 30).

Coated nWO3 and nZnO: an antimicrobial comparison over 24h

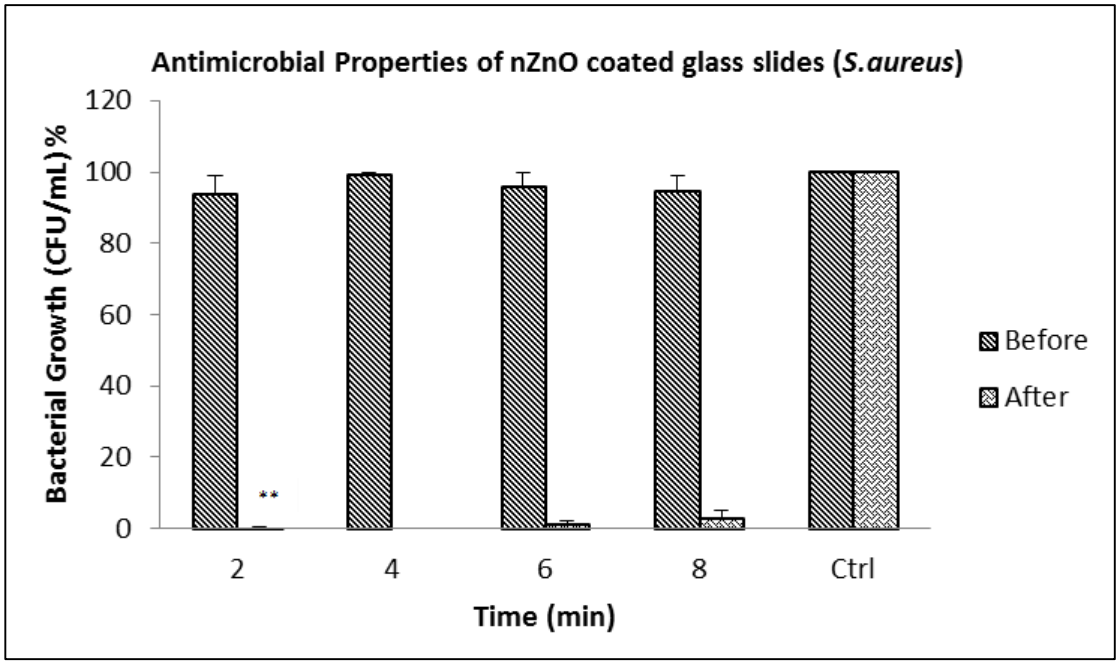

Figure 29 - The glass samples were coated (10,000µg/ml) with nZnO for different time periods and an antimicrobial test was conducted. Comparison of the "before" and "after" values demonstrate antimicrobial activity (Before and after 24h incubation). n =3, ±SEM, $p < 0.01$.

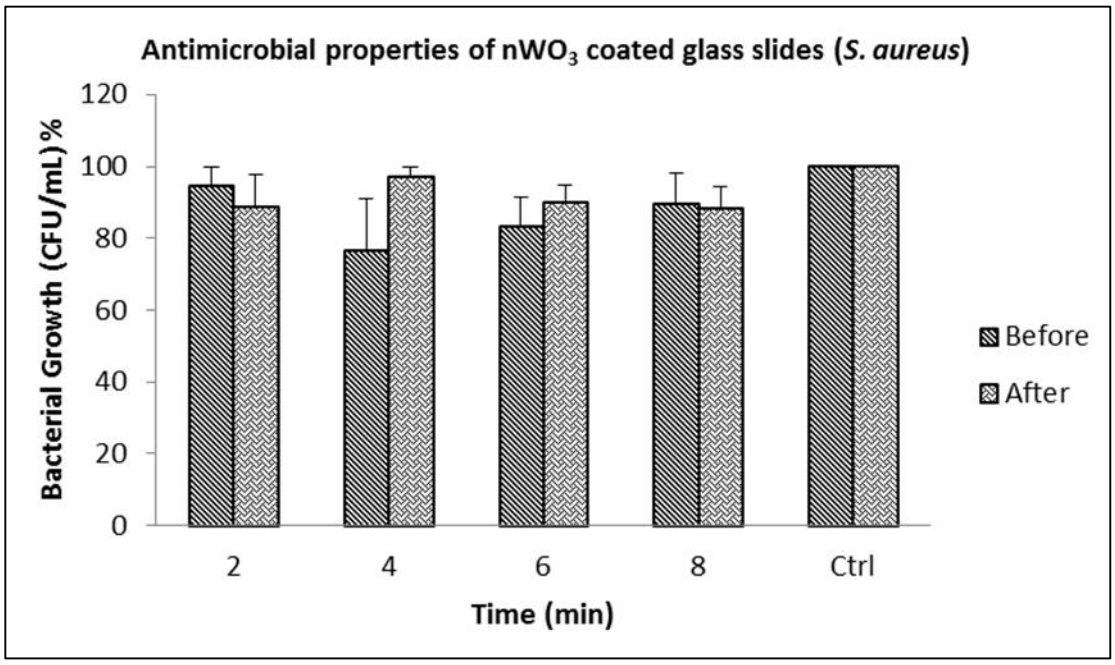

Figure 30 - The glass substrates were coated (10,000µg/ml) with nWO_3 for different time periods and an antimicrobial test was conducted. Comparison of the before" and "after" values demonstrate the lack of antimicrobial activity (Before and after 24h incubation). n =3, ±SEM

3.3.4 Quantification of the coating thickness

Based upon microscopy and antimicrobial results, a coating period of 2 min was therefore chosen as a fixed time for most future coatings. The thickness of this coating can be calculated as follows:

Equation 1 $V/A = t$

Where t is thickness and V equates to the volume of the NP suspension that flows through the nozzle and A is the relative area that is covered by this suspension.

If each sample is coated for a period of 2 min and the flow rate is 5 µl/min, then the final volume of the total deposited NP suspensions will equate to 10 µl/min.

Also assuming that the diameter of the deposition area is 7 cm then the given area for a coated region can be depicted as:

Equation 2 $A = \pi 3.5^2$

And since 10µL = 0.01cm^3, then:

$$0.01\ cm^3 / 28.26\ cm^2 = 3.54 \times 10^{-4}\ cm$$

This value, represents a thickness of 3.54 µm that is extremly thin. Micrographs in Figures 31 and 32 are a representations of how the surface of the substrate changes when a thin coating is applied to its surface.

Distribution of nZnO on a coated sample

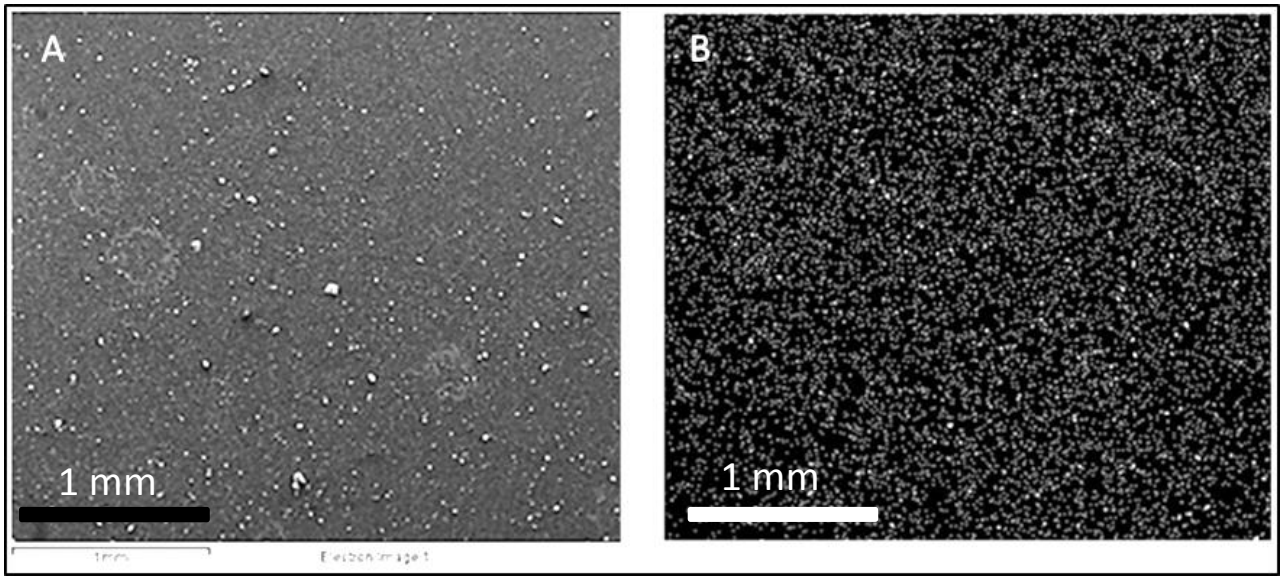

Figure 31 - The coated nZnO substrate is visualised using scanning electron microscopy. A) A coated surface. Debris present is the result of preparation or environmental factors (dust particles and etc). B) The uniform distribution (EDX) of nZnO throughout the surface of the substrate. This demonstrates the ability of EHDA to uniformly coat a future implant. Coating time = 2 min.

Comparison of coated and non-coated surfaces

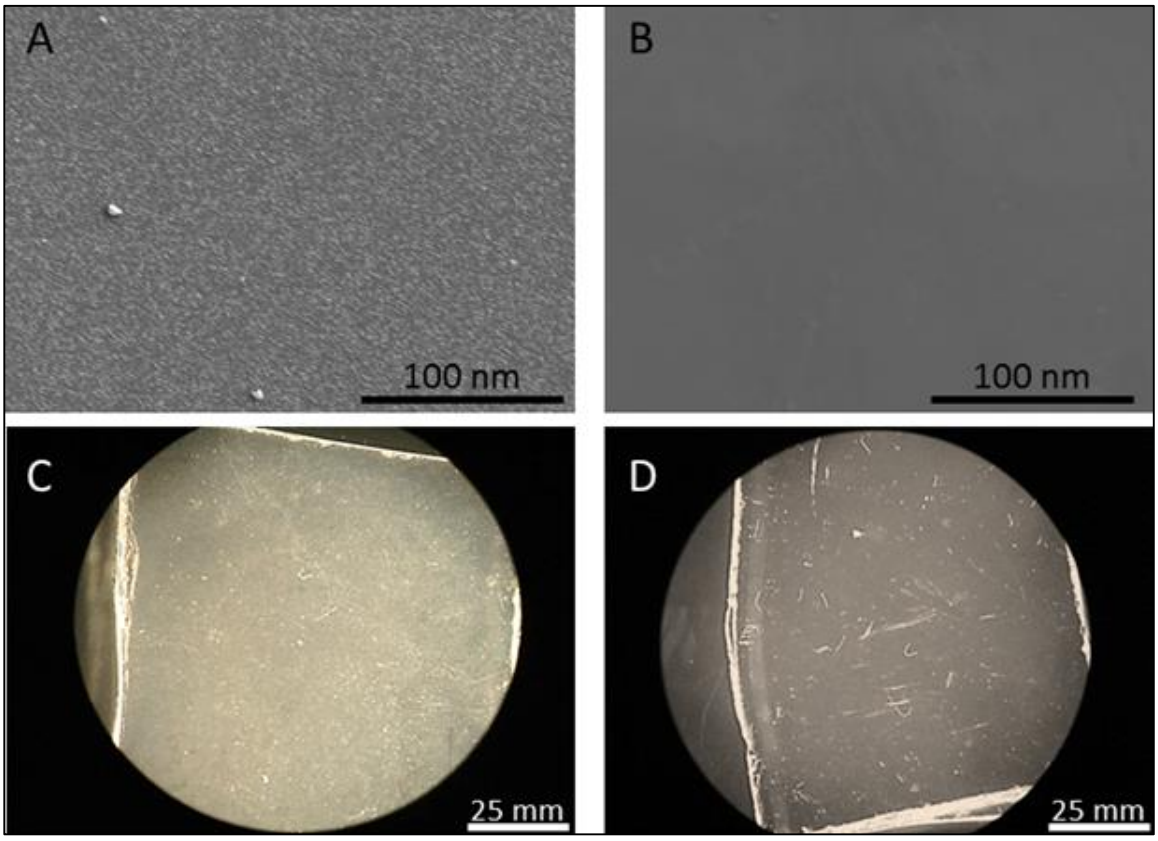

Figure 32 - Comparison of nano-coated and uncoated glass substrates. A) An electron micrograph of a nZnO coated surface, B) Micrograph of the uncoated sample, C) nZnO coated samples visualised using light microscopy, D) Uncoated sample. In both cases there is a clear difference between the coated and the uncoated samples.

3.3.5 Antimicrobial activity of coated samples: contact killing

NPs at concentration of 10,000 µg/mL and various combinations (25% nZnO + 75% nHA, 50% nZnO + 50% nHA, 75% nZnO + 25% nHA and 100% nZnO) of nHA and nZnO were coated onto the surface of glass substrates and their antimicrobial activity against *S. aureus* was assessed. These studies were performed under two different sets of experimental conditions; bacteria suspended in PBS or ABS were placed onto the surface of each substrate in a humidified chamber. The results for the bactericidal effects of the coatings on ABS or PBS suspended bacteria are shown in Figure 33.

The bactericidal effect of coated nZnO and nHA mixtures elicited a reduction in populations of bacteria as the concentration of nZnO increased. Furthermore there was a significant ($p < 0.05$) dose-dependent reduction when the control sample was compared to both the lowest and highest concentrations of coated nZnO. A similar effect was observed when PBS-suspended bacteria were placed onto the surface of the coated material. However the antimicrobial activity was more significant ($p < 0.001$) between the control and the 100% coated nZnO samples (Figure 33).

Antimicrobial activity of coated samples in both PBS and ABS

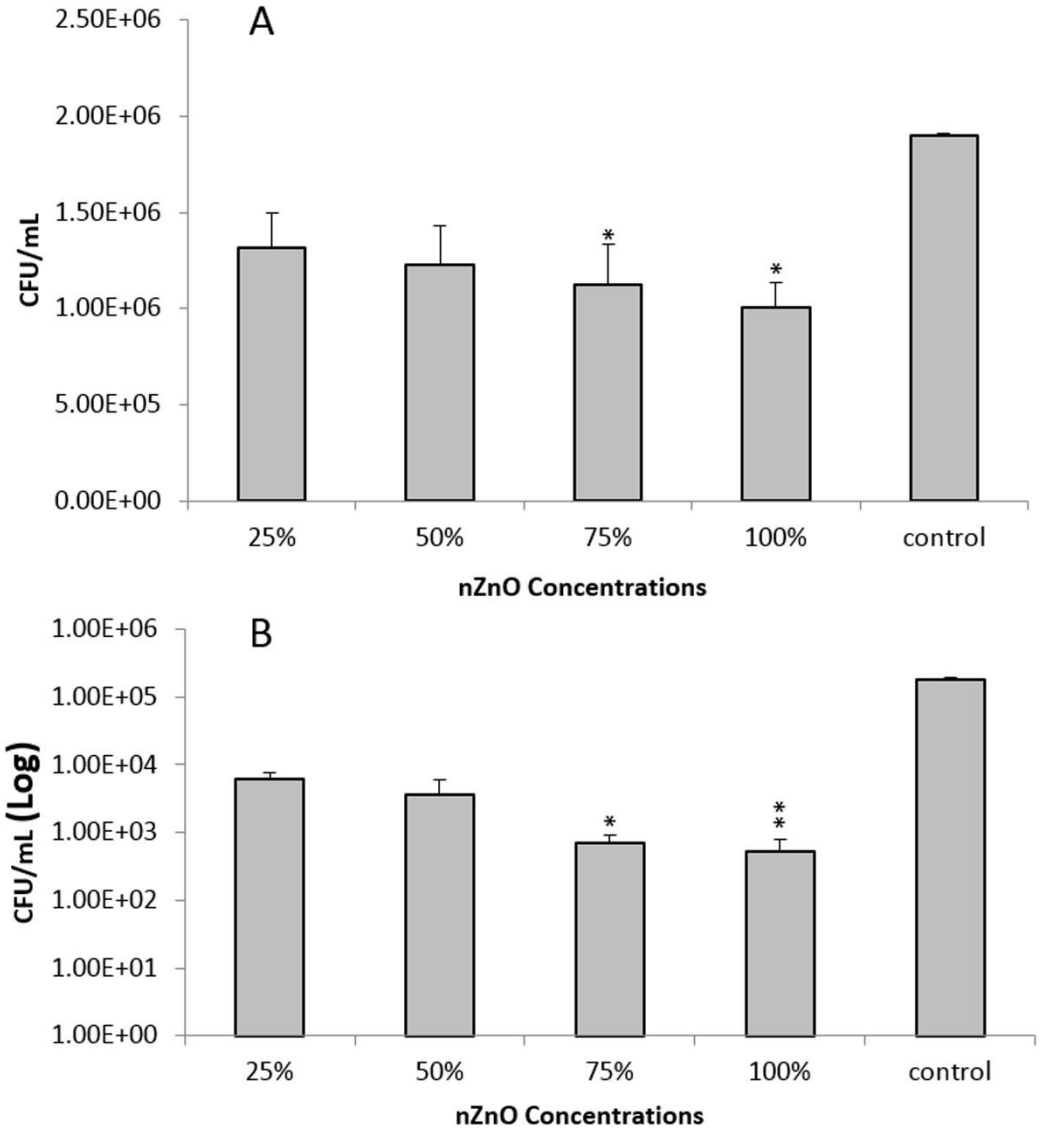

Figure 33 - Bactericidal effects of nZnO coated substrates A) Antimicrobial effect of coated nZnO + nHA composites on *S. aureus* in adult bovine serum (ABS). The coated glass samples are coated with different concentrations of nHA and nZnO. B) Antimicrobial effect of coated nZnO + nHA composites on *S. aureus* in PBS. Coated mixtures have bactericidal effects as the concentration of nZnO increases. Lines compare the antimicrobial effect of the control with the 100% and 25% nZnO coated samples, ** = $p < 0.001$, * = $p < 0.05$, n =4, mean ± SEM.

3.3.6 Antimicrobial activity of coated samples: micrograph analysis

Further investigations as regards to the characterisation of bacteria on the surface of the coated material were conducted using scanning electron microscopy (SEM). Obtained micrographs revealed a substantial presence of adherent bacteria on the surface of the uncoated sample (Figure 34A), in contrast to the sparse population of bacteria on the surface of the coated sample (Figure 34B). The increased amount of debris on the coated sample can be explained as remnants of bacteria killed by the nanoparticulates. The coating itself (Figure 34C) also indicates the uniformity of this antimicrobial coating. Furthermore, while many bacterial cells on the uncoated surface displayed signs of cell division, individual cells on the nZnO coated surface were clearly physically damaged when observed at higher magnification (Figure 35). The healthy bacteria are depicted as going through the normal cell division process on an uncoated surface whereas the bacteria that are positioned upon the coated samples show a cluster of NPs attached onto their surface of the single bacterium. Limited evidence for direct contact killing of bacteria via NPs are currently presented. These micrographs provide some evidence for the direct contact between the NPs which could eventually lead to cell rupture and cell death.

Bactericidal activity of nZnO coated substrates

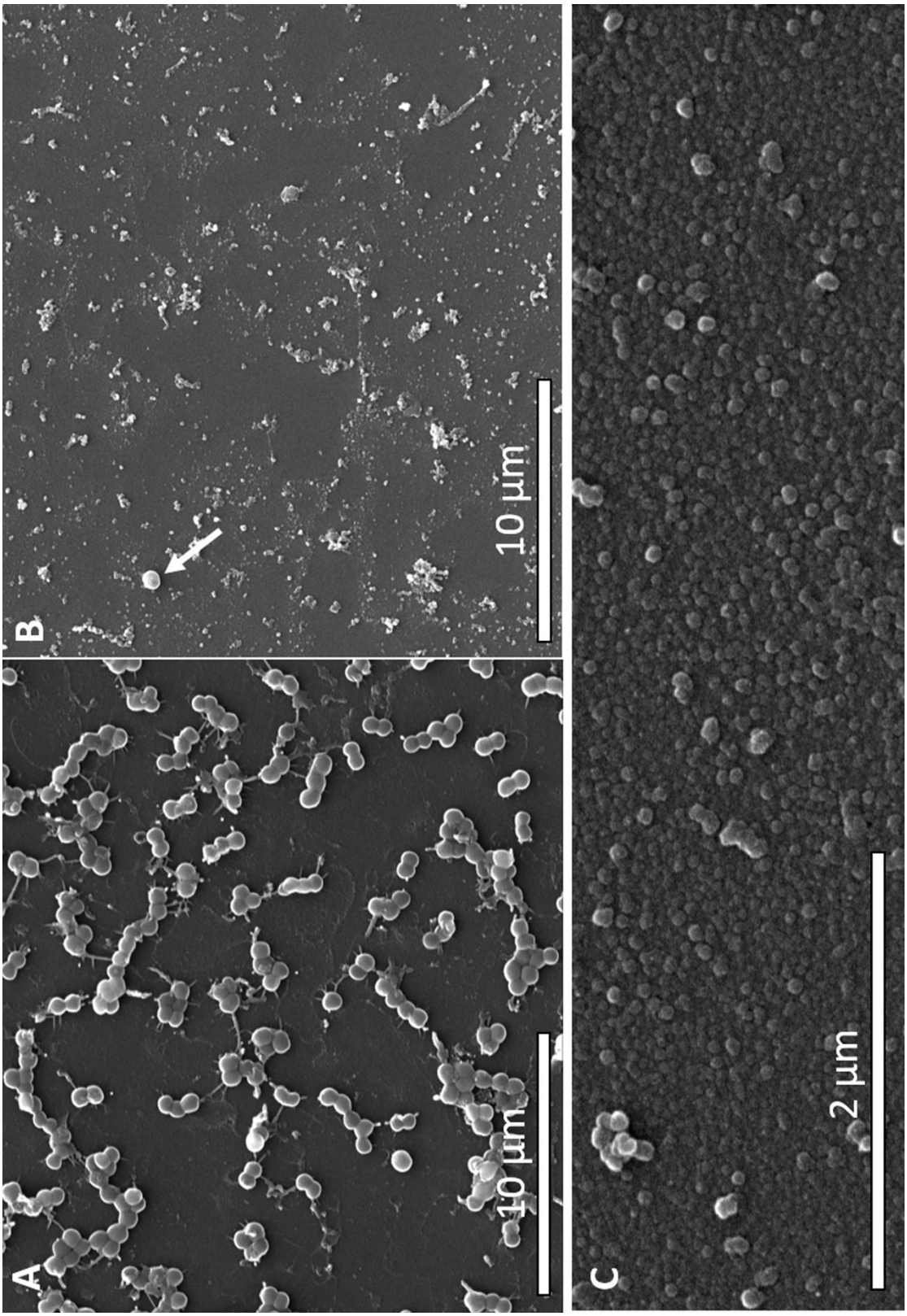

Figure 34 - A qualitative assessment on the antimicrobial effect of nZnO coated onto glass samples. A) Bacteria present on a surface without the coating B) The black arrow indicates a single bacterium present on the coated surface C) High resolution image of coating showing uniform characteristics.

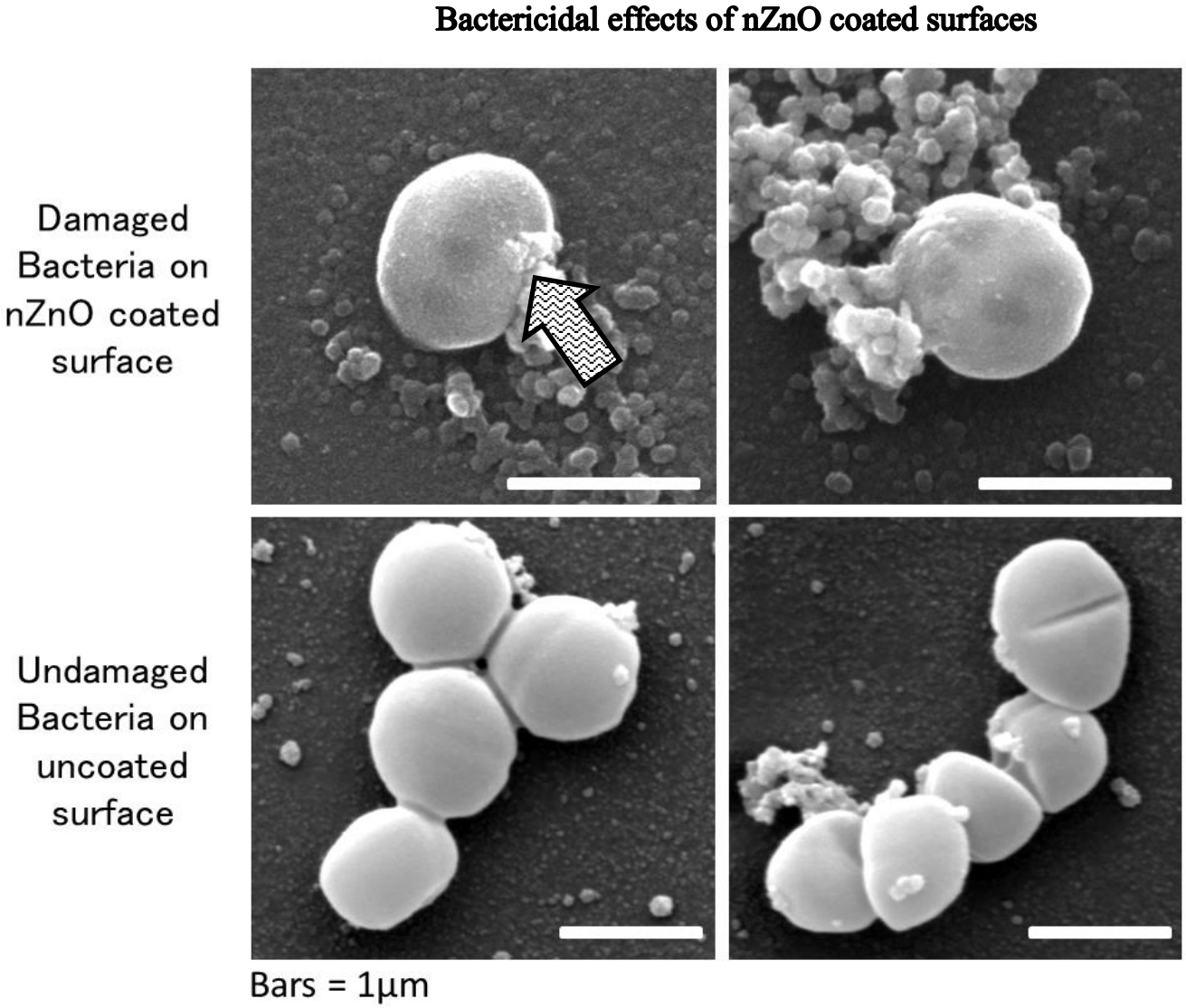

Figure 35 - Bactericidal effect of nZnO coated surface against *S. aureus*. Arrows indicate two potentially dying bacterium. While there is no direct molecular evidence, it can be stated that the membrane has been compromised as compared to the control bacterium. As the NPs physically rapture the membrane of bacteria, the interacellular components of the microorganism could be expelled into the extracellular environment.

3.3.7 Patterned nZnO surfaces

To explore novel ways for implant coatings and to further minimise the chance of coatings becoming detached from the surface of substrates, various patterned structures were devised and tested (Figure 36 and 37). These novel patterns were individually analysed and tested for their antimicrobial activity.

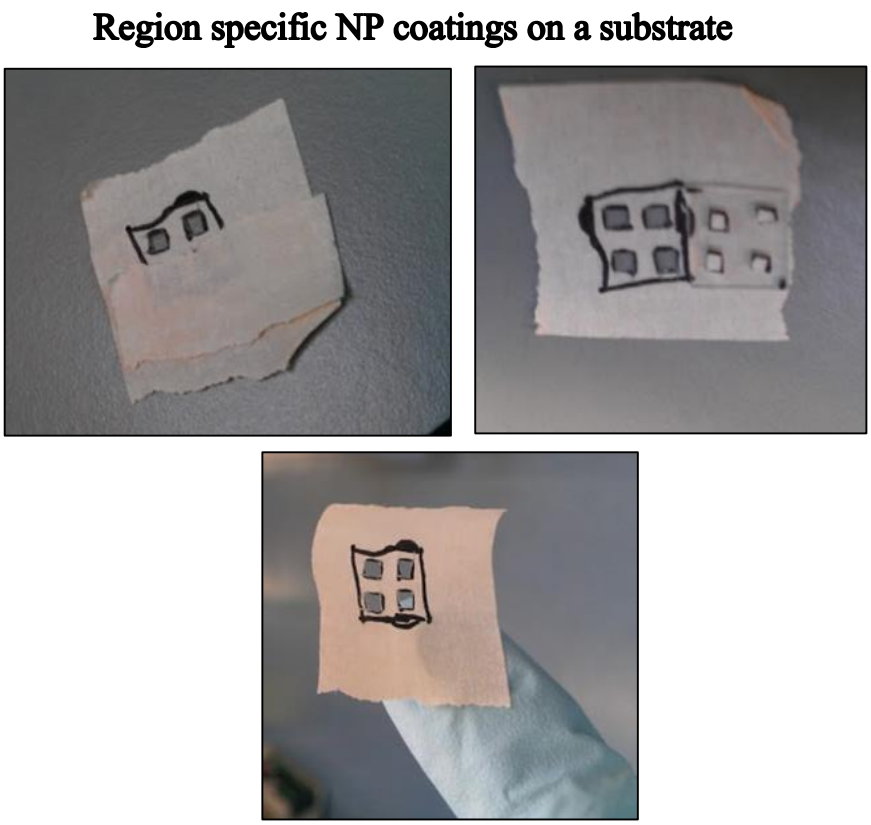

Figure 36 - Region specific coatings. The concept for a surface that has four different types of coating patterns on specific regions on a single sample. A sticky tape was used and four squared shaped structures were carved out of it. These structures were initially used for attaching grids that possessed different patterns. Each multi-grid attachment was placed under the nozzle and spraying was performed. The spray would travel through each grid and the coating will produce the relevant patterns on the substrate.

There were fundamentally four unique patterns utilised in this study. These patterns are depicted using images obtained by using optical microscopy (Figure 37). Two primary patterns identified as 1 and 2 in figure 37B, contain pillar-like structures with pattern 1 comprised of micro-structures that are larger pillars with each side measuring approximately 300 μm in length. Pattern 2 contains smaller sized structures that occupy more space in their provided environment. Patterns 3 and 4 (Figure 37B) are comprised of mainly rows. The nature of these rows differ, i.e.; pattern 3 has similar sized rows while pattern 4 contains elongated structures that can be up to 2.5 mm each, a length of an individual collection of patterns. A 3D representation (ScopeTek, minisee, China) of the surface of each coating is presented (Figure 37A) in order to graphically further clarify the structural integrity of each pattern structure. Application and utilisation of these custom made grids vary depending on how they are fixed onto substrates and therefore the initial concept for a rectangular shaped paper-based plate (Figure 36), which allows grid embedment to be visualised was devised and subsequently the final version that was used in final experiments (Figure 38).

3D and non-3D representation of patterned-based coated surfaces

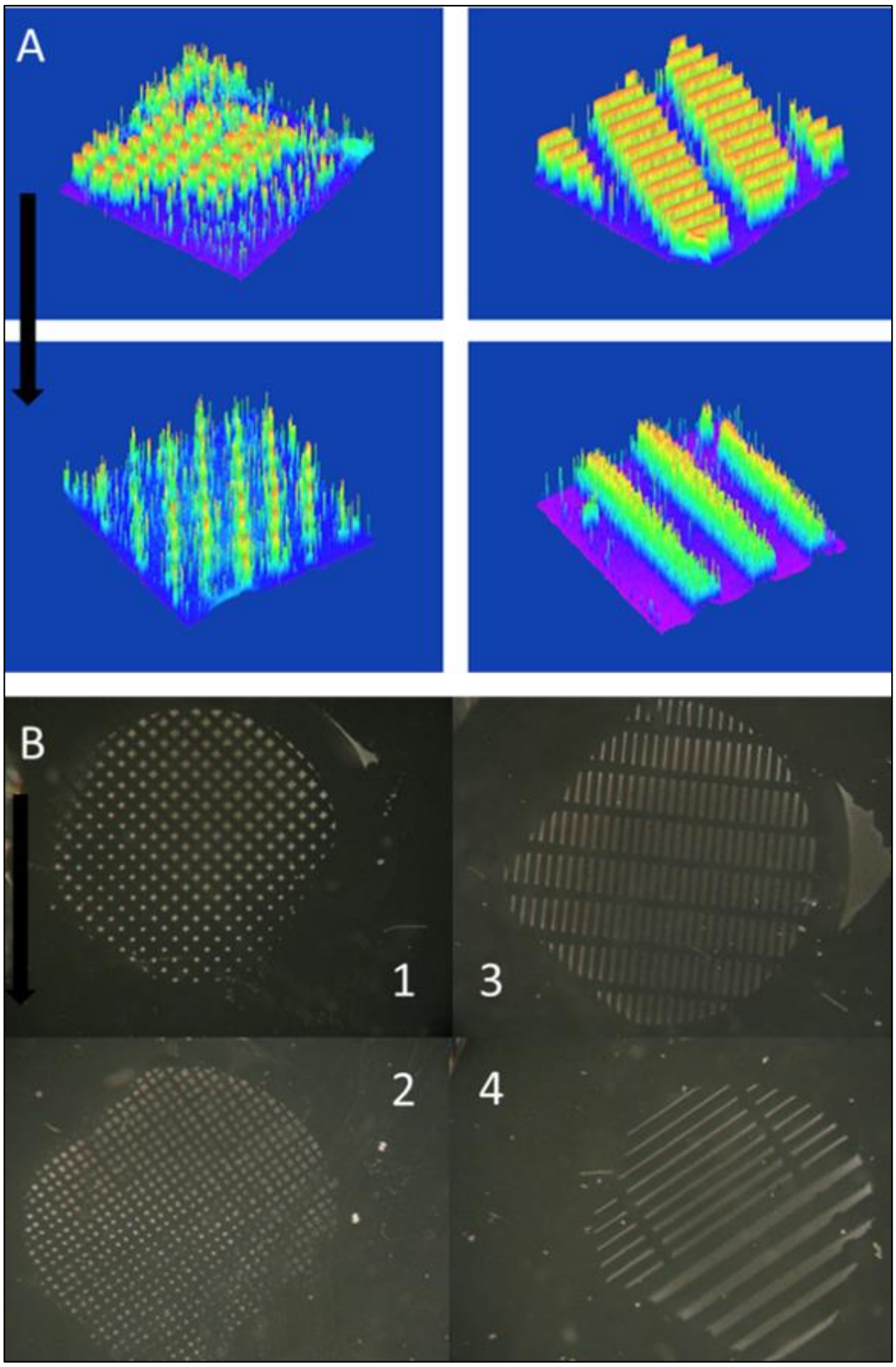

Figure 37 - The structure and shapes of the patterned coated surfaces. A) The 3D representation of the patterned structures (ScopeTek, minisee/ImageJ). B) Patterned structures using light microscopy. 1 and 2) pillar-shaped patterns with large and small sizes 3) Rectangular-shaped patterns 4) Line-shaped rectangular patterns with various thickness and size. Diameter across each pattern = 2.5 mm.

Customised grids for coating NPs onto surfaces

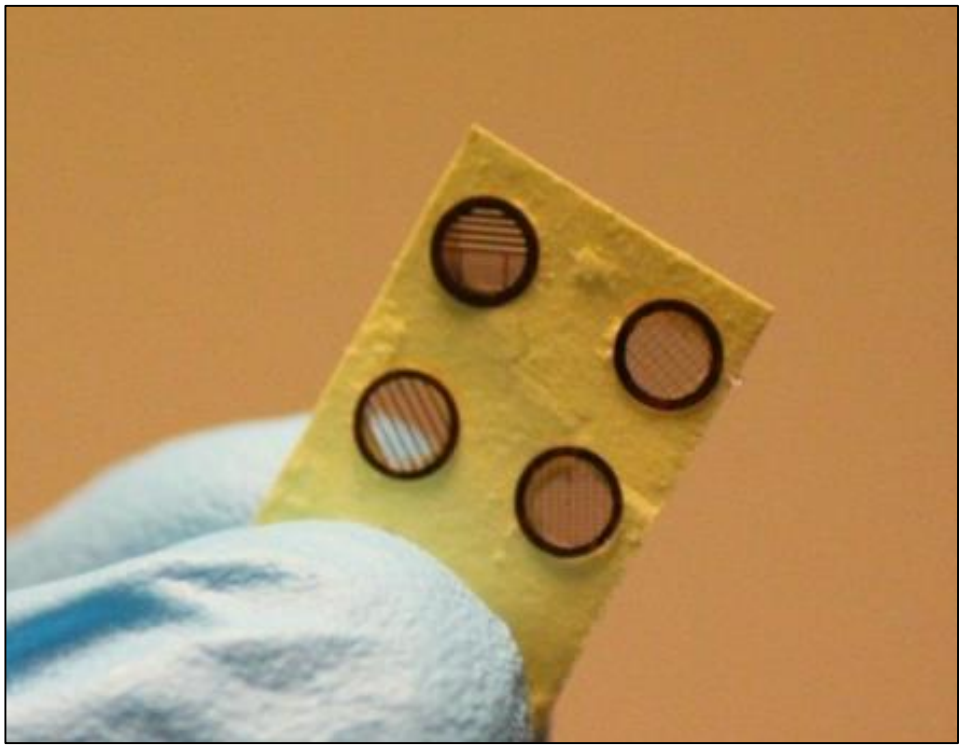

Figure 38 - A novel method of coating patterned structures onto substrates. This sample has been designed so that while spraying, the resulting nanoparticulate-suspension deposition corresponds to each individual grid presented. The size of each grid is approximately 25 mm and therefore multiple coatings with different shapes can be utilised on a single sample. If a single or multiple grids are to be used, others are easily covered. These qualities can be useful for both biological and imaging purposes.

3.3.7a The antimicrobial properties of patterned structures

Antimicrobial assays indicated that, compared to control, regions with small square shaped pillars are essentially more effective in killing bacteria (Figure 39). Large clusters and agglomerations of nZnO are not as effective and while not significant as compared to the control ($p < 0.05$), they cannot be branded as "effective" as nano-coatings and therefore providing a valuable insight into how future nano-based coatings could be designed.

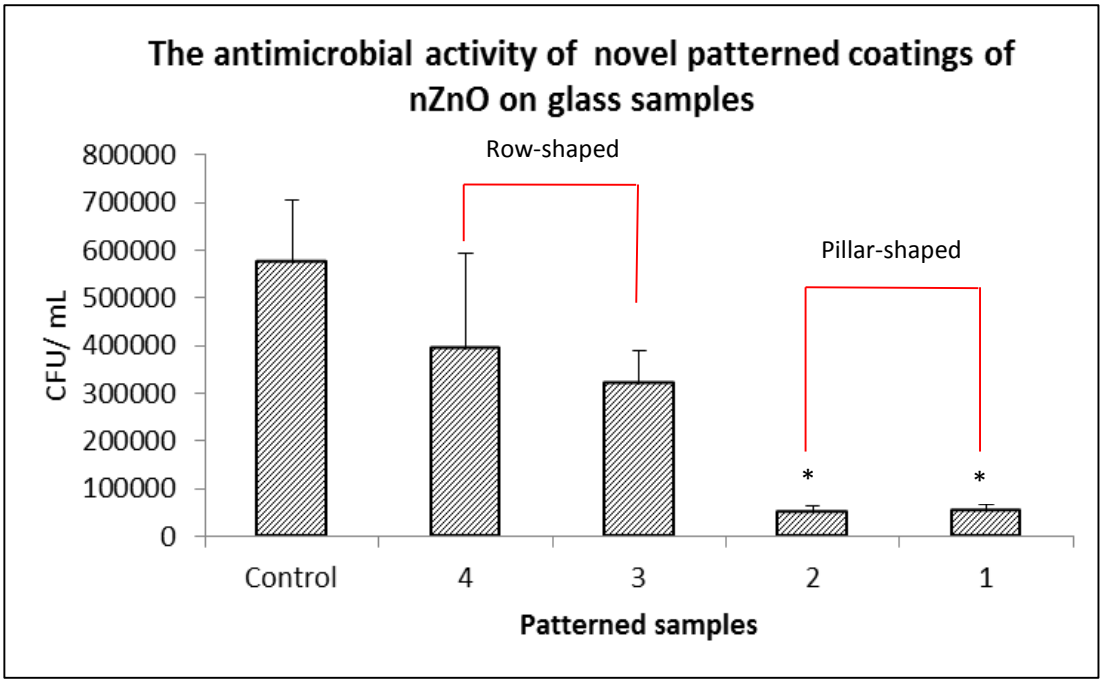

Figure 39 -The antimicrobial activity of the patterned samples compared to control. Patterns 1 and 2 elicit significant antimicrobial activity when compared to control and patterns 3 and 4. (All pattern numbers refer to patterns identified in figure 37), * = $p < 0.05$, n = 3, ±SEM.

The current results support the hypothesis that metal oxide NPs can be utilised as antimicrobial agents. An evaluation of the initial results (obtained from the MIC and MBC studies) supports this concept. In both the MIC and MBC studies, it was observed that NPs such as copper (II) oxide (CuO) and the novel silver mixtures (70% wt Ag + 30% ZnO and CuO) are highly antimicrobial. The results also indicate that a nanoparticulate such as WO_3 is possibly antimicrobial with more inhibitory properties than bactericidal. The values obtained as regards the MIC suggest that WO_3 is able to inhibit the growth of bacteria, almost as efficiently as the other nanoparticulates tested. This in itself is a novel finding because until recently tungsten oxide nanoparticulates had not been tested for their antimicrobial properties and were only utilised for industrial purposes (Lu et al., 2012). Furthermore, the MIC and MBC values for CuO are among the lowest in the present study. These findings are not surprising since the antimicrobial potential of CuO has been previously documented (Vargas-Reus et al., 2012). As a result of its toxicity towards eukaryotic cells, CuO is unlikely to be utilised for any medical related purposes in the near future (Fahmy and Cormier, 2009). Based on both the MIC and MBCs, both silver mixtures instigated strong bactericidal effects. Furthermore, time-based bactericidal studies confirmed that these mixtures were able to cause a significant reduction in bacterial population in a relatively short period of time. It is a well-known fact that silver NPs alone can show strong bactericidal effects against both gram positive and negative species (Morones et al., 2005, Sondi and Salopek-Sondi, 2004, Shahverdi et al., 2007). However, over-use of silver in various compounds, such as in cosmetics and solely as an antimicrobial agent will almost certainly contribute to the acquisition of new types of bacterial resistance (Chopra, 2007). Finally, the obtained results for both the MIC and MBC determinations for nZnO show that these NPs are

not able to display any visible antimicrobial activity within the provided time frame. This is possibly due to the nature of the experiment that will be addressed in the limitations section. Subsequently results for these experiments indicated that nZnO is antimicrobial (against both *E. coli* and *S. aureus*) and in contrast to our previous finding, nWO_3 lacks this ability. A similar pattern of killing was further confirmed when nWO_3 and nZnO coated samples were submerged and exposed to suspensions of bacteria. This confirmed that tungsten oxide is not a suitable novel antimicrobial for the purposes of the current study. A coated sample floating in medium with suspended bacteria is not a direct way of determining the antimicrobial activity of a coating and it is possible that the antimicrobial activity is partly due to elution of ions as compared to direct physical contact. Therefore further experiments were conducted with nZnO as the key NP under consideration.

In the human body and indeed within the structure of the bone there is no specific homogeneity, being comprised of nerves, blood vessels as well as areas within the trabecular bone that appear almost "lifeless". Therefore it is hard to mimic an environment whereby all these conditions are equally met. Tested nZnO under two different environments (ABS and PBS), indicates a phenomenon that has previously been observed in some recent studies (Premanathan et al., 2011). The results indicate that pure nZnO particulates seem to be selective towards *S. aureus* and while exerting an antimicrobial effect on *E. coli*, its effect is unquestionably less significant and scattered, with some low concentrations of NPs showing enhanced antimicrobial activity at higher concentrations. This finding is therefore relevant for applications related to medical coatings. Since most bone implants, predominantly orthopaedic, suffer from infections often caused by gram positive pathogens, this result is encouraging. Indeed it is suggested that nZnO is also highly antimicrobial to some

pathogens that are involved in dental-related infections, i.e. both facultative and anaerobic species (Vargas-Reus et al., 2012).

Using *S. aureus* suspended within different environments (as described above), the antimicrobial activity of coated surfaces was tested. The antimicrobial test method used in this study was novel since it allowed the investigator to closely monitor the interaction between the surface of a coated sample and the suspended bacteria. The low amount (in volume) of bacterial suspension that is placed onto the surface of the coated substrates allows for a closer interaction between the nanoparticulate coated surface and bacteria. Indeed if one considers the shape of these NPs (rod shaped structures, with sharp edges), their importance as agents capable of "stabbing" bacteria becomes apparent. It has been demonstrated that in nature, the process of natural selection has evolved mechanisms in order to develop such defence against pathogens. One remarkable example of this naturally occurring nano-surface defence is the cicada wing. The nanopillars present on the cicada wing surface have the capability to penetrate and kill bacteria (Hasan et al., 2013). Of course there is no direct correlation between the present study and a naturally occurring antimicrobial, however qualitative results obtained (with both *S. aureus* and *E. coli*) suggest membrane disruption and cellular disintegration, possibly due to physical interaction between the NPs and bacteria. These findings indicate that in both environments the nano-surfaces with an ascending concentration of nZnO can be bactericidal. Many of the current antimicrobial coatings for bone implants depend upon release of bactericidal concentration of various ions (Lee et al., 2005) or elution of antibiotics from within their structure (Popat et al., 2007). An increase in utilisation of nanotubes as an alternative method is a prime example of coatings where bactericidal agents are loaded within or deposited upon these nanostructures (Das et al., 2009).

The present system provides a coating that encompasses these preferred qualities. Having developed a reliable coating system, a new innovative method for creating novel patterns was investigated and tested for their antimicrobial properties.

Initial question was to investigate whether each unique coating pattern has a distinct

antimicrobial “profile”. Upon examining this hypothesis the results suggest that this is indeed in the case. Studies have shown that micro-patterned structures as coatings can have significant antimicrobial activity against multiple species (May et al., 2014), others assert that the presence of these structures on the surface of the medical devices prevents bacterial adhesion without the presence of any chemical intermediate (Reddy et al., 2011). It is therefore important to point out that these different shaped nano-based patterns on a substrate manifest into unique antimicrobial profiles that can be advantageous for future coatings and should be investigated further.

Importance of the work

	Relevant significance of the current research
1	The application of multiple experimental methods in order to test various NPs for their potential antimicrobial activity
2	Providing novel evidence for the antimicrobial activity of a composite that is comprised of two independent NPs.
3	Observing the physical interaction of NPs against both *E. coli* and *S. aureus*, providing provisional evidence for this phenomenon.
4	Confirming previous findings that nZnO is selective towards gram-positive species (Premanathan et al., 2011), especially *S. aureus.*

Limitations and disadvantages

1	Methods used for the inhibitory and bactericidal studies need to be modified and carried out in more controlled environments.
2	A suitable *in vivo* system would have been much superior for judging the "true" antimicrobial potential of the coated systems.

Chapter 3

nZnO as a biocompatible implant coating material

1. Introduction

Apart from their antimicrobial activity, the biocompatibility of NPs, particularly that of nZnO, is of outmost importance because of their potential toxic effect towards eukaryotic cells (Bai et al., 2010). It is understood that, when in suspension, most NPs can cause eukaryotic cell death or apoptotic. This chapter focuses on the synergic activity of two nanoparticulates, namely nHA and nZnO with eukaryotic cells. The following is a review of their physiochemical effects as directed to bone and its microenvironment.

1.1 Nano-HA

Chemical modifications to the surface of bone implants affect cell behaviour, shape and metabolic activity. Therefore, based on observations, a vast expanse of materials as well as methodologies have been devised in order to improve bone integration (Wennerberg and Albrektsson, 2009). One of the first materials used for surface enhancements was hydroxyapatite (HA). This biomaterial is chemically related to the bone matrix and therefore its properties are ideal for an implant coating (see general introduction). While nHA has been used for a number of years, active research is being carried out to further study its effects on osteoblasts and bone formation. It has been established that nanostructures are of particular interest in that they can promote osteoconduction, bioresorption and make more intimate contacts with the structure of bone (Noor, 2013). This close proximity of the surface of the coating and bone

structure allows for apatite formation which is a direct result of ion exchange between the coated surface and body fluid. Recent studies indicate that HA solubility and therefore calcium release increases if this biomaterial is in a nano-form (Meirelles et al., 2008). Furthermore, bone grafts made with this nanoparticulates demonstrate increased bone healing through osteoblast activation (Noor, 2013).

1.2 Nano-ZnO

During the process of implantation, NPs can be scraped off the implant surface and be distributed within the body, which can lead to potential toxicity. Studies have shown that ingested nZnO particles display slow absorption rates and a decreased systemic absorption when compared to zinc ions alone *in vivo*. It has been further suggested that most NPs, regardless of size or surface charge, are excreted through faeces, indicating that while not entirely safe, the majority of NPs are excreted (Lee et al., 2012a). Another study indicated that upon oral injection tagged nZnO particles were able to penetrate several organs but no traces of these tagged NPs were found in the bone. These NPs were compared to two different fluorescent agents that were both detected upon ingestion (Lee et al., 2012b). However, orally administrating NPs into subjects does not simulate the scenario where an implant is inserted into bone, the main difference would be the immobility of the NPs on coated materials.

The cytotoxic effects of nZnO have been extensively investigated and no cause of toxicity has been determined. A study looking at the mechanistic effects of suspended nZnO against macrophages concluded that apoptotic events did not occur because of the physiochemical properties of nZnO or the conventional major phagocytic oxidant generating pathway (Wilhelmi et al., 2013). Furthermore the

study indicates that these apoptotic events are concentration based. As the concentration of the nanoparticulates increases, ROS-mediated pathways are triggered that result in DNA damage and therefore cell necrosis. The authors finally concluded that these mechanisms are not entirely known and thorough investigations are required (Wilhelmi et al., 2013). A recent separate study monitoring the toxic effects of nZnO particulates concluded that sub-acute exposure of these nanoparticulates in mice results in minimal inflammatory responses, challenging the contradictory nature of ZnO nanoparticulate research (Adamcakova-Dodd et al., 2014).

1.3 Coated nHA

While the use of nHA has been extensively investigated in both fields of dentistry and orthopaedics, less is known about its nano-state. A study measuring the osteoblast activity on porous titanium surface indicates an improvement of proliferation and differentiation when exposed to nHA coated surfaces as opposed to a plain porous Ti-based implant (Shi et al., 2013). Nano-HA facilitates biocompatibility and osteoconductivity among other factors. However, because of its slow biodegradable nature, it is often demonstrated that its application in conjunction with other organic or synthetic materials such as PLGA or collagen will enhance its drawbacks (Christenson et al., 2007). A quality that seems to be universal to most biocompatible NPs, and especially, nHA, is its crystal structure. Researchers claim that nanophase HA has a crystal structure that bears a close resemblance to that of bone. This observation is enhanced by evidence provided in multiple studies that have shown *in vivo* evidence for increased bone formation when metal-based implants were coated with nanophase HA (Li, 2003, Zakaria et al., 2013). Therefore

it can be inferred that nHA provides changes in cellular interactions that ultimately lead to an increased tissue response.

1.4 Coated nZnO

Limited studies have been conducted as regards to the function of nZnO particulates for medical implant coatings. Most of these studies have been conducted very recently, making this field relatively unexplored (Zaveri et al., 2010, Seil and Webster, 2008, Brunner et al., 2006). A recent study demonstrated found that a novel polyvinyl chloride (PVC) nanocomposite incorporating fine ultra-sonicated nZnO particulates can enhance fibroblast density after 18 hours of incubation (Paul et al., 2014). In contrast, a recent study indicates that increasing concentrations of nZnO nanoparticulates in polymer matrices causes a decline in cell viability. Other means of incorporating ZnO into coatings have also been used recently. The following investigations are an attempt to understand the biocompatibility properties of nZnO particulates relevant to bone cells.

2. Materials and Methods

2.1 Nanoparticles utilised for coating

Metal oxide NPs were synthesised using the flame pyrolysis method as used by Johnson Matthey plc (JMTC). The average surface area was determined by Brunauer Emmett Teller (BET) analysis at JMTC. Nano-HA particles were made by the process of wet precipitation between calcium hydroxide ($Ca(OH)_2$) and orthophosphoric acid (H_3PO_4). Handling and storage of these NPs was performed in a manner to avoid biological and environmental harm. NP suspensions were

collected, dried and incinerated. The NPs tested were: Zinc Oxide (nZnO),Titanium dioxide ($nTiO_2$), Cupric Oxide nCuO and nHA. Both nZnO and $nTiO_2$ were subsequently analysed by transmission electron microscopy (See Chapter 2, section 3.1).

2.2 Nanoparticulate suspension-derived supernatants

Nano-ZnO, $nTiO_2$ and nCuO particulate suspensions (10,000 µg/mL) were placed in 2% FCS DMEM and left in a shaking incubator for 10 days at 37°C. After 10 days samples were removed and transferred into a 50 mL centrifuge tube and spun at 1000 RPM (160 *g*) for 5 min. The supernatant from each sample was removed and filtered using a 0.22 µm filter (EMD Millipore, UK). Osteoblast-like cells (UMR-106 and MG-63) were seeded at a density of 1×10^5 per well in a 24 well plate. A volume of 1 mL of DMEM (with 2% FCS, 1% P/S) was added to each well and incubated at 37ºC, 5% CO_2 for 24 h to allow a cell monolayer to develop. The medium in each well was replaced with filtered supernatant or plain media (control) and incubated for 0, 2 and 4 h respectively.

2.3 Nanoparticulate suspension and composites

Nanoparticulate suspensions: Different concentrations (2500, 5000 and 10,000 µg/mL) of nZnO suspension were made in 100% ethanol and sonicated thoroughly prior to electrohydrodynamic atomisation (EHDA) spraying.

Nanoparticulate composites: For preparation of the composite mixtures, two different suspensions of nZnO and nHA were made with equal concentrations of 10,000 µg/mL (100% nHA, 25% nZnO + 75% nHA, 50% nZnO + 50% nHA, 75%

nZnO + 25% nHA and 100% nZnO). From these suspensions a known volume was added to produce the required concentration of NPs within each composite.

2.4 Biocompatibility and cell proliferation studies

2.4.1 Cell culture

UMR-106 (Rat osteosarcoma), MG-63 (human osteosarcoma) and human mesenchymal stem cells (hMSC) were used in this study. The majority of investigations were carried out using UMR-106 cells. Human MSCs were utilised for qualitative adhesion observations. MG-63 cell-lines were utilised for both qualitative & quantitative adhesion observations as well as ELISA studies.

Frozen cells were quickly thawed and cultured in high-glucose DMEM with 2% FCS, 1% penicillin and 1% L-glutamine. The cells were incubated for 48 h at 37ºC, 5% CO_2 and then detached using Trypsin/EDTA. Trypsinised cells were resuspended with 5 mL of medium, placed in 10 mL tubes and centrifuged at 800 *g* for 5 min. Supernatant was removed from each tube and fresh media was then added to the cell pellets. Osteoblasts were dispersed, suspended, counted and seeded onto coated samples with a density of 1×10^4 cells. Samples were incubated at 37ºC, 5% CO_2 for 2 h to allow cell-substrate adhesion.

2.4.2 Proliferation assay

The proliferation of the UMR-106 cells was assessed using Alamar Blue (alamarBlue® -AbD Serotec). The reagent was diluted with normal growth medium (1:10 dilution) and stored at 4ºC prior to use. A population of 1×10^4 osteoblasts were seeded onto coated glass samples in a 24 well plate (n = 4 per condition). Seeded cells were left for a period of 15-20 min in the incubator to ensure adhesion and 1

mL of medium was added to each well for overnight incubation. At 1, 5 and 10 days 10% of the volume of the medium in each well was replaced with reagent medium. The plate was then incubated for a period of 4 h and 100 µL of the supernatant was removed from relevant wells and added to a 96 well (Black Falcon) plate. Fluorescence was measured using a fluorescent plate reader (FLUstar OPTIMA, BMG Labtech, Germany) at wavelengths of 570 nm (excitation) and 600 nm (emission).

2.4.3 Cytotoxicity Assay

LDH release from UMR-106 cell lines was measured using a commercially available kit (LDH-Cytotoxicity Assay Kit II (500 assays) (ab65393)) and carried out according to the manufacturer's instructions.

1) **LDH release: osteoblasts exposed to NP suspension supernatants**

To examine the possible effects of released ions on osteoblast viability, nZnO particulates were suspended in 2% FCS DMEM (10,000 µg/mL) and left in a shaking incubator for 1, 5 and 10 days at 37°C. Nano-TiO_2 particulates were also tested in a similar manner. At each time point, samples were removed and transferred into a 50 mL centrifuge tube and spun at a speed of 160 *g* for 5 min. The supernatant from each sample was removed and filtered (0.22 µm , EMD Millipore) Osteoblasts were seeded at a density of 1×10^4 per well in a 96 well plate. A volume of 100 µL of DMEM (with 2% FCS) was added to each well and incubated at 37ºC, 5% CO_2 for 24 h to allow a cell monolayer to develop. The medium in each well was replaced with 100 µL of the filtered supernatant or Lysis Buffer (positive control) and incubated for 40 min. The plate was centrifuged at 600 *g* for 10 min and 10 µL of the supernatant was transferred to a new 96 well plate. A volume of 100 µL of the LDH

reaction mix was added to each well and incubated for a further 30 min. Absorbance for all samples and controls was measured at a wavelength of 450 nm using a plate reader (FLUstar OPTIMA, BMG Labtech, Germany).

2) LDH release: osteoblasts exposed to supernatants derived from nano-coated samples

The coated samples were placed in a 24 well plate containing 2 mL of 2% FCS DMEM in each well. The samples were then left in a shaking incubator (37ºC, 200 rpm) for periods of 1, 5 and 10 days. In parallel, 1×10^4 cells per well were seeded into a separate 24 well plate and incubated at 5% CO_2. A volume of 1 mL of DMEM from each time point was subsequently added to cells. Osteoblasts were then incubated for a further 24 h and 100 µL of each well was removed and dispensed into a 96 well plate and LDH release was measured.

2.4.4 Alkaline phosphatase activity

The differentiation of the UMR-106 cells on the nZnO coated samples was determined by measuring alkaline phosphatase release. A population of 1×10^4 cells were seeded onto coated glass samples in a 24 well plate and left at 37°C in an incubator with 5% CO_2 for 1, 5 and 10 days respectively. For the ALP assay, one tablet of 4-nitrophenyl phosphate disodium (SIGMA-aldrich, Dorset, UK) was mixed with 8 mL 0.1 M Trizma Hydrochloride (pH = 9.5) and 15 µL of 2 M $MgCl_2$. Before addition of the reaction solution to the cells, each well was washed with PBS three times. A volume of 1 mL of the reaction solution was added to each well containing

the cell seeded coated samples. The 24 well plate was left at room temperature for approximately 10 min for the reaction to take place. Addition of 0.5 M NaOH was then used to stop the reaction. Subsequently, 100 µL aliquots were removed from each well and transferred into a 96 well plate and the absorbance read at 405 nm using a plate reader (FLUstar OPTIMA, BMG Labtech, Germany).

2.4.5 Cytokine release measurements

ELISA was performed in order to quantify cytokine release. MG-63 human osteosarcoma cells were seeded onto glass samples (as described previously) and cytokine release (TNF-α and IL-6) were subsequently measured according to the manufacturer's protocol (Thermo Scientific, UK).

2.5 Microscopy

2.5.1 NP characterisation

1) Transmission electron microscopy: ZnO along with TiO_2 NPs were placed in 5 mL of distilled water and sonicated to provide a homogenous suspension. Carbon film grids (400 Mesh Cu, Agar scientific) were briefly dipped into the nanoparticulate suspension and left at room temperature to air dry. The grids were transferred into the TEM (Philips CM 12) and subsequently analysed.

2.5.2 Cell morphology

1) Optical microscopy: Standard inverted light microscopy (Nikon Eclipse TE2000-5) was used to observe cellular growth at every stage. A population of 1×10^5 of cells

were seeded onto coated samples and their morphology and distribution was monitored over time.

2) Scanning electron microscopy (SEM): Both coated and uncoated substrates that were seeded with cells were placed into 3% Glutaraldehyde (SIGMA Aldrich, Dorset, UK) in 0.1 M Cocadylate buffer (SIGMA Aldrich) for a period of 24 h. Each sample was then dehydrated using ascending concentrations of ethanol: 20%, 50%, 70% and 90% for 10 min each and 100% ethanol for 30 min. Finally the samples were dried using hexamethyldisilazane (HMDS) (SIGMA Aldrich) for 5 min. Samples that lacked the presence of cells were cleaned with 100% ethanol and processed without the dehydration process. Furthermore, glass samples were mounted onto stubs and made conductive by the application of conducting carbon cement (Agar Scientific, UK) between the sample and the stub. All samples were gold coated and directly transferred into the scanning electron microscope (FEI Quanta 3D FEG) with an average working distance of 12 mm and an accelerating voltage of 5kV.

2.5.3 Immunofluorescence

Cells were fixed with 4% paraformaldehyde (PFA), incubated for 10 min in permeabilisation buffer (PBS with 0.2% Triton X-100) and subsequently blocked with 2% bovine serum albumin (BSA). Samples were incubated with primary antibody (4 mg/mL mouse anti-paxillin; Santa Cruz, Inc., U.S.A.) for 24 h at 4°C. Subsequently NP coated coverslips were washed with PBS and incubated for 45 min at room temperature in the dark with Alexa Fluor® 568 conjugated rabbit anti-mouse secondary antibody (Invitrogen Molecular Probes, U.K.). Alexa Fluor® 488-phalloidin staining was applied to visualise F-actin (Invitrogen Molecular Probes,

U.K.). Imaging was performed with a Leica DM4000 epi-fluorescence microscope (Leica, Solms, Germany).

2.5.4 Sirius red assay (collagen assay)

The Sirius red assay is often used to stain for collagen deposition. This solution was obtained from the Bart's and The London School of Medicine, (The Royal London Hospital). Samples were coated with 100% nZnO, 100% nHA and 50% nZnO + 50% nHA. An identical population of osteoblasts (1×10^5) was seeded upon coated and uncoated samples. All samples were incubated overnight at 37ºC, 10% CO_2. The medium in each well was removed and all samples were gently washed with PBS and transferred into a new 12 well plate. Subsequently, 100 µL of the Sirius red solution was added to each sample in order to fully cover the surface. All samples were left submerged in the solution for 1 h and immediately washed with 70% ethanol. Samples were left at room temperature for a further 15 min to dry and then mounted onto glass slides for microscopy. Normal images were obtained using a 650D DLSR. Magnified micrographs were obtained by utilising a DEM130 (1.3 M pixels, MiniSee). Image thresholding was conducted using ImageJ, This refers to a software-based technique whereby an image background is changed in order to highlight the regions of interest.

2.6 Statistical analysis

One way ANOVA (GraphPad Prism 5) was used for focal adhesion studies and student's t-Test were used to analyse the difference between quantitative measurements. When, $p < 0.05$, the results was considered statistically significant.

3. Results

3.1 The effect of NP supernatants on osteoblasts

Osteoblasts were exposed to supernatants derived from three different nanoparticulates: nZnO, $nTiO_2$ and nCuO, each at 10,000 µg/mL. Figure 40 demonstrates the morphological change for the seeded osteoblasts. At hour 0 there were no visible morphological changes present, where hour 0 represents the morphological state of the cells after 5 min of exposure to supernatants. The morphological changes become evident after 2 h of incubation. At this stage, stark differences can be observed between the control and osteoblasts, particularly with UMR-106 cells exposed to nCuO NP supernatants. The morphology for both MG-63 and UMR-106 cells was compromised, resulting in cellular detachment. Furthermore, the effect of nZnO supernatants on UMR-106 becomes more evident as the incubation time increases. While still attached to the surface of the culture flask, their morphology dramatically changed. Cells no longer exhibited their characteristic "flattened" shape and as a result many gaps emerged between individual and their neighbouring cells. This extreme response was not observed for MG-63, however compared to the control and hour 0, cells possessed elongated, thinner and well defined protrusions, indicating the possible inception of cellular detachment. At 4 h, nCuO supernatants visibly destroyed both cell types. Furthermore, no structural or morphological change was observed in both cell types upon exposure to supernatants of $nTiO_2$ NPs.

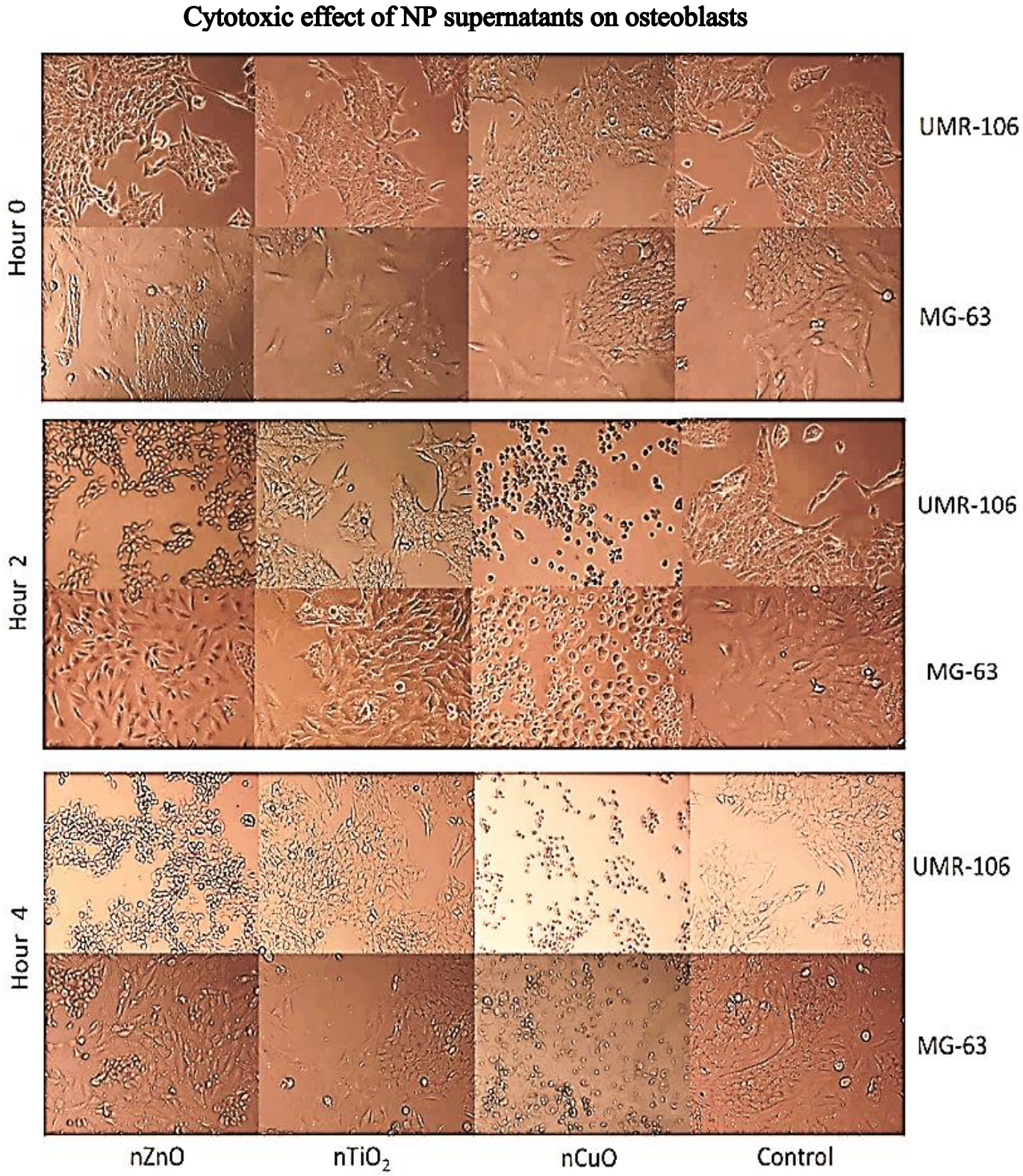

Figure 40 - Supernatants of nZnO, $nTiO_2$ and nCuO on osteoblast-like cells (UMR-106 and MG-63) after 0, 2 and 4 h of incubation. The morphological differences at each time point are taken into consideration as to assess the toxicity of each supernatant.

3.2 Effect of nZnO on morphology of osteoblast-like cells

Osteoblasts (UMR-106) were cultured on different concentrations of nZnO coatings (2500 µg/mL, 5000 µg/mL and 10,000 µg/mL). Bright field microscopy revealed greater number of cells at 2, 24 and 48 h and minimal cell death (Figure 41). Cell interaction with nZnO at different exposure times to coated samples was further characterised by SEM. UMR-106 and MG-63 cells revealed a spindle shaped morphology, characteristic of a normal osteoblast (Figures 42 - 46). Cell morphology was also largely normal in hMSCs, with no signs of physical cellular stress (Figures 47 - 49). Cellular stress based upon electron micrographs are often depicted as numerous large blebs (sphere like protrusions) occurring on the surface of the individual cell, indicating the process of apoptosis. Osteoblasts also displayed filopodia projections that are in close contact with the nZnO surface or in proximity to neighbouring cells. Adhesion to coated nZnO in culture was further investigated by immunofluorescent imaging of the focal adhesion protein paxillin. Cells adhered to higher concentrations of nZnO or the mixture of this NP with nHA showed spreading features, with increased punctate paxillin staining and stress fibres (Figure 50 and 51). Thus nZnO coatings allow osteoblast attachment and focal adhesion formation.

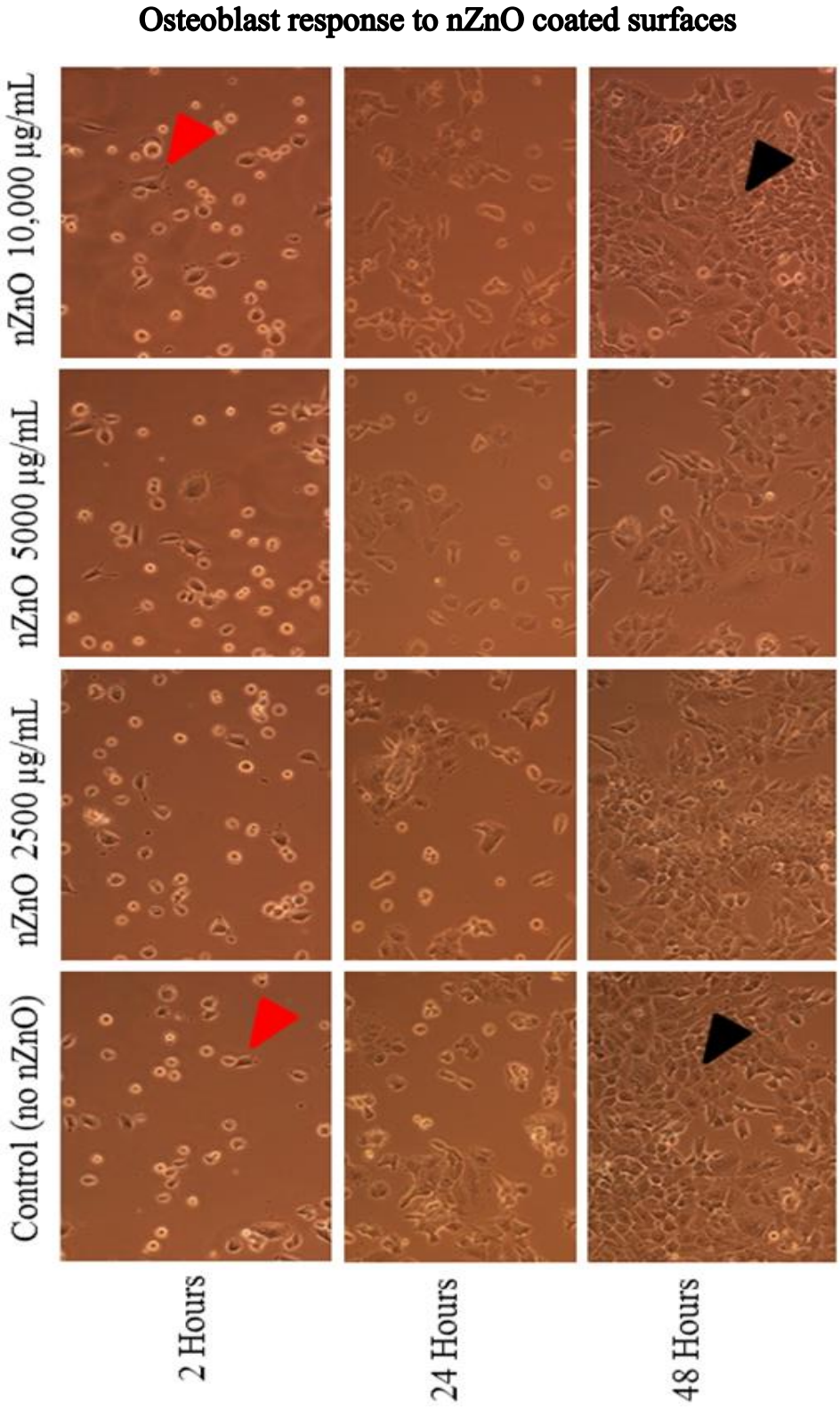

Figure 41 - Seeded UMR-106 (osteoblast-like cells) on the surface of nZnO coated glass samples. The samples were coated with increasing concentrations of nZnO to observe any morphological changes. Phase images show increased numbers of cells at 2, 24 and 48 hours. Red arrows indicate initial attachment of osteoblasts to the substrates after 2 hours of incubation and Black arrows show the similarity of osteoblast confluency between a coated and non-coated substrate.

Filopodia extension: Osteoblast-like cells attached to a nZnO coated surface

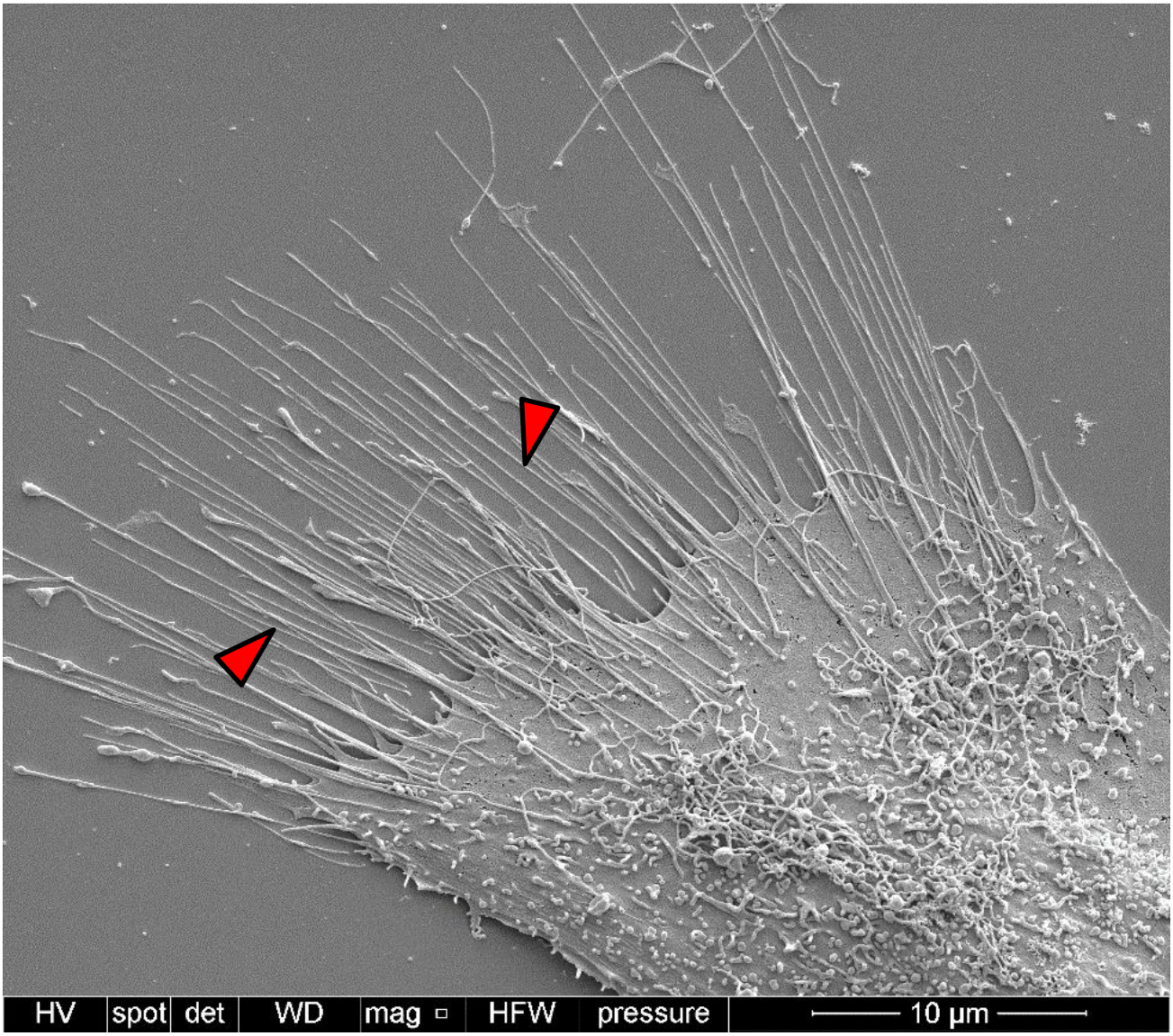

Figure 42 - Osteoblast-like cells (UMR-106) attached to the nZnO coated substrates. An osteoblast like cell is extending its filopodia (red arrows) projection to adhere to the coated surface.

Filopodia outreach: Multiple osteoblast-like cells attached to a nZnO coated surface

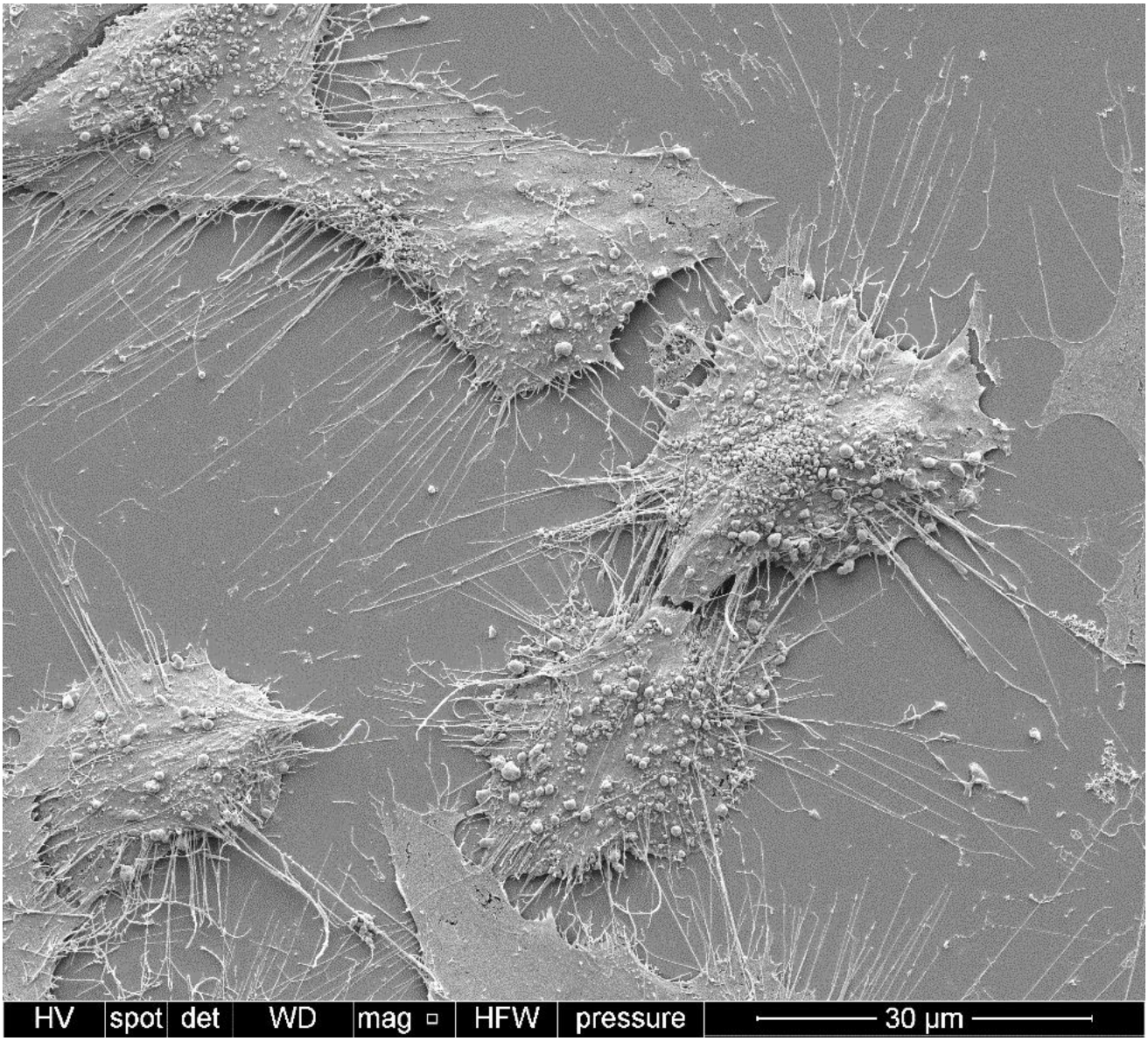

Figure 43 - Osteoblasts exhibiting projection-like structures in order to secure and settle onto the nZnO-coated surface.

Communicating: Two osteoblast-like cells attached to a nZnO coated

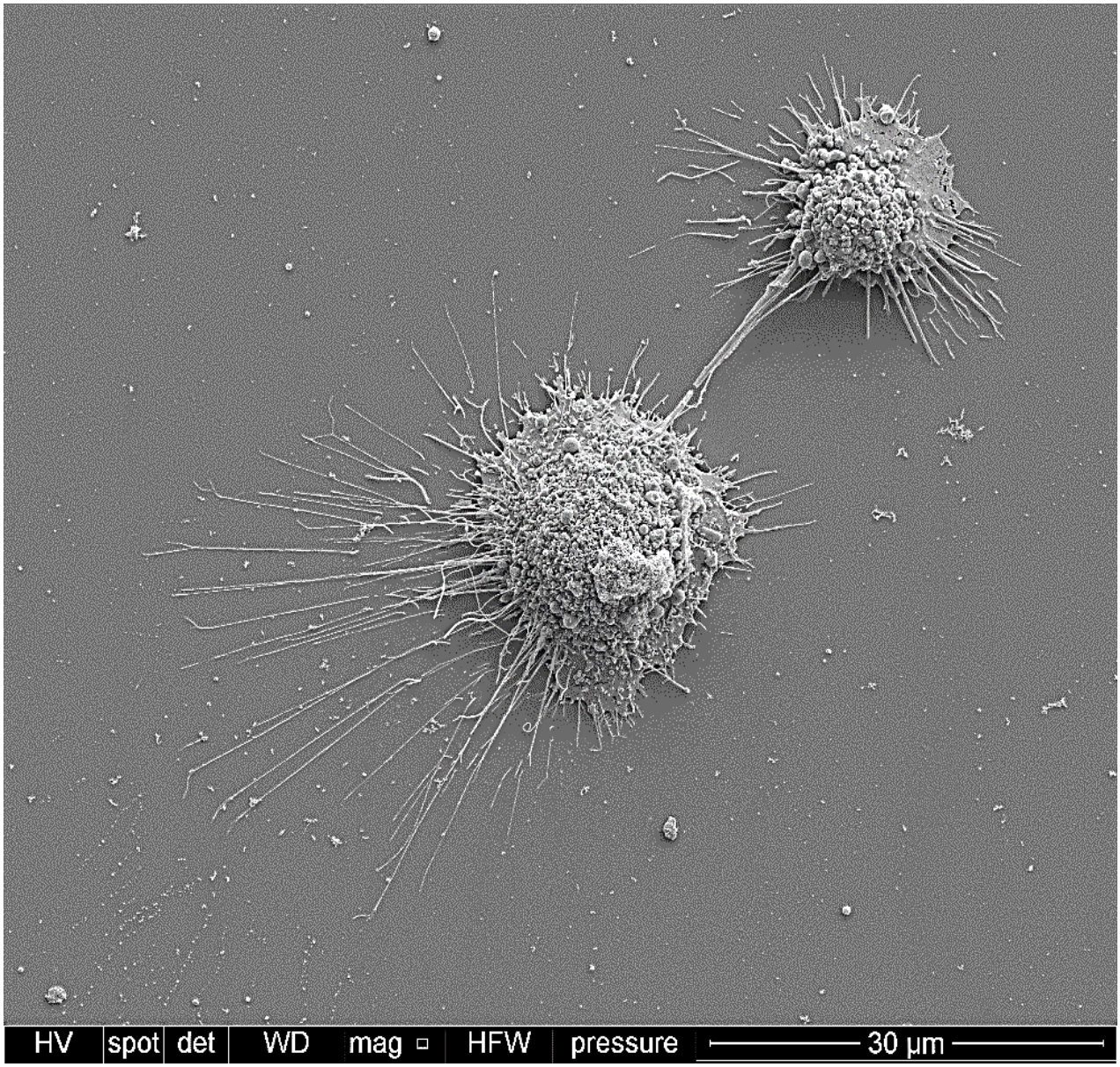

Figure 44 - MG-63 osteoblasts on a nZnO coated surface. Micrograph shows two communicating cells on a surface coated with nZnO particulates.

Interaction on a coated surface: Osteoblast-like cells seemingly interacting while adhered onto nZnO coated surface

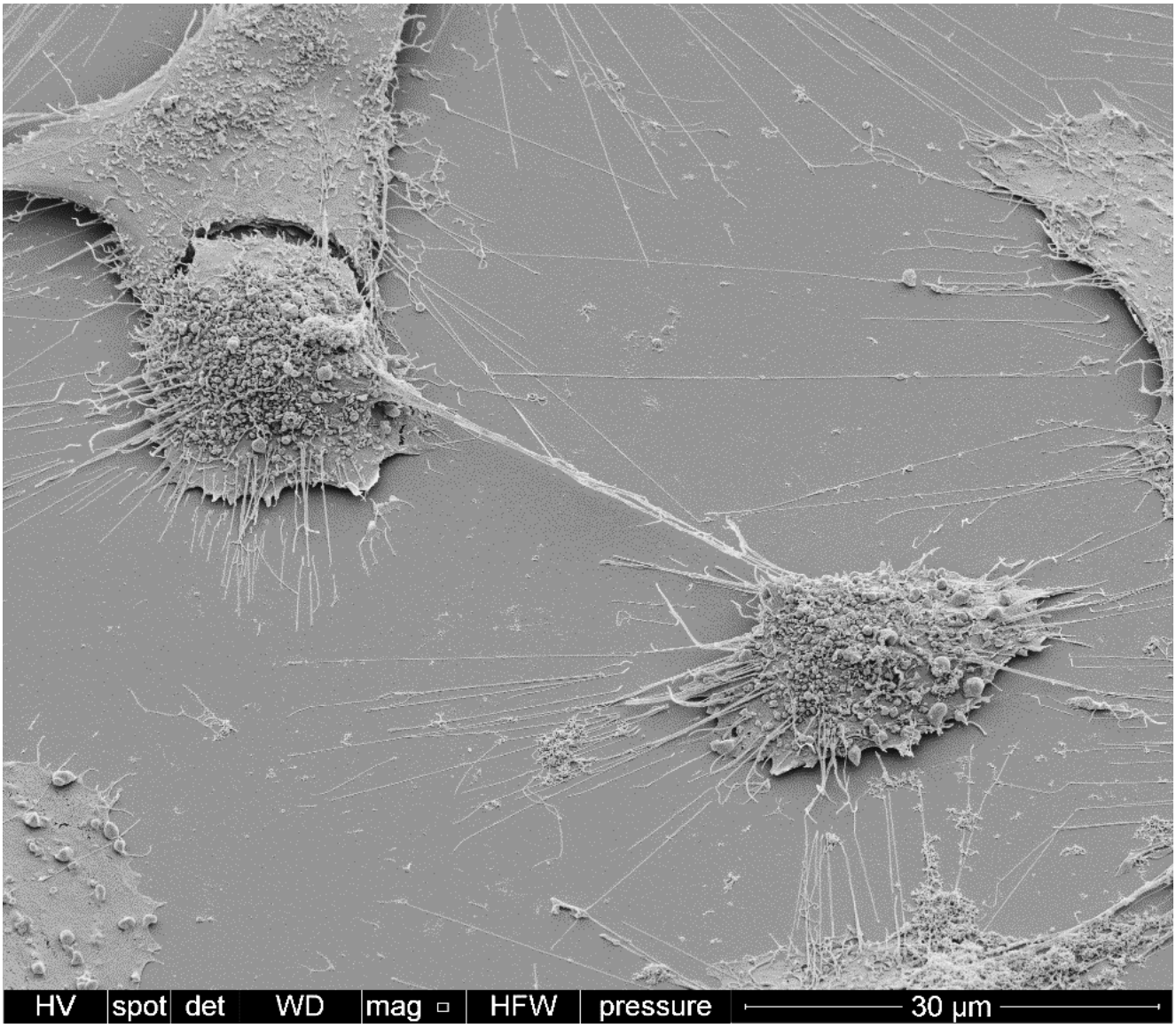

Figure 45 - MG-63 cells on nZnO coated surfaces. Human osteoblast-like cells on a coated surface, surrounded by other already adhered osteoblasts.

Dividing cells: Human osteosarcoma cell lines

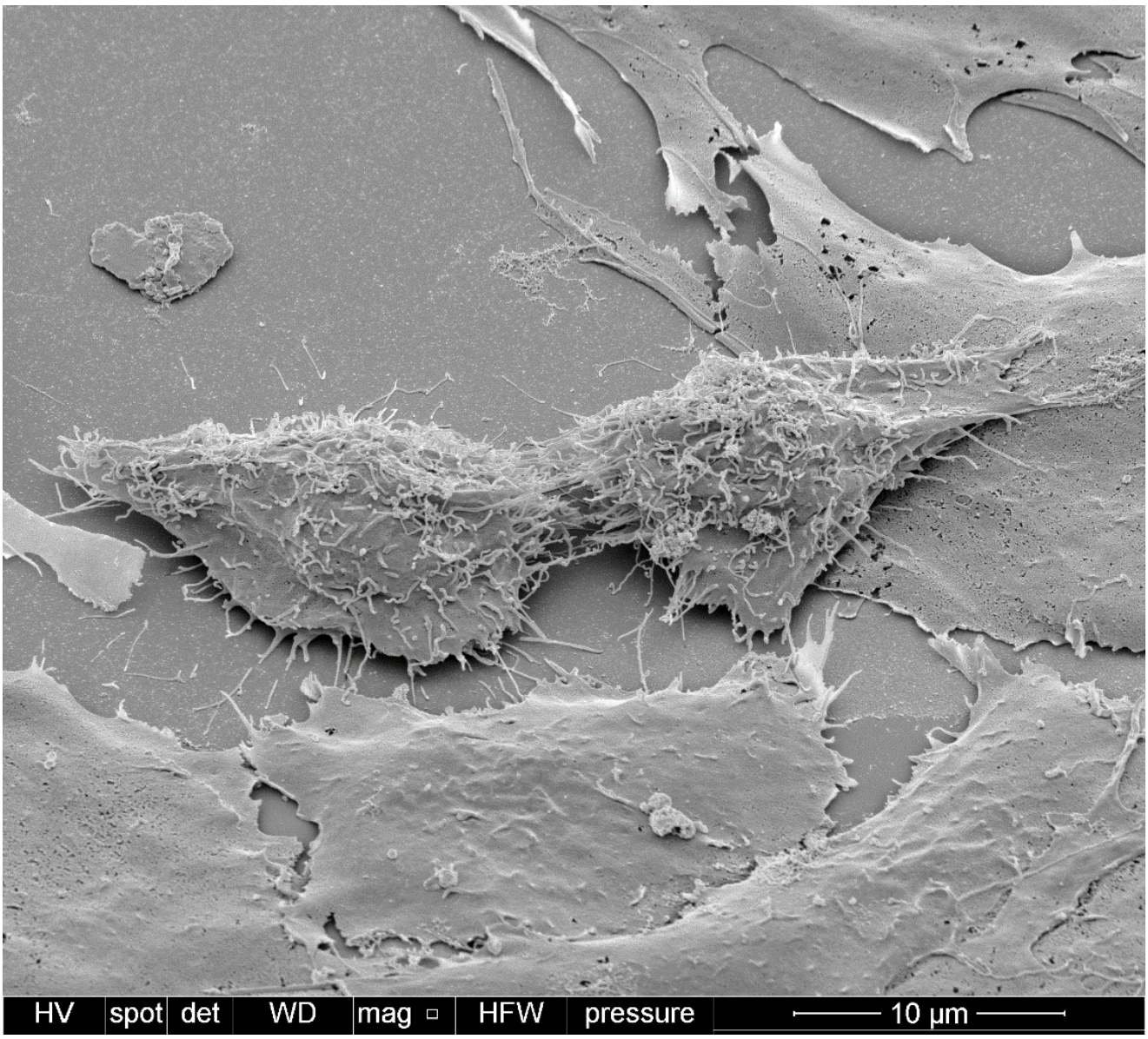

Figure 46 - Two MG-63 (osteoblast like cells) interacting on the 100% nZnO coated surface (10,000 µg/mL). The uniformly nZnO-coated surface is visible below and beneath the cells. The active mini cell membrane filopodia suggest a very healthy, metabolically active cell.

A mesenchymal stem cell adhering onto a nZnO coated surface

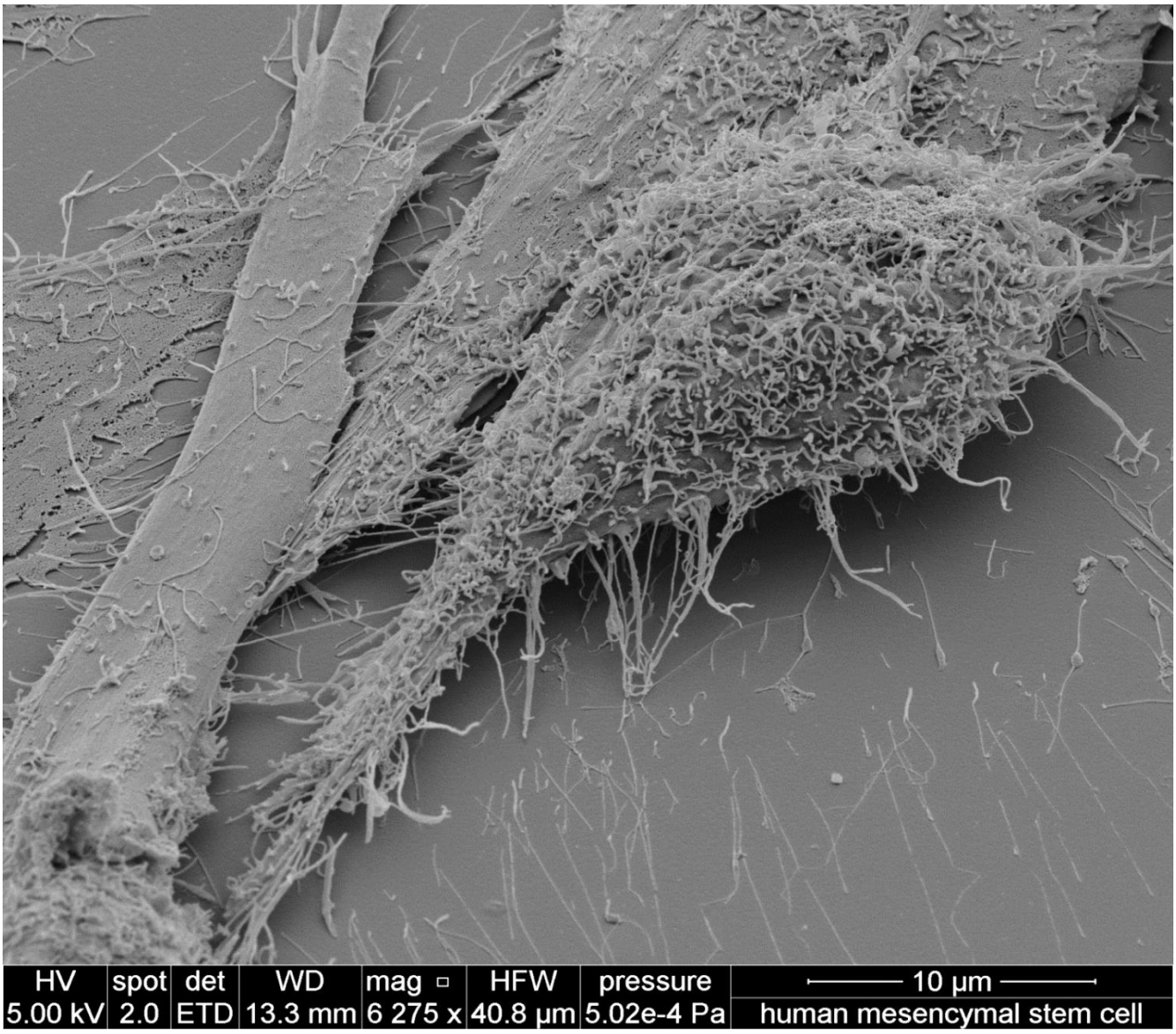

Figure 47 - hMSC cells are able to attach to the surface of composite coated substrtaes. An SEM and an optical representation of mesenchymal stem cells adhered to the surface of nano-coated substrates.

A group of flattened hMSCs on a nano-coated surface

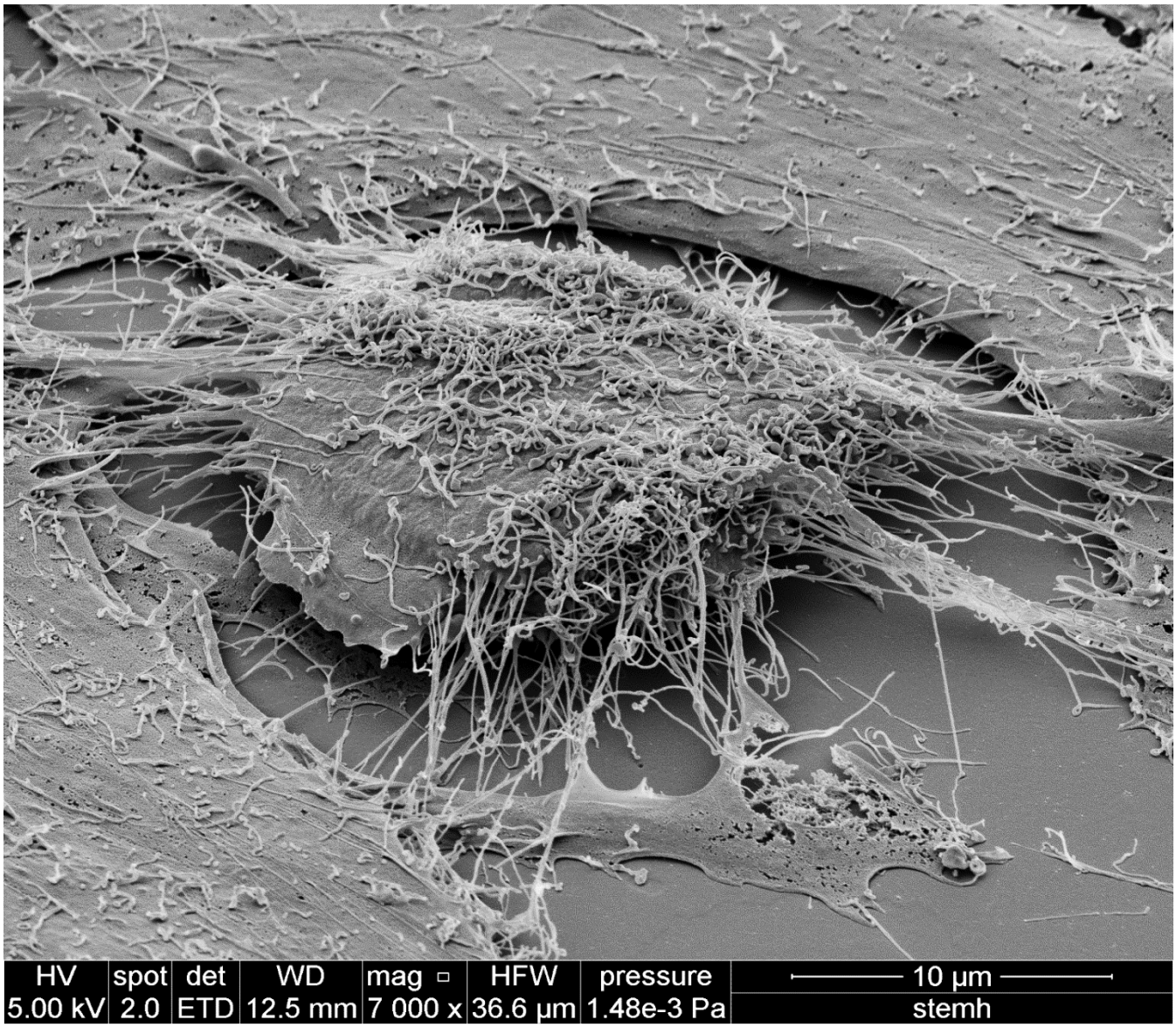

Figure 48 - hMSC adhered to the nZnO coated surface. C & D) Cells adhered to a suitable surface and eventually become flattened. Other attached cells can be observed in close proximity to all these adhering cells.

Cell adhesion: hMSCs are capable of forming a healthy looking monolayer on a nano-coated surface

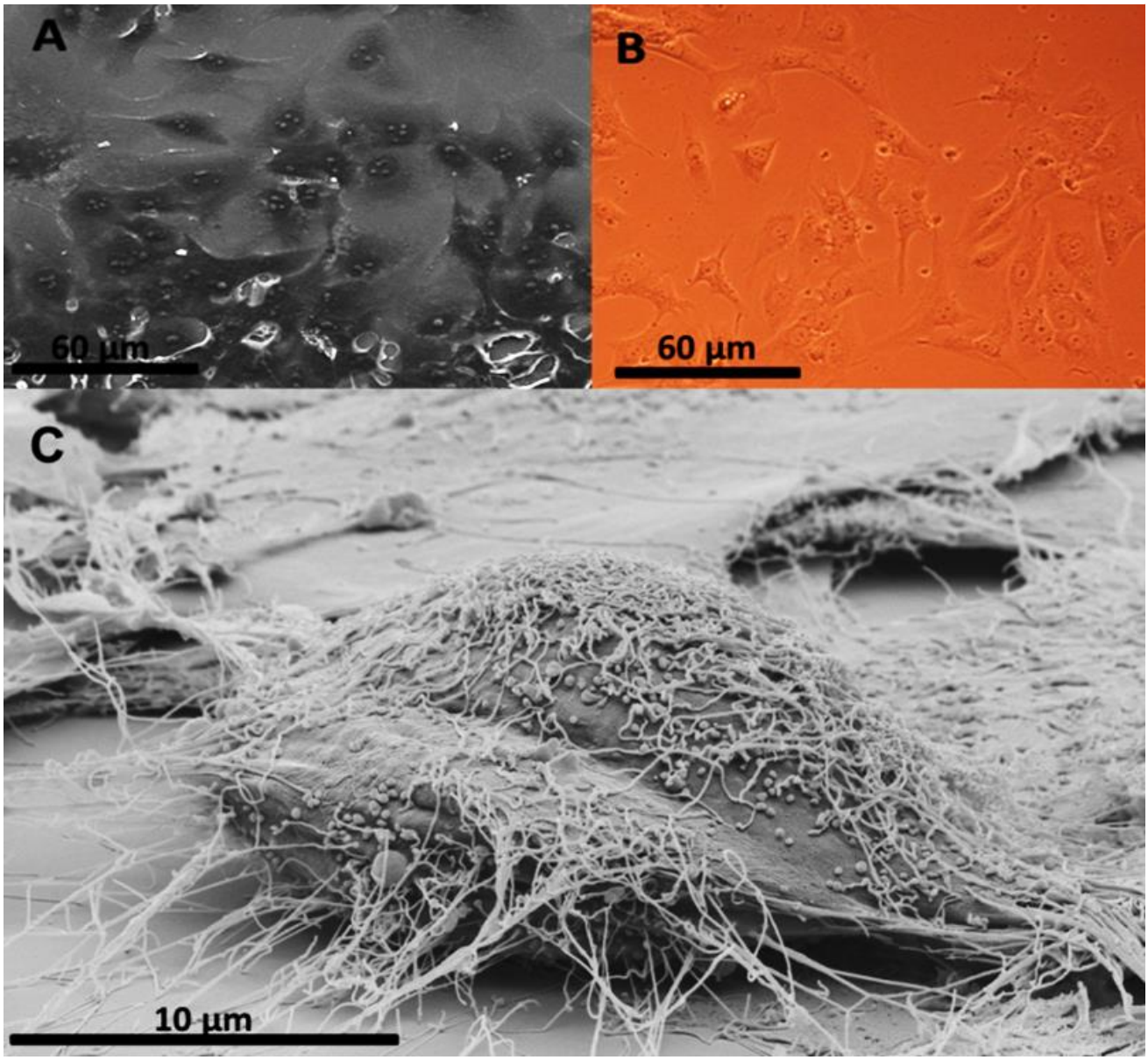

Figure 49 – Mesenchymal stem cells on a nZnO coated surface. A) Electron micrograph of a cell monolayer of hMSCs, B) Light microscopy representation of the same monolayer, C) Electron micrograph showing a cell elongating its filopodia for an appropriate place to adhere

Phalloidin, a toxin that binds to actin filaments allows clear visualisation of the structural integrity of fixed cells. Actin filaments are visualised as red fine structures that are viewed within the cytoskeleton of the cell. The present findings suggest that cells attached onto all coated samples, have a stable morphological integrity. Adhesion points, whereupon osteoblasts make contact with the nano-coated surface, are highlighted by the level of paxillin expression. The red-coloured adhesion markers (highlighted by the white arrows) specify regions where cells have made contact with the surface of the coating. Qualitative assessment of the level of paxillin expressed in each individual staining suggests an increased expression present for samples that have an increased concentration of nZnO coated on their surfaces. This observation is verified by the quantitative analysis of the paxillin expression points (Figure 52). The focal adhesion counts for UMR-106 cells show no significant difference between all coated samples as compared to the control or within multiple samples. This is different for MG-63 focal adhesion counts where there is a significant increase in counts ($p < 0.01$) of nZnO + nHA composite coatings in comparison to other coatings. Furthermore, the nZnO alone coating has the second highest focal adhesion counts as compared to nHA and the uncoated surface (control).

Comparison of osteoblast focal adhesion points on nano-coated surfaces (MG-63)

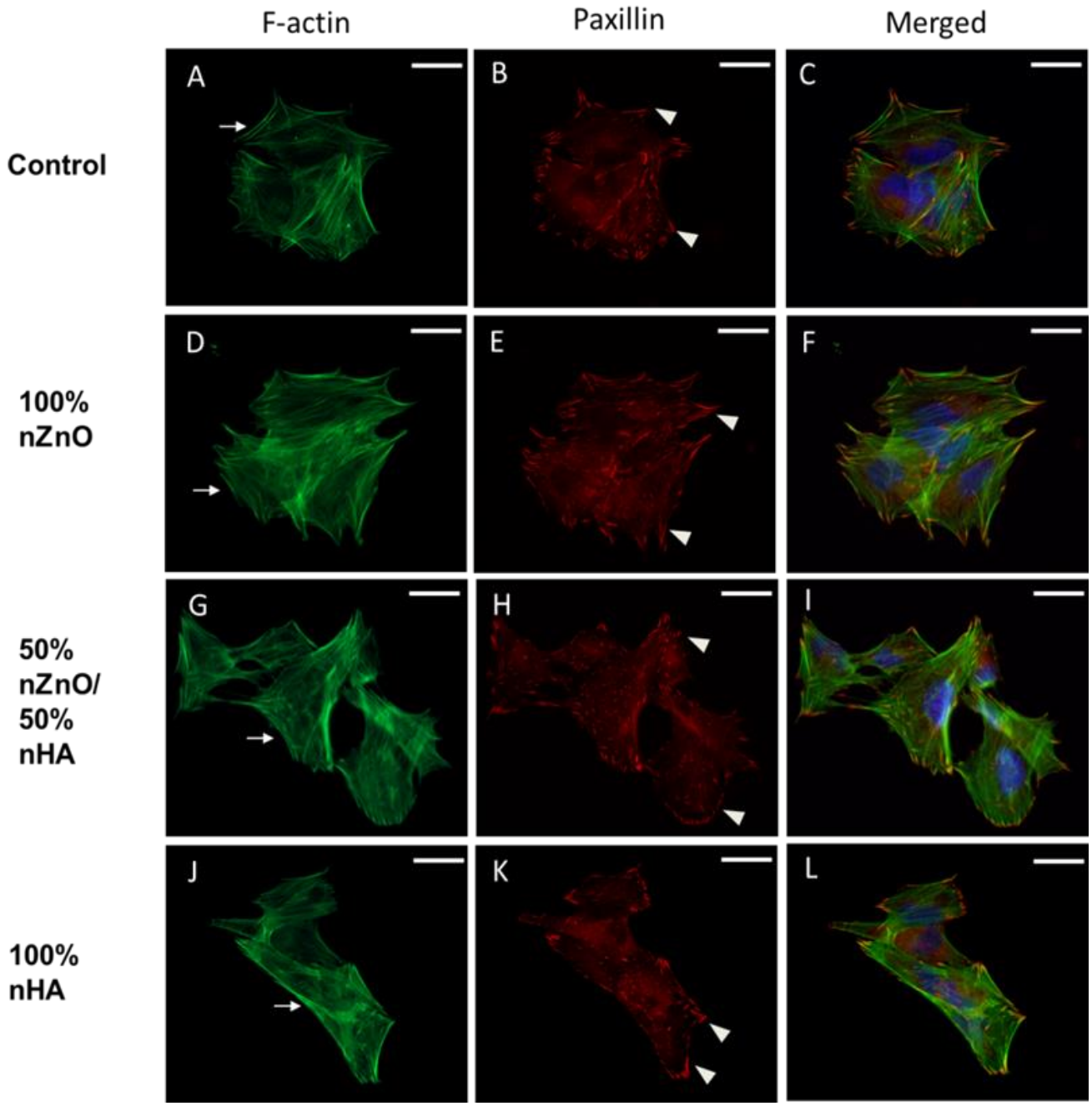

Figure 50 - Effect of nZnO and nHA on actin cytoskeleton and focal adhesions. Fluorescent images of actin filaments (arrow heads in A, D, G, J) and focal adhesions (arrows in B, E, H, K). Human osteoblast-like cells (MG-63) cultured for 24 hours on 100% nZnO, nHA and 50% nZnO coatings show more marked focal adhesions (E, H, K) compared to control (B). Scale bars = 50μm (Memarzadeh et al. 2014).

Comparison of osteoblastic focal adhesion points on nano-coated surfaces (UMR-106)

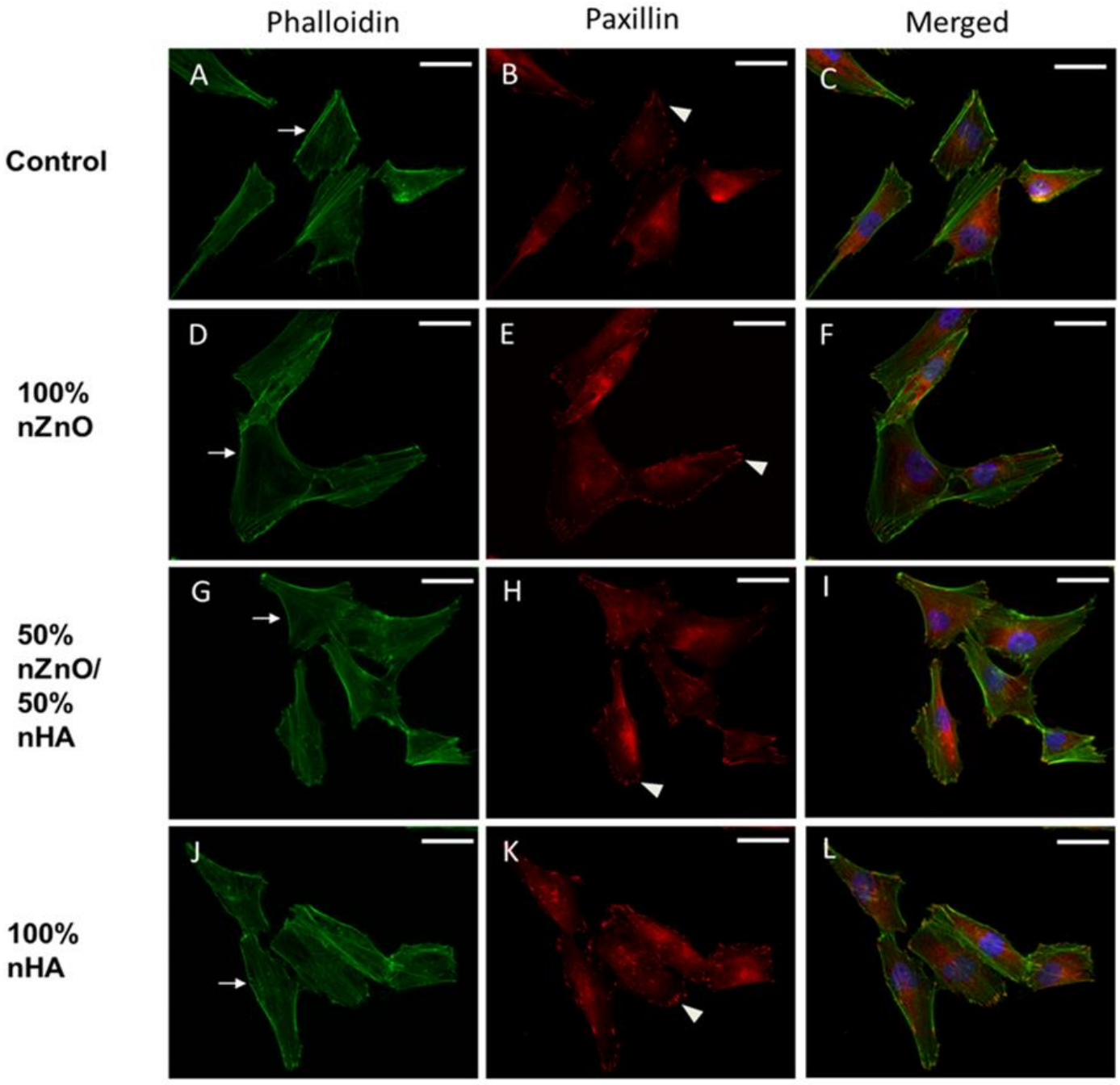

Figure 51 - Effect of nZnO and nHA on actin cytoskeleton and focal adhesions. Fluorescent images of actin filaments (arrow heads in A, D, G, J) and focal adhesions (arrows in B, E, H, K). Human osteoblast-like cells (UMR-106) cultured for 24 hours on 100% nZnO, nHA and 50% nZnO coatings show more marked focal adhesions (E, H, K) compared to control (B). Scale bars = 50μm (Memarzadeh et al, 2014).

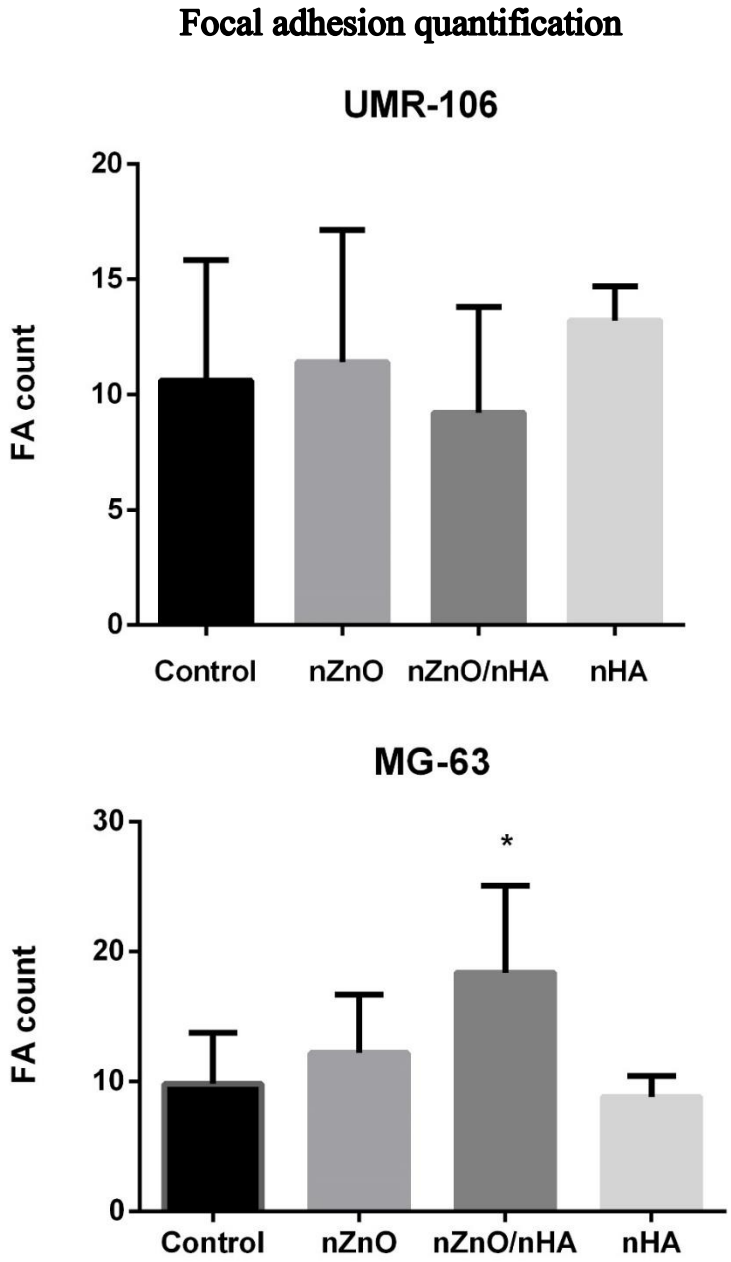

Figure 52 - Comparison of focal adhesion points of osteoblast-like cells on coated samples. No significant change in focal adhesion (FA) expression (paxillin) was observed for UMR-106, while MG-63 cultures on composite mixture of 50% nZnO and 50% nHA showed an increase in FA expression. n =5, $p < 0.01$, SD+.

3.3 Osteoblast cytotoxicity, viability and proliferation

Lactate dehydrogenase (LDH) production and release from supernatants derived from suspended NPs (TiO_2 and ZnO) (Figure 53 and 54) and coated nZnO (in cell culture medium) were measured from UMR-106 cells (Figure 55 and 56). No significant LDH release was observed under both conditions.

Moreover, osteoblasts seeded on NP surface coatings demonstrated an increase in proliferation (Figure 57) and alkaline phosphatase release (Figure 58), with the higher nZnO percentages showing an increased activity in both. While the general trend for proliferation for days 5 and 10 is increasing as the concentration of coatings of nZnO is increased, this trend does not apply to cells seeded onto composites of nZnO + nHA (50% nZnO + 50% nHA and 25% nZnO + 75% nHA). Osteoblasts seeded on the composite mixtures do not show any significant proliferative activity between days 5 and 10. This trend was found to be similar when findings for ALP activity was similarly evaluated. In both cases, the relative activity of cells when seeded onto mixtures of nHA and nZnO show decreased activity when compared to a sample with no coating.

In addition, measurement of cytokine release (TNF-α and IL-6) revealed that no inflammatory response was induced when cells were allowed to adhere on coated surfaces (data not shown).

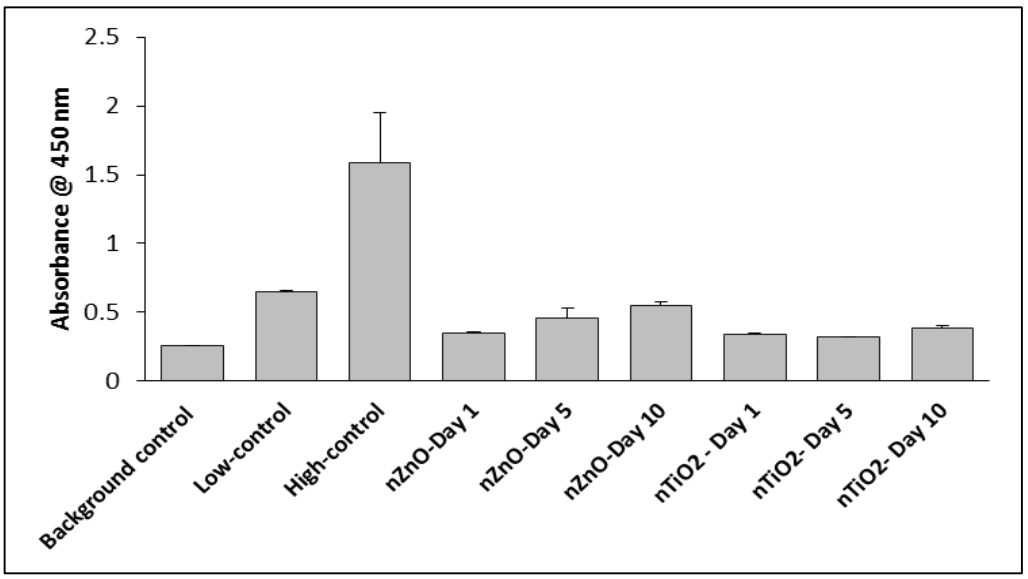

Figure 53 - Cytotoxicity assay. Lactate dehydrogenase (LDH) release from cells exposed to supernatants of suspended nZnO and $nTiO_2$. Each suspension was incubated for an extended amount of time (1, 5 and 10 d) and its supernatant tested on UMR-106 cells; n = 4, ±SEM

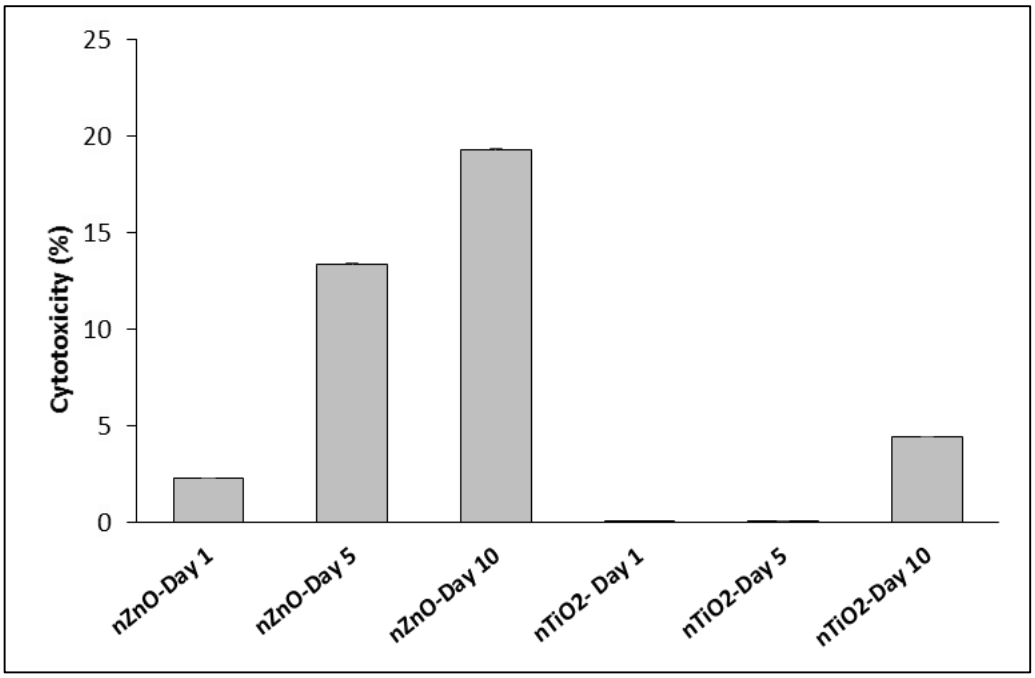

Figure 54 - Percentage cytotoxicity instigated upon UMR-106 cells by supernatants of suspended nZnO and $nTiO_2$. n =4, ±SEM.

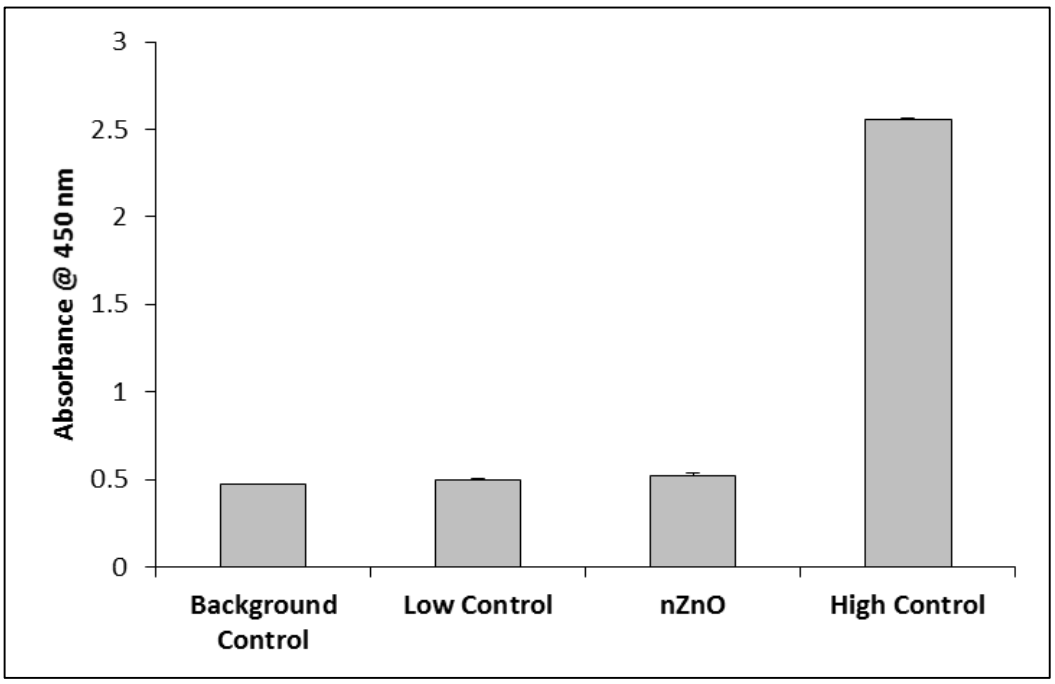

Figure 55 - Cytotoxicity assay. Lactate dehydrogenase (LDH) release from the seeded UMR-106 cells (1×10^4). High-control = lysis buffer + osteoblasts, Low Control = cell culture media + osteoblasts, Background control = cell culture media. n =4, ±SEM.

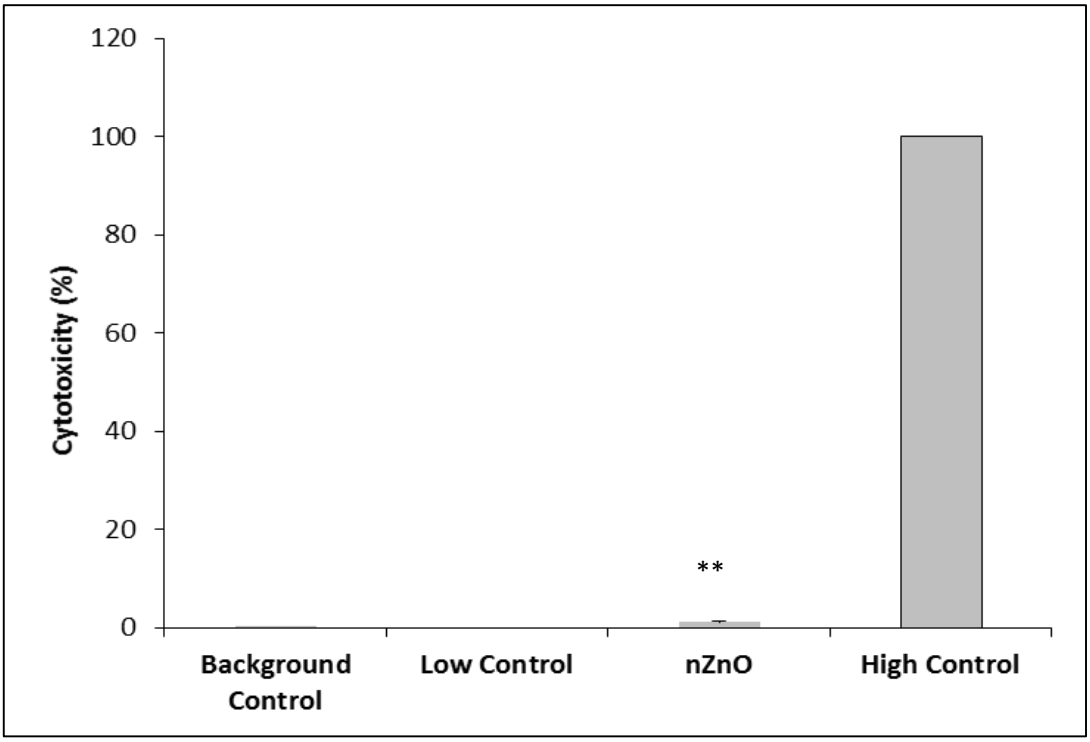

Figure 56 - Percentage cytotoxicity of coated nZnO samples instigated upon osteoblasts. n =4, ±SEM. Significance compares the level of toxicity of the nZnO coated substrate to both background and low control, $p < 0.05$.

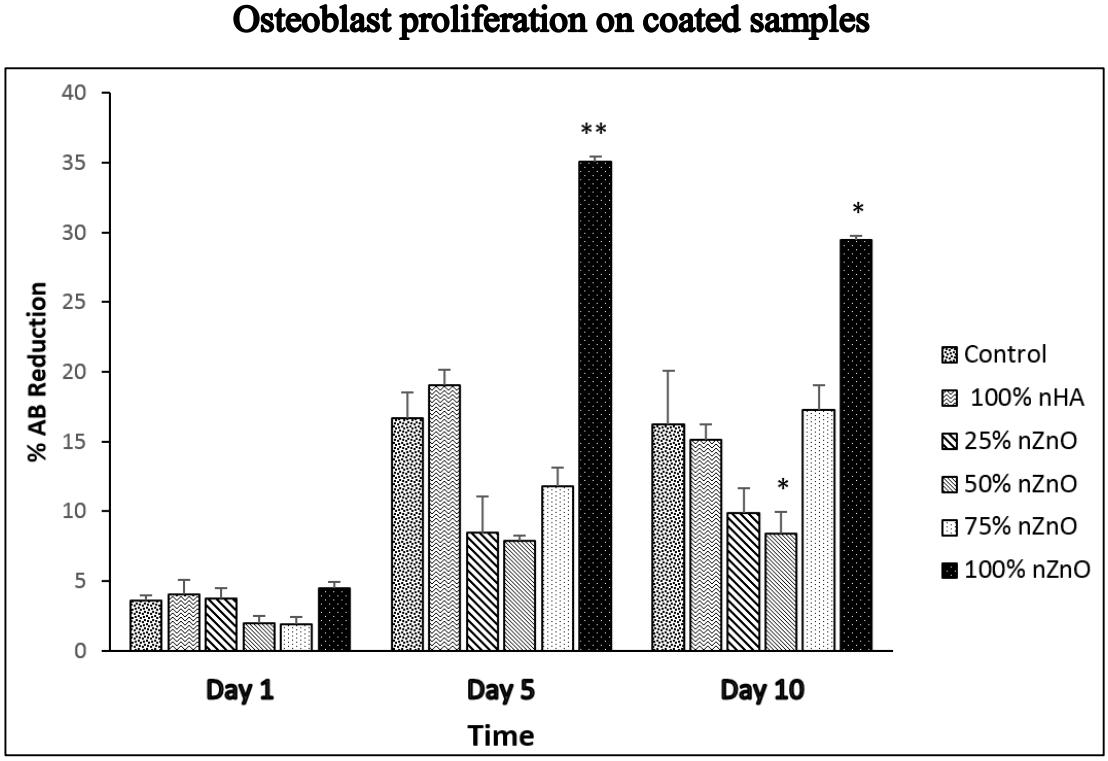

Figure 57 - Proliferation assay (AlamarBlue) of UMR-106 cells. Cells were monitored on mixtures of coated samples at three time points, day 1, day 5 and day 10. Mean ± SEM, n=4, * = $p < 0.05$, ** = $p < 0.001$.

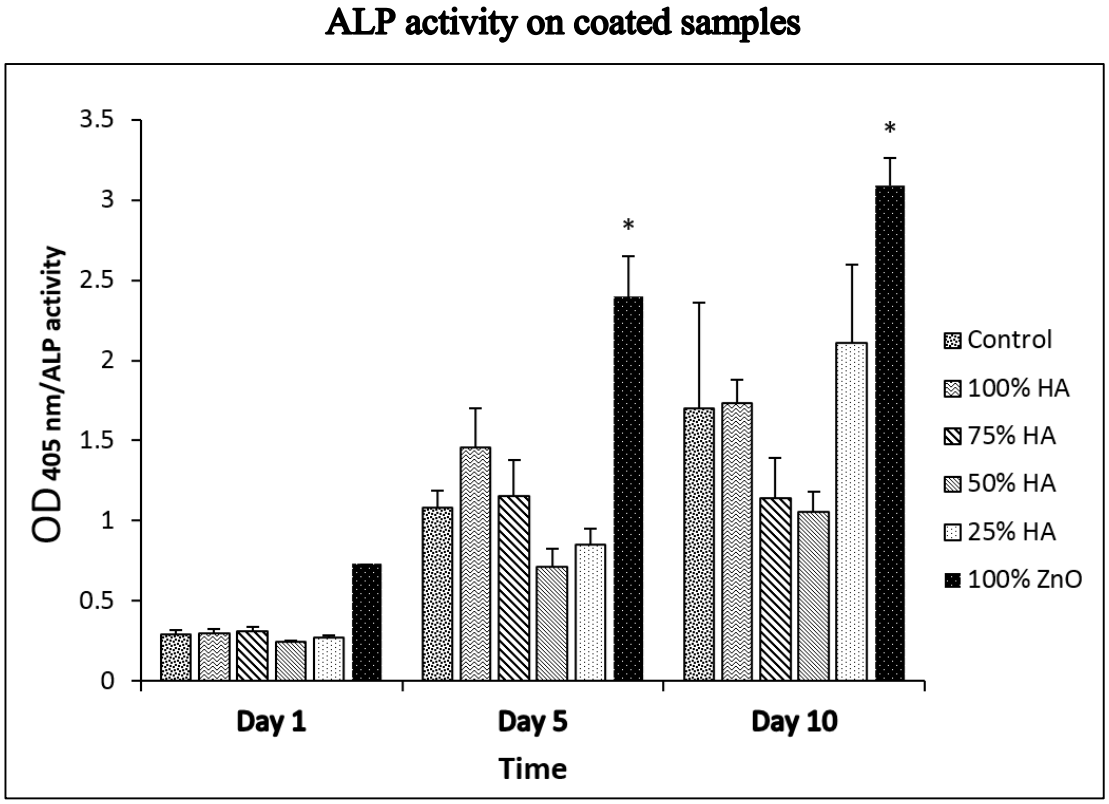

Figure 58 - Alkaline phosphatase (ALP) activity in UMR-106 cells. ALP release was measured from cells on coated mixtures at 1, 5 and 10 days. The asterisks indicate the ALP release between 100% nZnO and both 50% and the control. Mean ± SEM, n=4, * = $p < 0.05$

3.4 Collagen expression

Collagen expression for each sample was observed using Sirius red staining. Regions where collagen expression was prominent are stained red with a yellow background. Samples coated with 50% nHA + 50% nZnO and 100% nZnO showed an increased level of collagen production as compared to the control and 100% nHA. Also a comparison between these two samples indicates an equal level of collagen deposition. This was visualised when observed with an optical microscope, where a clear distinction between stained regions and the other non-stained regions were evident (Figures 59). At day 5, dispersed collagen expression for all samples was observed, the homogeneity of these scattered regions being greater for the 50/50 composite where stained regions were not so confined to a specific region and were comprised of smaller stained regions that together form the broader stained regions. At day 15, a more concentrated collagen deposition at all regions can be observed. This was very well defined and distinct for all samples compared to control, particularly on the 100% nZnO coated substrate. An additional observation to identify regions stained for collagen was carried out by adjusting the threshold for the colour red (Figure 60 and 61). This allowed for a unique insight into the distribution of collagen production on each specific substrate, giving an accurate comparison between all samples.

Collagen staining of osteoblasts on nano-coated samples

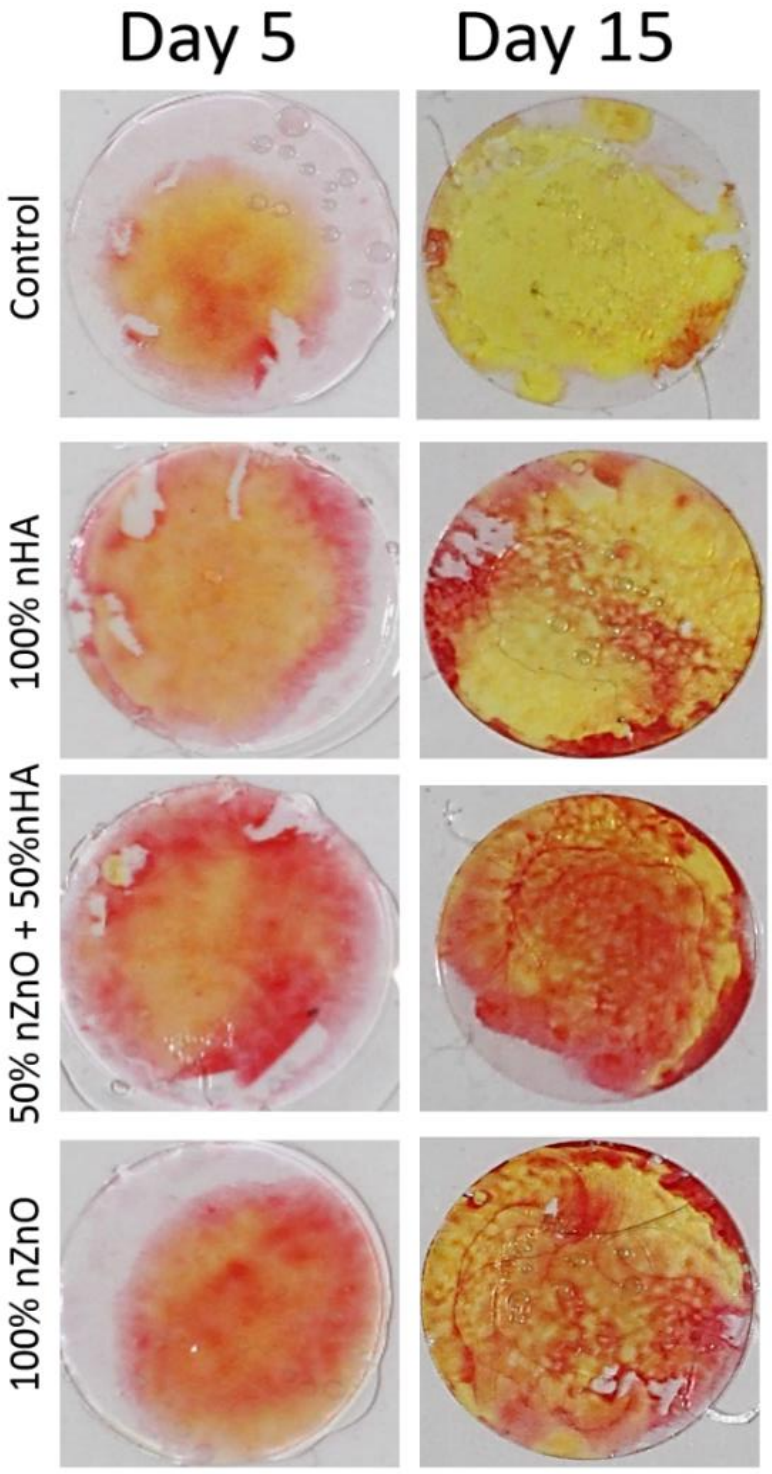

Figure 59 – Sirius red stained osteoblasts (UMR-106) seeded onto coated glass substrates for 5 and 15 days. Red regions indicate collagen expression. Controls = uncoated coverslips.

Relative collagen distribution on nano-coated samples

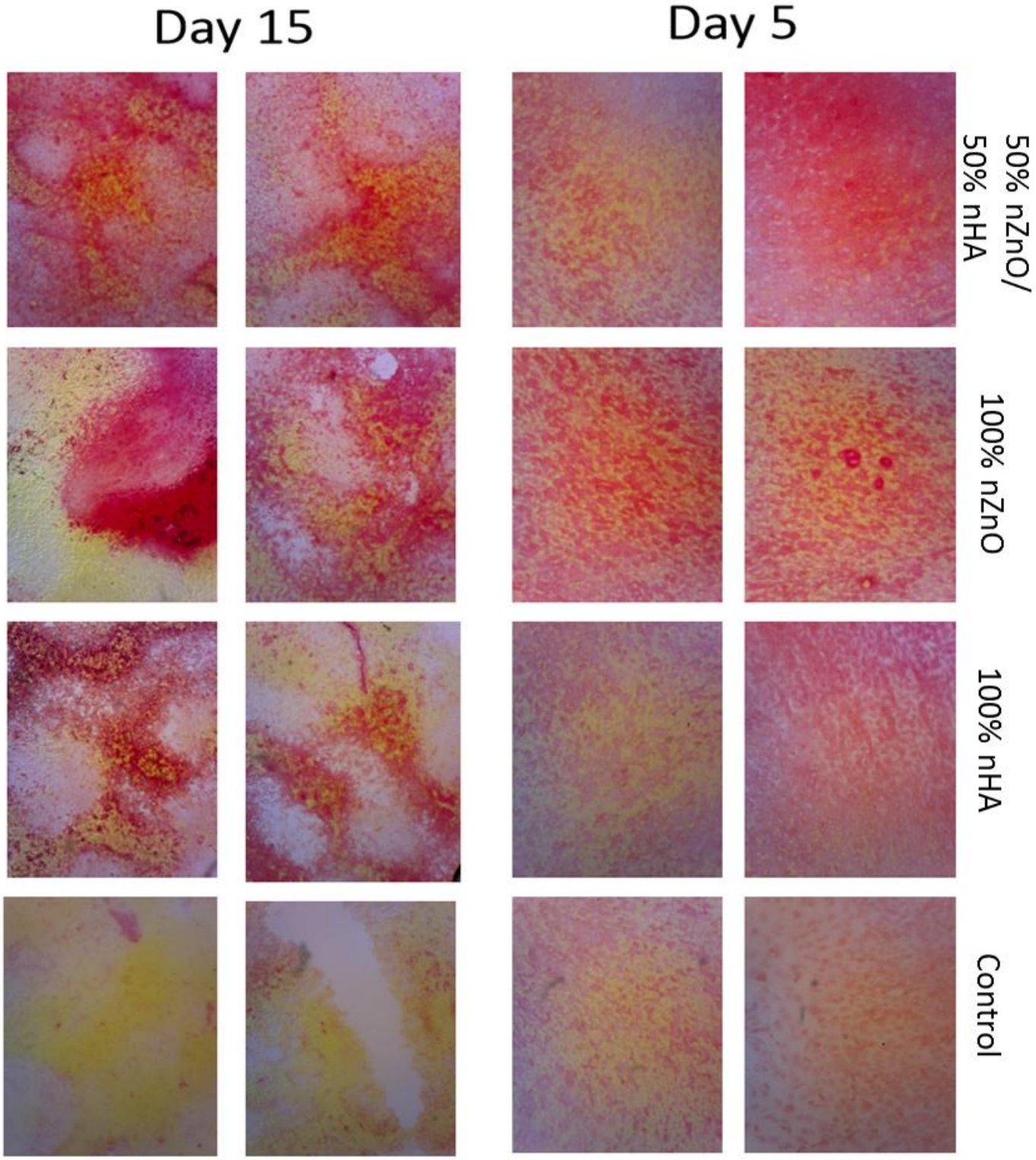

Figure 60 – Collagen staining of osteoblast cultures after 5 and 15 days. 50% nZnO + 50% nHA, 100% nZnO and 100 nHA coated surfaces were compared to control. Regions stained with the colour RED are considered to be comprised of collagen type I. Light microscopy = objective x4.

Image thresholding: distribution of collagen on coated samples

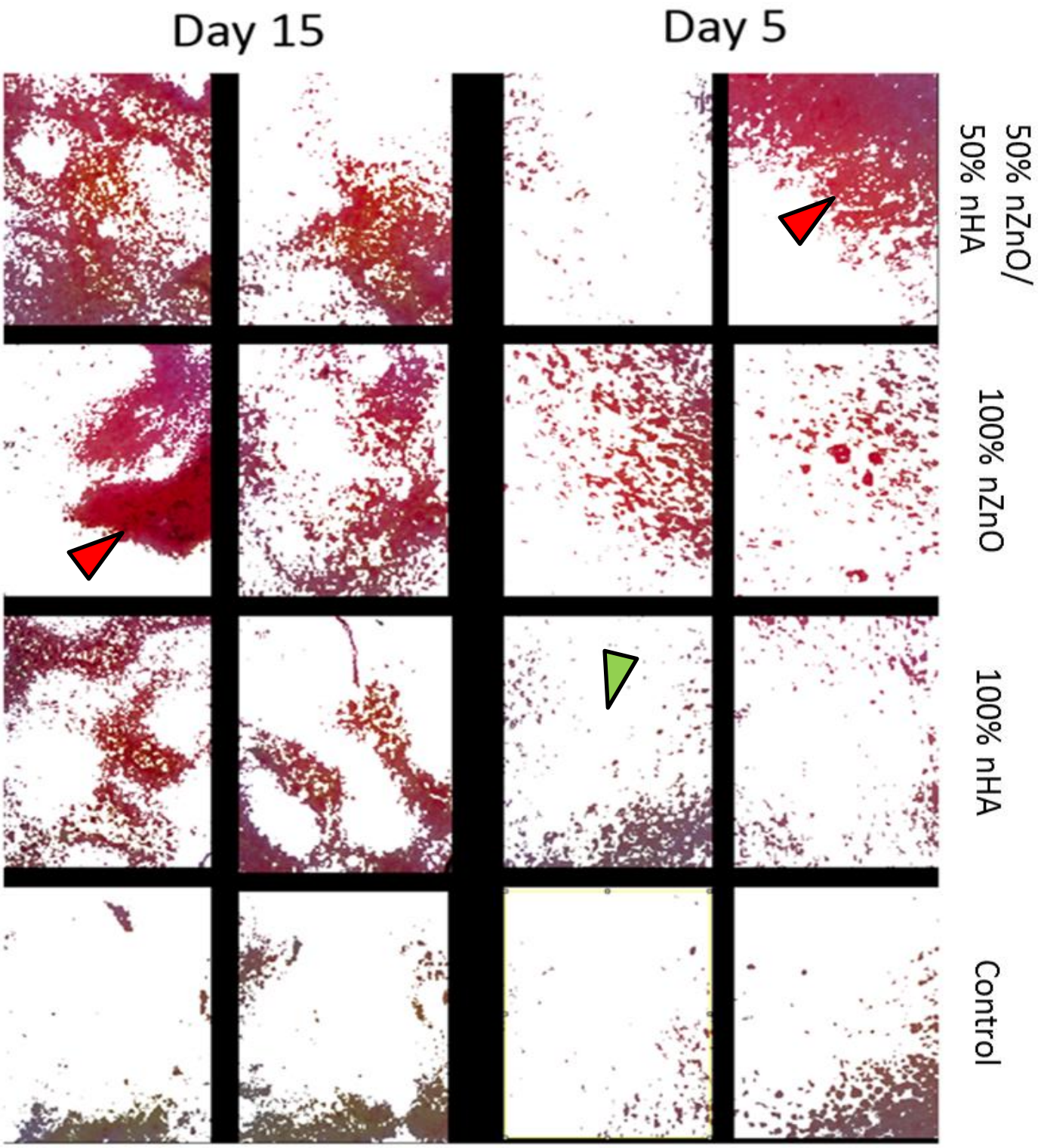

Figure 61 – Threshold-adjusted stained regions. These adjusted micrographs highlight regions of interest for each sample. All stained regions are considered as clusters of osteoblasts that have expressed collagen type I and the white regions are not stained. Thresholding refers to an image processing technique where a specific region of interest is singled out against the background to highlight the region of interest. In the present case the region of interest are stained with Sirius red for Collagen. Red arrows depict regions of stained collagen while the green arrow depicts non-stained regions

4. Discussion

It is essential to provide evidence for the biocompatibility of a prospective bone implant. The term biocompatible refers to an object with overall properties that are not detrimental *in vivo*. This implies that upon exposure to osteoblasts or other relevant cells, the nano-coated prototype remains non-toxic or refrains from causing an inflammatory response or cell death (Williams, 2008). A series of limited but thorough studies have been carried out in order to address this particular issue.

Previous chapters in this thesis dealt with the toxicity of various NPs against given species of bacteria. It is also necessary to observe the "indirect effect" of some of these NPs on eukaryotic cells, i.e. osteoblasts. The term "indirect" refers to the effect that these NPs instigate when not in direct contact with eukaryotic cells, i.e. the exposure of cells to NP-derived supernatants. Some studies have concluded that most nanoparticulates, and certainly those tested in this study (nZnO, $nTiO_2$ and nCuO) instigate direct damage to multicellular organisms (Moore, 2006, Mortimer et al., 2010, Wang et al., 2009). There is, currently, no direct evidence as to how this direct damage maybe caused. The current consensus in this research area speculates that the toxic nature of the NPs is solely due to the amount of ion release into their surrounding environment, while other studies suggest that these effects are a combination of different factors such as ROS generation and direct contact (Sharma et al., 2009a). Indeed, NPs are often produced via different procedures and therefore their effects on cells may also differ. The important distinction between direct and supernatant exposure of cells is the removal of the "physical" aspect of the nanoparticulates. Our previous provisional investigations indicate that lower concentrations, as compared to NPs used for obtaining the present supernatants, are detrimental to eukaryotic cells. CuO supernatants are more toxic than other metal

oxide derived supernatants on immediate exposure to cells. An immediate morphological change and a separation of the cells from the flask indicated that CuO supernatants are toxic to both cell-lines tested. This observation is in accordance with work that has been reported on the effect of copper on various eukaryotes (Chen et al., 2011, Mortimer et al., 2011). This morphological change can also occur when cells are exposed to nZnO supernatants; however no change is evident when compared to cells exposed to $nTiO_2$ supernatants. Considering the high concentration of nanoparticulates, these findings are not surprising and essentially highlight the intricacies involved with testing for "cytotoxic effects" of these agents. By observing these results and evidence for osteoconductivity of titanium dioxide it can be deduced that $nTiO_2$ coated implants are an option for a biocompatible coating (Wu et al., 2012). However this agent is optimally bactericidal under certain conditions (i.e. when exposed to UV or normal light) and therefore cannot be utilised as a coating that needs to be enclosed in a closed biological environment (Fu et al., 2005). Qualitative observations of cell adhesion assays indicated much potential for nZnO. Since all other nanoparticulates were excluded as regards to their biocompatibility, nZnO was tested for its direct effect on osteoblasts.

Results obtained from time based cell culture studies on nano-coated substrates did not demonstrate any adverse morphological difference between osteoblasts cultured onto high concentration coatings and those cultured on low concentrations. Recently, a study investigating the effect of ZnO on osteoblasts has shown that synthesised ZnO nanoflowers have the capability to promote cell adhesion, osseointegration, growth and proliferation (Park et al., 2010). The current nZnO coated prototypes show that at 10,000 µg/mL, a relatively high concentration, osteoblasts are able to adhere and proliferate, without displaying signs of toxicity.

Additional evidence provided by electron micrographs confirmed these findings by showing cells with elongated filopodia and projections that lead to cells adopting a flattened shape on the nano-coated surfaces. In addition, cellular communication and division is also evident, whereupon osteoblasts undergo the process of mitosis on a surface coated with nZnO. These results are reinforced by comparative observations made with assessment of paxillin expression in osteoblasts. Paxillin is part of a larger complex of proteins, the so called focal adhesion proteins. These proteins include paxillin, vinculin and alpha-v beta 3 integrin. Briefly, their main function is to increase cellular adhesion and therefore reduce cell migration (Turner, 2000, Wozniak et al., 2004, Yano et al., 2004). Integrins bind to the extracellular matrix such as collagen and fibronectin, allowing the cell to attach to a suitable substrate. Furthermore, expression of paxillin can be seen in the current studies whereupon osteoblasts exposed to coatings with increased concentrations of nZnO express an equal or more levels of paxillin. Limited studies have confirmed the role of calcium and zinc in promoting the expression of focal adhesion points (Nayab et al., 2005, Xu et al., 2013). Comparatively, the expression of paxillin is relatively higher in samples that contain increasing concentrations of ZnO NPs. However this only applies to cells derived from human origin (MG-63), whereby focal adhesion points on coatings with mixtures of nHA and nZnO showed significant difference as compared with other samples. Focal adhesion counts showed no significant difference between all coated samples for rodent based osteosarcoma cells (UMR-106). This stark difference between multiple cell types highlights the intricate processes involved in cell adhesion and how cellular behaviour is likely to be species dependent. In general, exposure to high concentrations of nanoparticulates can be detrimental (Sharma et al., 2009b). When eukaryotic cells are introduced to a toxic

environment/material, the phospholipid bilayer may rupture and intracellular compartments of the cell escape to the extracellular medium. Release of the enzyme lactate dehydrogenase (LDH) is a useful indicator of cytotoxicity (Huang et al., 2010). In the present study, to examine exposure of cells to supernatants of $nTiO_2$ and nZnO, the supernatant derived from nZnO did not elicit significant toxicity when compared to osteoblasts placed in normal media. Although eliciting a greater response than $nTiO_2$, there was no significant increase in toxicity between days 5 and 10. Similarly, low LDH release was detected when cells were cultured onto nZnO coated surfaces.

In order for early bone formation to occur, the conditions surrounding the implant should provide a suitable environment for osteoblast attachment and proliferation. Therefore it is essential that the implanted prosthesis has the capability to be both osteoconductive and biocompatible. This study showed an increase of proliferative activity after 5 and 10 days for all coated samples; this effect was greater with both 100% nHA and nZnO coated samples. ALP activity was also assessed using osteoblastic cells (UMR-106). A time dependent increase in ALP was observed with all samples and was associated with samples having a higher percentage of nZnO. This effect could be due to the role that Zn^{2+} plays in regulating the metabolism of bone. Studies report that zinc deficiency decreases calcium deposits in the extracellular matrix (ECM) (Hie et al., 2011). In fact ALP contains Zn as a cofactor and its deficiency causes the dissociation of phosphomonoester, an enzyme hydrolysed by ALP that is directly related to bone mineralisation (Alcantara et al., 2011). Furthermore, the surface charge of each coating (nHA and nZnO), could have an effect on the ion release of these particles, as adsorption of ions onto the surface of the material is a possibility once a composite is formed. It can be hypothesised

that the reduction in ALP and proliferation, once osteoblasts are exposed to composites, are likely to be the cause of this adsorption, however the main mechanism behind this phenomena remains unknown and should be researched further. Furthermore it was also observed that after 5 days of incubation the cell metabolic activity decreased, indicating extracellular matrix formation by osteoblasts, which includes an increase in collagen production. Collagen synthesis is often considered as a well-defined sign of osteoblast differentiation and, a deficiency of zinc could affect its biosynthesis (Seo et al., 2010). Observations in this study confirm these previous findings. At day 5 the collagen (predominantly collagen type I) production is less prominent for all samples when compared to day 15. This is in agreement with findings that show collagen synthesis occurring at the late stages of incubation as opposed to early incubation (Alcantara et al., 2011). A quantitative observation by the same group suggests that samples lacking zinc, would decrease the ECM biomineralisation which indicates a decline in collagen type I production. The production of collagen is important for several reasons. Both *in vivo* and *in vitro* studies have shown that collagen has evolved to serve as an important component of bone that allows for its involvement in bone strength, toughness and multiple independent roles in biochemical modifications of its structure (Viguet-Carrin et al., 2006). The current investigation also confirms another hypothesis which states that collagen production at the early stages (day 1) of mineral deposition is much slower and almost non-existent as compared to the later stages when the ECM is fully formed. Furthermore, utilising a colour thresholding approach on collagen production indicates that nZnO and nHA can promote collagen production at an early stage. In conclusion, proliferative, biocompatibility and morphological assays conducted *in vitro* suggest that osteoblasts together with human mesenchymal cells

can reside and potentiate bone formation when placed upon or are exposed to supernatants of concentrations of metal oxide NPs. Coated ZnO NPs can also instigate a positive response in osteoblasts, promoting the initiation of ECM formation that in turn will mediate osteoblast differentiation leading to collagen production. Indeed, further evidence is required to validate the present findings via mechanistic and molecular studies.

Importance of work

Relevant significance of the current research	
1	Providing evidence that EHDA-coated nZnO samples are non-toxic to relevant eukaryotes, such as osteoblasts.
2	Establishing that nZnO coated substrates are both biocompatible and osteoconductive.
3	Understanding the potential for novel nano-patterned structures.
4	Providing novel evidence for the adhesion of osteoblasts to a nano-ZnO surface in addition to highlighting the superiority of nZnO in up-regulating focal adhesion-related genes.

Limitations

Relevant significance of the current research	
1	Molecular evidence is required to fully establish the current hypothesis of biocompatibility (i.e. expression of genes that might have had an effect on osteoconductivity of cells).
2	No *in vivo* or *ex vivo* studies have been carried out.
3	The mechanical stability of the coatings is still under investigation.

Chapter 4

1. Future innovations

The following chapter will discuss concepts and ideas relevant to this thesis. These require further validation and their absolute validity of these findings needs to be strengthened with further additional experiments. The following segments constitute of four sections in which various novel aspects as regards to further biological and physical capabilities of nZnO will be reviewed. These results are based upon careful observations of some of the author's findings.

1.1 The role Ion release from NPs

Ion release is an important factor in both antimicrobial and osteoconductive processes (Kim et al., 2005). It is important to quantify the amount of ions released into the surrounding environment. While there is no clear evidence as to what mechanism is exclusively responsible for the toxicity of nZnO, *in vivo* and *in vitro* studies have shown that its effects on both eukaryotic and prokaryotic organisms can be ion-based (Brun et al., 2014, Ng et al., 2013). Based on findings present in this thesis it has been deduced that a supernatant of ascending concentrations of ZnO NPs can have an adverse effect on eukaryotic cells while allowing the growth and attachment of cells when these NPs are coated onto a surface. Studies were carried out in on an attempt to understand the quantity of ions released into the surrounding medium and whether this release is consistent with the antimicrobial activity of nZnO at different concentrations. In fact further experimental results indicate that cytotoxicity of nZnO of sizes ranged between 30-60 nm (identical to that of this

study), corresponds to that of solutions of Zinc chloride (Miao et al., 2010). Since Zinc ions are the main cause of antimicrobial activity in a solution of ZnCl, these results are fascinating and suggest that ion release could play a major role in the way that these NPs cause both their bactericidal and cytotoxic effects. However the majority of studies have overlooked the ability of nZnO coatings to release ions, the aim for conduction of the following studies was to analyse this and compare the results to that of ion release of suspended ZnO NPs.

1.2 ROS generation

Reactive oxygen species (ROS) are considered to be one of the predominant mechanisms by which NPs cause bacterial damage. Studies suggest that H_2O_2 is the dominant species behind such ROS-based antimicrobial activity (Dwivedi et al., 2014). Mechanistic experiments with oxides have yielded numerous and contradictory results. Conducted experiments on magnesium oxide (MgO) NPs (Makhluf et al., 2005) suggest that because of the presence of this metal oxide, ROS production and thus membrane damage is possible, although alternative mechanisms of actions such as direct contact related to damage to bacteria were also proposed. Other studies indicate that slurries made from powders of ZnO and MgO can independently release hydrogen peroxide (Sawai, 2003) While others suggest that ROS generation is not exclusively responsible for the antimicrobial activity of NPs and various other factors may be involved (Tam et al., 2008) . The production of H_2O_2 was shown to be directly related to an increase in concentration of NPs (Sawai et al., 1996). The physical presence of NPs in suspension also allows direct contact killing (Vargas-Reus et al., 2012) that does not allow an accurate quantification of

other factors involved. The following study attempts to provide evidence for the involvement of hydrogen peroxide in the antimicrobial activity of nZnO particulates.

1.3 Nano-coating stability

Bone implants within the body are exposed to variety of forces such as bending, torsional, axial compression, axial tension and shearing forces (Isidor, 2006). Given the fact that nano-based coatings are being proposed in the current study, one can investigate the effect of the dynamic environment present within the structure of the bone. This dynamic environment of forces also consists of biological components such as blood and marrow. The present study is an innovative method, designed to observe the shear stress/forces applied to a surface by these biological components. This is an important factor because more often than not, coated surfaces are prone to degradation when positioned within bone. Naturally, metal corrosion is a multifactorial phenomenon and depends upon mechanical, geometric and other important parameters. This often causes the release of debris into the surrounding environment, these are often metal based and nano in size (Jacobs et al., 2003). The present study is an indirect but innovative attempt to observe the effects that the physiochemical environment might have on a surface of an implant. This investigation utilises the function of a 3D printed model in order to create a prototype to test the present hypothesis.

1.4 Pattern-based coated samples

Patterned-based coatings have been used in relation to nHA in recent years (Gu et al., 2012). However, patterned based investigations are almost exclusively applied to nHA which solely serves to enhance osteoblast adhesion and proliferation (Munir et al., 2012). Furthermore, various studies claim that ceramic based micro-patterns are

able to promote bone formation more than the conventional coatings (Halai et al., 2014). Apart from the biological response of cells to a patterned based coating, the hypothetical advantage of patterns is the potential of being less toxic when detached from the surface. It can be hypothesised that if the total surface area of prosthesis is taken into the consideration, then upon removal or a possible revision surgery, less surface detachment of a coating can be observed. It is known that NPs can travel throughout the body and into many organs and while not highly toxic and often cleared from the body via excretion at moderate concentrations (Baek et al., 2012), they can accumulate and cause gene alterations, inflammatory responses among many other undesirable side effects (Balasubramanian et al., 2010).

2. Nano-ZnO ion release capability

2.1 Methods

2.1.1 Suspension-based

Different concentrations (100 µg/mL, 500 µg/mL, 2500 µg/mL and 10000) of NPs were incubated at 37°C for 1, 5 and 10 days in 3 mL of deionised water (dH_2O) and subsequently centrifuged at 50,000 rpm for 20 min in order to separate the NPs from the supernatant. Half of the samples for suspension supernatants were filtered using 0.25 µm filters (Millex® syringe filter units).

2.1.2 Coated

For coated samples, concentrations of 2500 µg/mL, 5000 µg/mL and 10000 µg/mL of nZnO were chosen as coating concentrations. Glass samples were coated and prepared as stated in previous chapters. Duplicate coated nZnO substrates were

placed in tubes containing 3 mL of dH_2O at 37°C. In order to increase the chances of detecting any ion leaching from the surface of the substrates.

2.1.3 Ion chromatography

NP supernatants (filtered along with unfiltered) were measured using ion chromatography (Dionex ICS-1000 cation system). The system uses an isocratic pumping method that has electrolytic suppression to minimise background counts. Analysis times can vary depending on the number of samples used and ions of interest. Vials of 500 µL were filled with the supernatant content and placed within a sample rack for measurement using the AS50 autosampler. The ion release data was transferred to a computer and analysed.

2.2 Results

Findings indicate that filtering the supernatants had a positive effect on detection of Zn^{2+} ion release. An increase in ion release for filtered supernatants was observed in ascending incubation periods. This phenomena was not observed for unfiltered samples, indicating a possible need for further separation of NPs and the supernatants.

Ion release was detected for all concentrations during days 1 and 5 and only on day 10 was there a gradual peak observed for Zn^{+2} release with filtered supernatants. The difference between the ion release from the coated surfaces and suspended NPs was clearly evident (Figure 62) as the ion release for coated samples was considerably lower than that from suspension supernatants.

Zinc ion release: A comparison between suspended and coated NPs

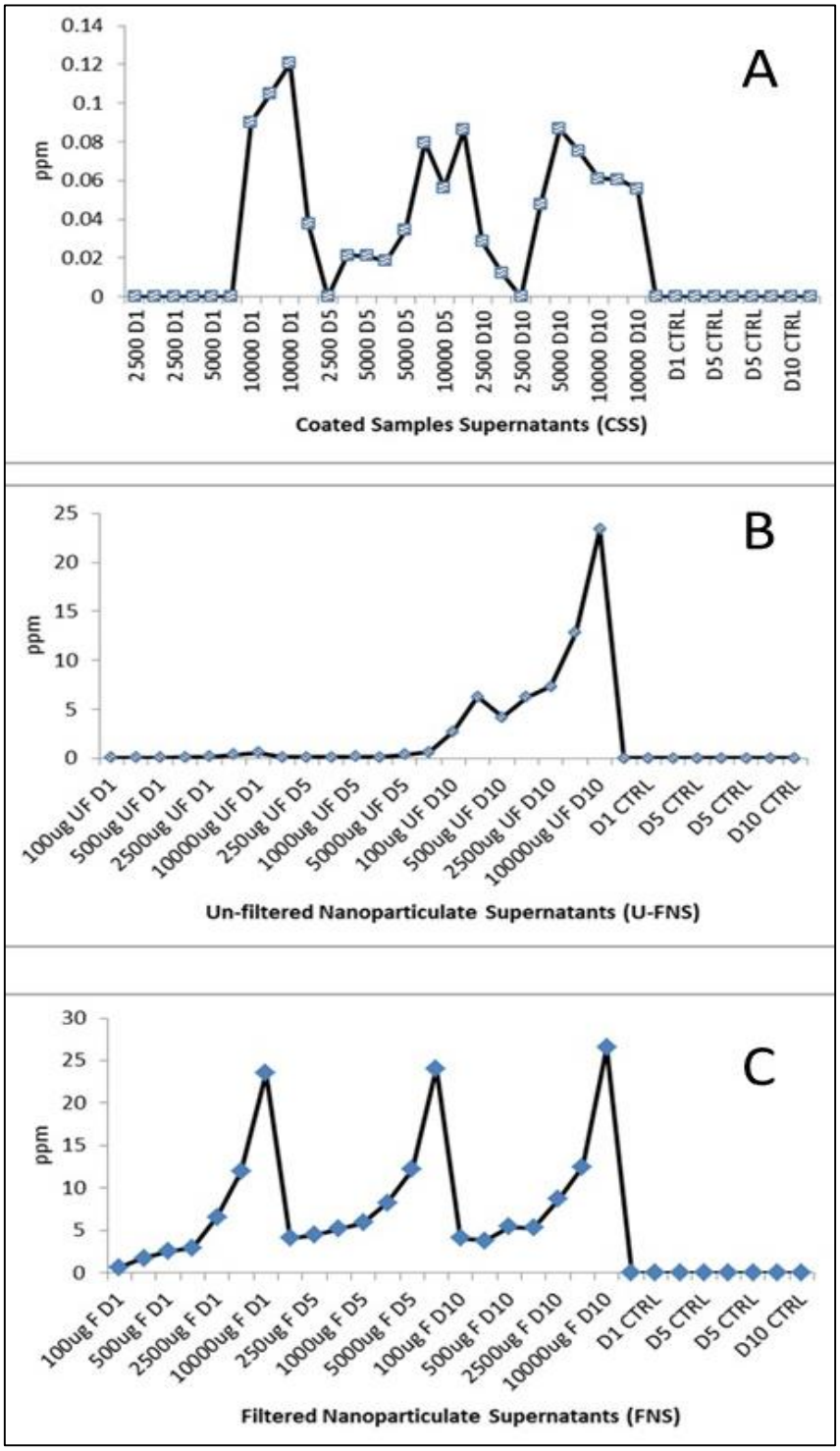

Figure 62 - Ion release measurements of supernatants of A) coated samples, B) unfiltered and C) filtered nZnO suspensions. All samples were compared to dH_2O (Control) that was incubated alongside all samples for the relevant period of time. n = 3 (for each condition and concentration).

2.3 Discussion

These provisional findings indicate that ion release from a nano-coated surface is minimal as compared to suspension-based ion release. Therefore it seems that "ion release" plays a limited role in the antimicrobial activity of nZnO via coated substrates. An important distinction between the stable NPs and when in suspension needs to be made. Current findings indicate that nZnO coated samples submerged into suspensions of bacteria, showed significant bactericidal activity as compared with innocuous coated NPs and the uncoated samples (Memarzadeh et al., 2012). If the assumption for this activity is based solely upon ion release, then this is a contradictory finding, since not much is released into the surrounding environment from the coated samples. The same deduction cannot be made for suspended NPs and their mode of antimicrobial action and ion release is indeed one of the main mechanisms for their antimicrobial activity. The results can however shed some light on the fears of "excess ion release" that could cause cytotoxicity to eukaryotes such as osteoblasts. The antimicrobial activity of NPs and their mechanistic behaviour are extremely complex and further evaluations of evidence are required in order to achieve a firm conclusion.

2.4 Conclusion

It is important to distinguish the difference between the ion release of individual NPs in suspension and those that are coated onto a substrate. Here preliminary evidence is presented that coated NPs release lower amount of ions into their surrounding environment. This could have important implications as to determine the main mechanism underlying the antimicrobial property of coated nZnO particulates.

3. Hydrogen peroxide release

3.1 Methods

3.1.1 Nanoparticles

Nano-ZnO particulates were prepared at concentrations of 10,000, 5000, 2500 and 1000 µg/mL in PBS (Table 5). All concentrations were thoroughly sonicated and then vigorously shaken at 2500 rpm in order to insure a stable suspension.

3.1.2 Bacteria

Species of bacteria used were: *S. aureus* (Oxford strain; NCTC. 6571) and *E. coli* (NCTC 9001).

3.1.3 Hydrogen peroxide assay

Using a hydrogen peroxide colorimetric detection kit (Hydrogen Peroxide Assay Kit - abcam UK, ab102500) the release of H_2O_2 into the surrounding medium was quantified. Samples were prepared and analysed based upon the assay protocol provided by the manufacturer.

Hydrogen peroxide release was analysed by observing the difference in release between multiple concentrations of nZnO suspended in PBS (Table 5), similar analysis was carried with the bacterial species exposed to the different concentrations of nZnO. Bacterial species were at populations of ~ 10^7/ mL suspended in PBS. All experiments were carried out at room temperature.

3.2 Results

Exposure of *S. aureus* resulted in no increase in concentrations of hydrogen peroxide (Figure 63). In addition to these results at concentrations of 10,000 µg/mL of nZnO in PBS, increasing quantities of superoxide was quantified. The outline for all bacterial suspensions in NP supernatants is described in table 4. Superoxide release from suspensions of *E. coli* with nZnO was evident and can be quantified using the suspensions at 5000 µg/mL and 10,000 µg/mL nZnO. The release profile for hydrogen peroxide differs between *S. aureus* as compared to that of E. *coli*. No visible H_2O_2 release for nZnO concentrations of 5000 µg/mL and lower was observed; however minimal release was observed for the 10,000 µg/mL concentration of nZnO (Figure 63).

Mixtures of NP supernatants and bacteria

Table 4 – Supernatants for different concentrations of suspended NPs were mixed with O.D. adjusted bacterial suspensions. NP supernatants in PBS were also tested for hydrogen peroxide release without exposure to bacteria. The black arrows annotate the mixing action, i.e. *E. coli* suspension + 1000 µg/mL NP supernatant.

µg/mL(NP supernatants)	*E.coli*	*S.aureus*	PBS
1000	☑	☑	☑
2500	☑	☑	☑
5000	☑	☑	☑
10000	☑	☑	☑
PBS	☑	☑	

Hydrogen peroxide release from Bacteria (*S. aureus* and *E. coli*), NPs and their combinations

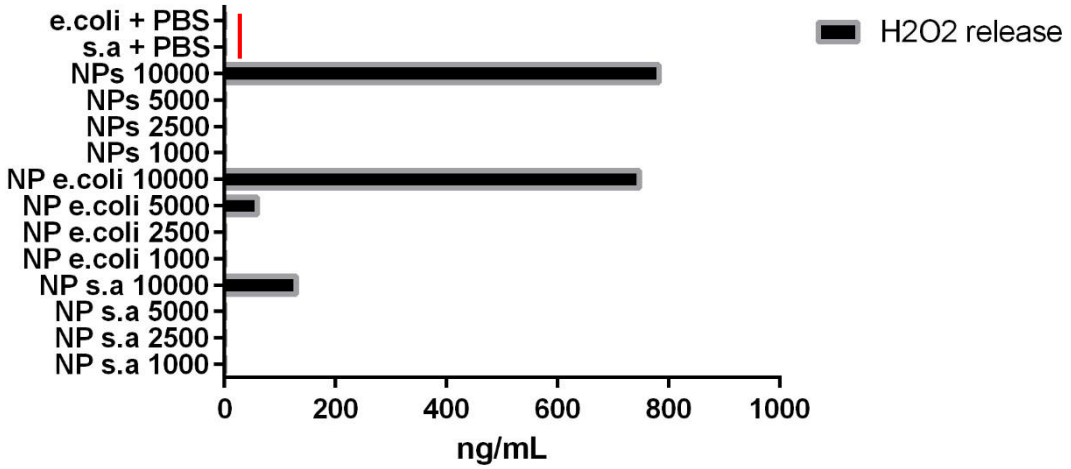

Figure 63 - Comparison of H_2O_2 release between *S. aureus* and *E. coli* when exposed to different concentrations of ZnO NP. ZnO nanoparticle suspensions and bacteria (NP s.a and NP e. coli) were also tested for H_2O_2 release independently. The red line depicts the controls, n > 3, all concentrations on the Y axis are µg/mL.

3.3 Discussion

The present preliminary results indicate that hydrogen peroxide release differs when *E. coli* is compared to *S. aureus*. NP suspensions elicit less H_2O_2 release when exposed to *S. aureus* as compared with *E. coli*. This in turn indicates that *S. aureus* is somehow able to break down the production of this reactive oxygen species (Mandell, 1975). The current observation is strengthened by studies demonstrating that this break down is possibly based upon the activity of catalase activity produced by *S. aureus* (Makhluf et al., 2005).

3.4 Conclusion

According to these findings, NPs are able to independently produce H_2O_2 and that the amount released into the surrounding environment differs when exposed to either *S.*

aureus or *E. coli*. More thorough studies are required to establish a coherent mechanism for these effects.

4. Coating stability test

4.1 Methods

4.1.1 3-D printing

Ultimaker 2, a 3-D printer, (UCL, Institute of making) was used to print all the prototypes produced for the present experiments. A cylinder like structure was designed (CATIA VR3) in order to serve as the container of test samples. The programmed software was then transported to the 3-D printer and a prototype was printed using polylactic acid (PLA) in a layer by layer bases. A 3-D printer allows for great freedom as it allows for formation of each layer as a hotplate melts the polymer at a specific temperature (melting temperature of PLA is ~ 200°C) and subsequently building the forthcoming layers on top. The density of PLA used was chosen to be at 100% in order to allow the construct to have water-tight properties.

4.1.2 Coated samples

Glass samples were coated using concentrations of 10,000 µg/mL of nZnO and prepared as previously explained in Chapters 3.

4.1.3 Coating stability

With an aim to measure the effect of shear stress on the surface of the nano-coated samples, the cylindrical prototype was devised that allowed careful monitoring of the nano-coated surfaces. The 1 cm^2 nano-coated sample along with a non-coated sample was placed in each pocket, carefully designed in order to ensure the coated surfaces was positioned inside pockets created towards the inner region of the cylinder

(Figure 64). A magnetic stirrer was placed at the bottom of the cylinder in order to provide an artificial flow rate that allows for the measurement of shear force applied onto the NPs on the sample surface and eventually the measurement of the stress required for the particulates to be worn off the surface. The flow rate of the fluid can be measured (Day 1, 5 and 10) using a Laser Doppler Anemometry (LDA); that is normally used to measure the velocity of any specific liquid. Simulated body fluid (SBF) and olive oil were chosen in order to compare their qualities. Studies have confirmed that the viscosity of bone marrow differs in various bone types and also temperature dependent. Overall a fluid such as olive oil has rheological properties that are closer to that of bone marrow (Gurkan and Akkus, 2008). Olive oil has an increased viscosity (81 cP) as compared with SBF and therefore changes can be observed when applied to the nano-coated surface. The substrates were seated into the hollow pockets in order that the surface will be exposed to the moving fluid which can potentially simulate aspects of what occurs *in vivo*. In order to fill the space within the cylinder, three elongated arms were designed, each one having a pocket positioned at its extremity. These pockets were positioned in symmetrical fashion so that when samples are fixed within each one, equal exposure to the shear stress is taken place, essentially allowing all three samples to be processed at the same instance.

Each pocket with its sample is supported by an arm with a thickness of 10 mm and each of these three arms has a distance of approximately 10 mm from the centre of the cylinder. The substrate has the size of 1 cm^2 and less than 1 mm thick. Therefore the pocket needed to be slightly bigger and was designed in order that nano-coated samples are placed within it without any visible damage to the surface.

The dimensions of the pockets were: 10.5 mm and thickness of 1 mm and the outside of the pocket are 13 mm high, 12.5 mm wide and 3 mm thick. Hence, the substrate can fit into the pocket. The hollow space on the pocket is 10 mm high and 8 mm wide.

4.2 Results

The initial concept of the present investigation was to 3-D print a prototype (Figure 64) that is ultimately used to utilise a laser technology in order to measure the flow rate near the surface of the nZnO coated samples. However because of the nature of the material (a murky clear PLA) and its relative thickness, an accurate measurement could not be achieved using this technique, leading to the abandonment of laser guided flow rate measurement. Other options such as applying some form of coloured dye that would travel with the fluid in order to provide a visual approximation, followed by a measurement of fluid mobility nearby were proposed but discarded because environmental factors which lead to lack of dye control. Results for stirrer based immersion studies indicate that when placed in olive oil (Figure 65) at a fixed flow rate of 80 rpm, nano-coatings start to wear off after a 5 day period. This phenomenon was not observed with coated samples positioned in the SBF filled chamber.

An early design of 3-D printed coating stability test chamber

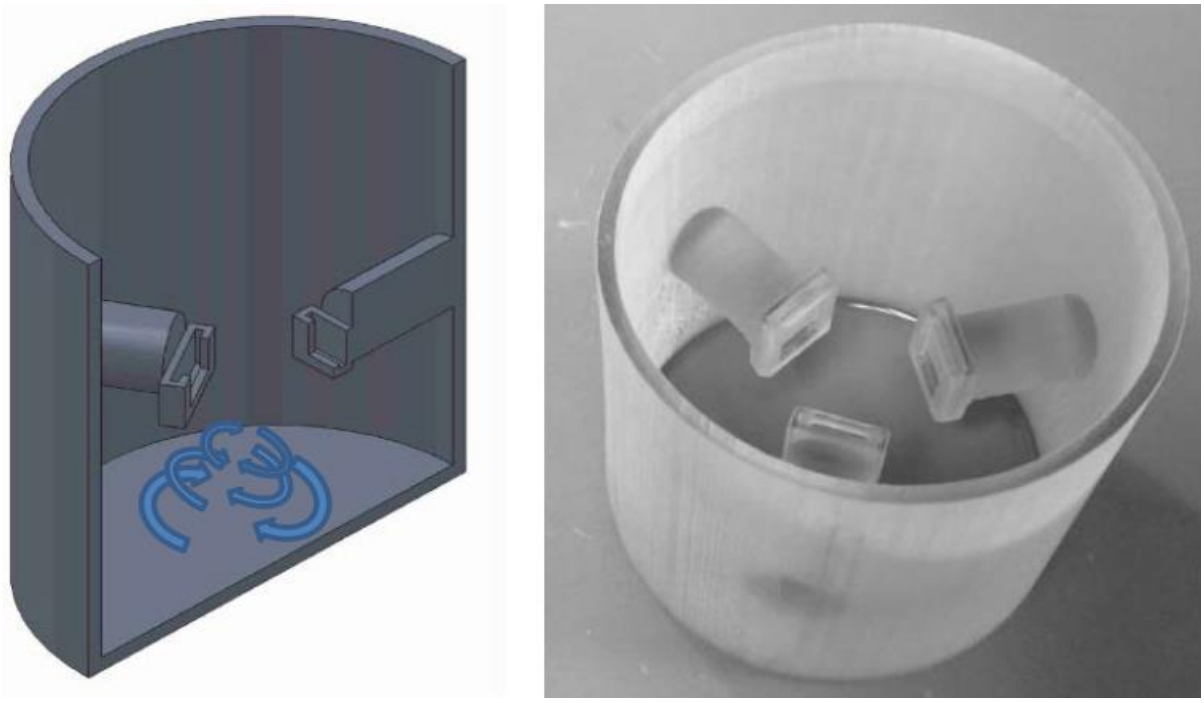

Figure 64 - The figure on the left represents the initial design of the prototype and the figure on the right is the final product. Using a stirrer the fluid within the chamber is moved and shear stress is applied to surface of each sample separately. A magnetic stirrer placed at the centre of the chamber is not the best option because it allows for potential errors in calculating the exact fluid flow near the nano-coated samples. A stirrer that allows for a uniform fluid flow is therefore a suitable future alternative.

Stability testing of nano-coated samples

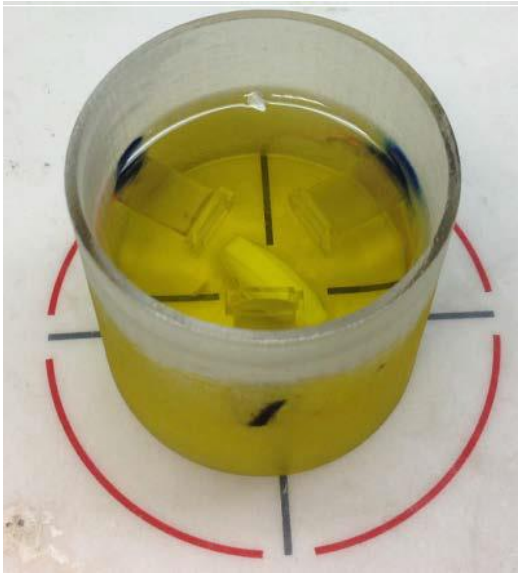

Figure 65 - The cylindrical prototype filled with olive oil and loaded with samples. The viscosity of olive oil is approximately similar to that of the bone marrow and therefore utilised. The motion of the oil within the chamber allows for close contact with the surface of coated NPs.

4.3 Discussion

The mechanical stability of a coating is of utmost importance for future medical implants. The present findings provide evidence for diversity of strength and stableness of our coatings. Furthermore by comparing the *in vitro* physiochemical effects (detachment of the NPs from the surface) that these environments instigate upon the coatings we can formulate an approximate idea about their stability. A 3D printed model allows for rapid prototyping. This permits for designing a device that permits researchers to manifest their ideas faster and relatively cheaper. While limited similar studies have been conducted before, there is much of evidence for an enhanced cellular behaviour in systems where use liquid flow enhances cellular attachment (Jacobs et al., 1998, Bancroft et al., 2003). It could be envisioned that a similar method could be utilised to measure the mechanical integrity of a coating. This could be achieved by analysing the shear stress applied to multiple surfaces for prolonged periods. A similar prototype, based upon the cylindrical nature of the current model is now being designed and used by the present research team (unpublished work) to study and observe the osteoconductive nature of nano-coated Ti samples in the presence of decellularised *S. domesticus* bone discs.

4.4 Conclusion

Nano-coatings can be highly antimicrobial and also enhance biocompatibility, however their stability is understudied. The current investigation adds insight into the novelty and provides some evidence that can be expanded into a larger area of investigation.

5. Osteoconductive patterned nZnO

5.1 Methods

5.1.1 Patterned-coated samples

All samples were created as explained in previous chapters. Individual the patterned regions (round in shape) on the glass slides comprised of 204 -210 of individual square shaped patterns. These square shaped patterns had equal sides, each measuring to150 µm. Furthermore, there were four patterned regions present on each glass sample (Figure 66).

5.1.2 Cell culture

A relatively small number of previously cultured UMR-106 cell lines (1×10^3 cells) were placed at the midpoint of the glass samples (n =3), between the patterned regions. All seeded samples were placed in a 12-well plate and incubated overnight at 37ºC, 10% CO_2 in DMEM (5% FCS, 1% P/S). *Proliferation assay:* AlamarBlue (abcam, UK) was used to quantify osteoblast proliferation (Figure 67) on nano-based micro-pattered surfaces. Glass samples were used for each time point (Days 1, 5 and 10). Controls were glass samples with no nZnO micro-patterns. Each sample was then removed and prepared for SEM (procedure explained in previous chapter 2).

5.2 Results

The nZnO-patterned coated surfaces revealed that organised homogenous structural relics can be coated onto substrates (Figure 68 – 70). These assemblies are almost always agglomerations of NPs because they are confined into a limited space provided by the grid (Figure 66). Considering the fact that controls in the current experiment were chosen as plan glass, a significant ($p < 0.05$) difference in

proliferative activity was observed after day 10 of incubation. This difference was also significant for day 5 but after 24 h of incubation no change between the two samples was observed (Figure 67). Closer analysis of each patterned region indicates that osteoblast-like cells have majorly adhered to coating regions as opposed to regions between the small square shaped coatings. This was evident at regions where there were lower number of cells per coated region, often with multiple osteoblasts adhered onto the squared regions (Figure 68). Furthermore, each square shaped NP pattern contains hundreds of tiny circular agglomerations of NPs, each with a diameter of ~ 4.5 – 5 µm, all concentrated at the centre of each square structure and only visible in its extremities.

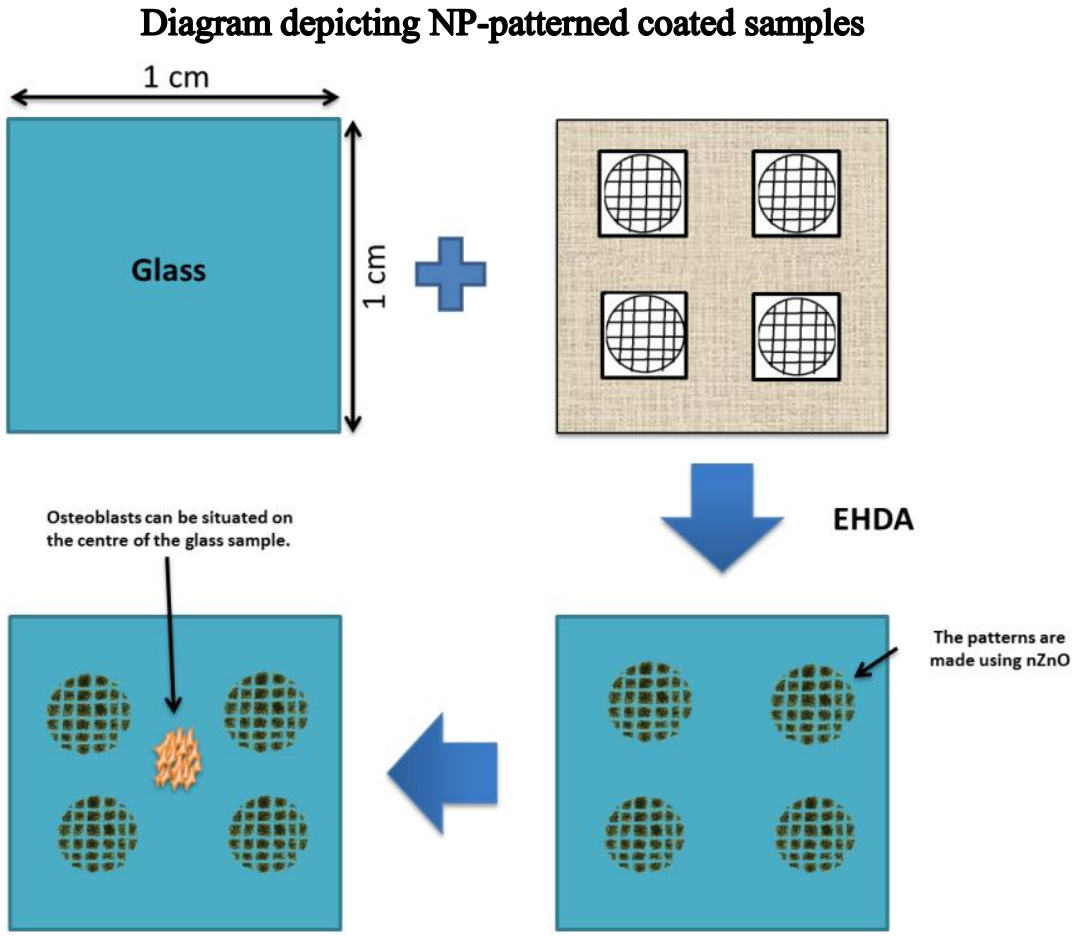

Figure 66 - A hypothetical diagram showcasing the possible osteoconductive ability of nZnO coatings. The patterned structures can hypothetically attract osteoblasts, showing the ability of nZnO as a patterned based coating.

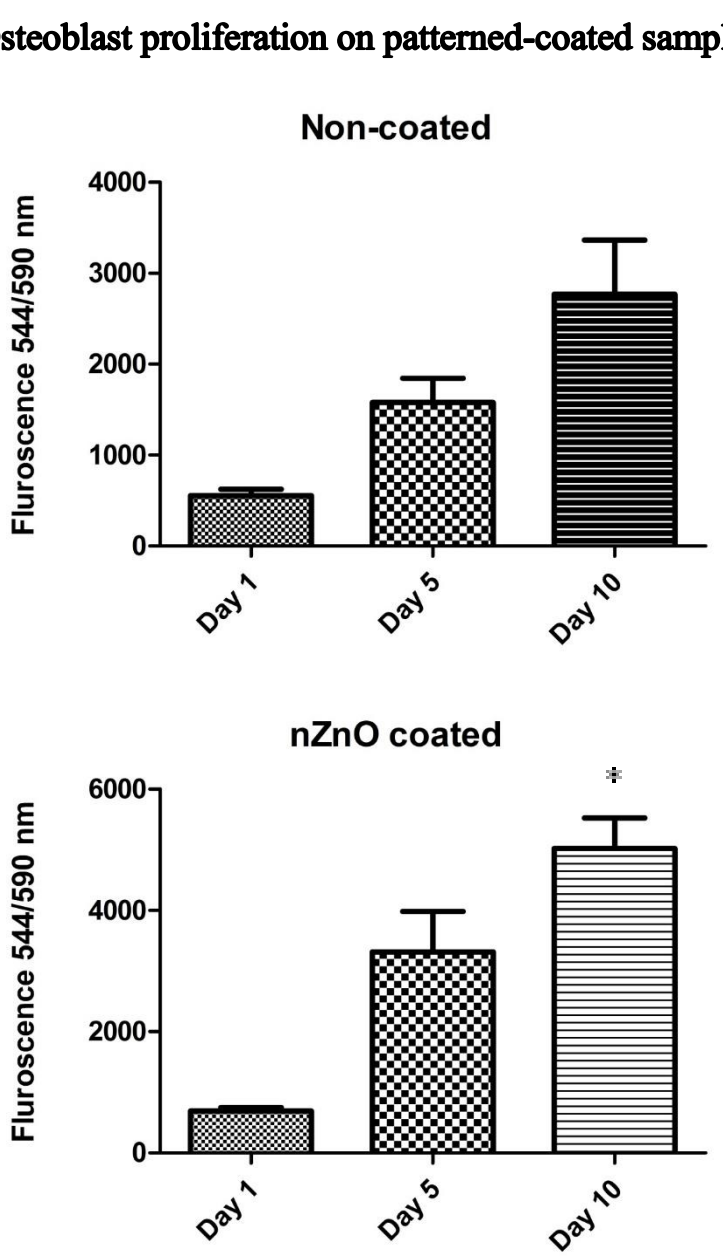

Figure 67 - An independent experiment comparing the proliferation of osteoblasts on 100% nZnO patterned coated samples compared to uncoated glass samples. While no significant changes are observed after days 1 and 5, a significant change in proliferation is observed on day 10 between cells cultured on nZnO and non-coated samples. n=3, ±SEM, $p < 0.05$.

Osteoblasts adhere to patterned nZnO coated glass

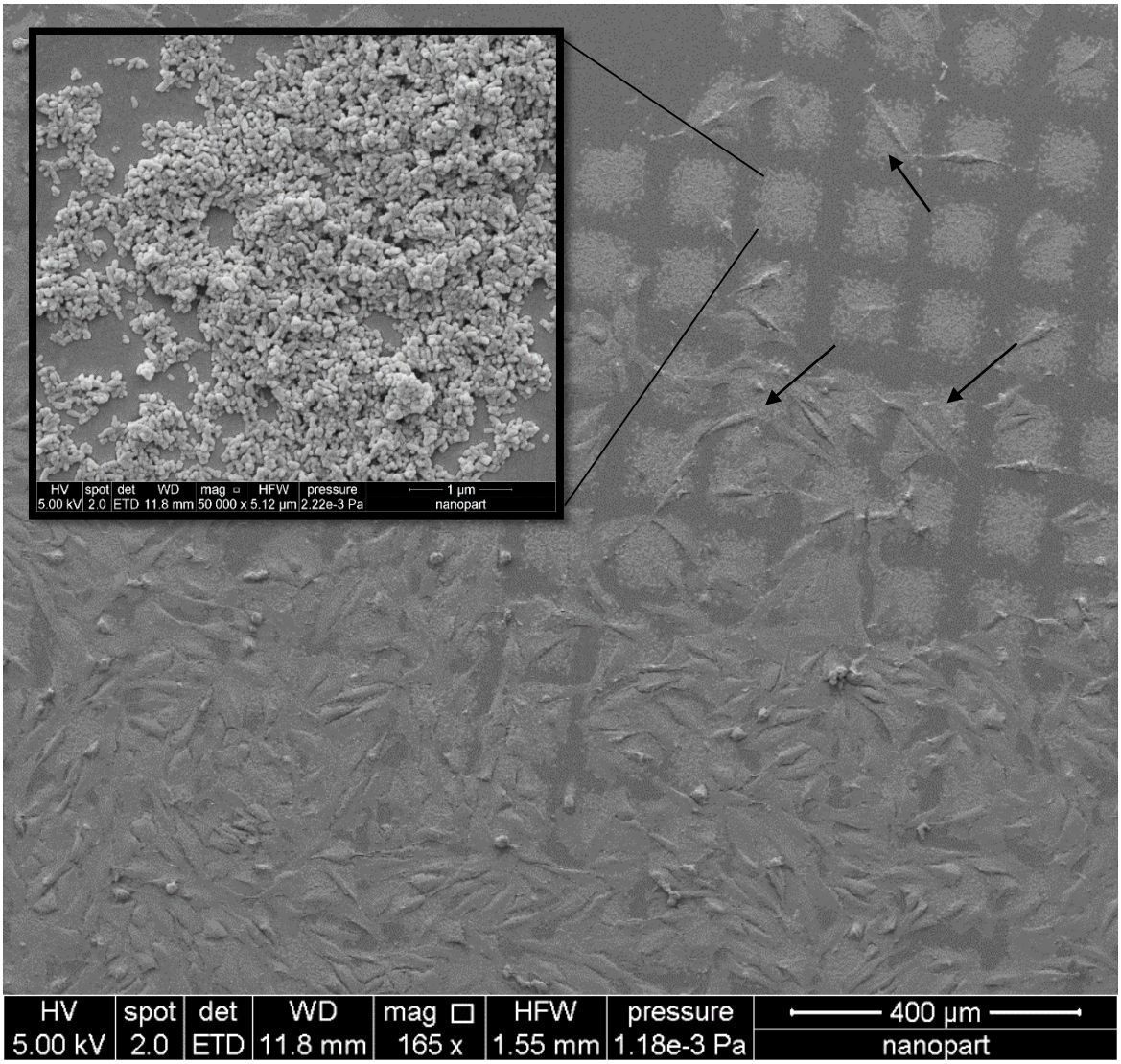

Figure 68 - Squared shaped nano-patterned coatings with osteoblasts seeded upon. The magnified region represents the structure of nZnO when coated as patterned structures. Each square shaped structure (150 µm) consists of smaller circular regions (5 µm). Osteoblasts are predominantly adhered to these coated regions (highlighted by the black arrows).

A single osteoblast attachment onto a coated surface

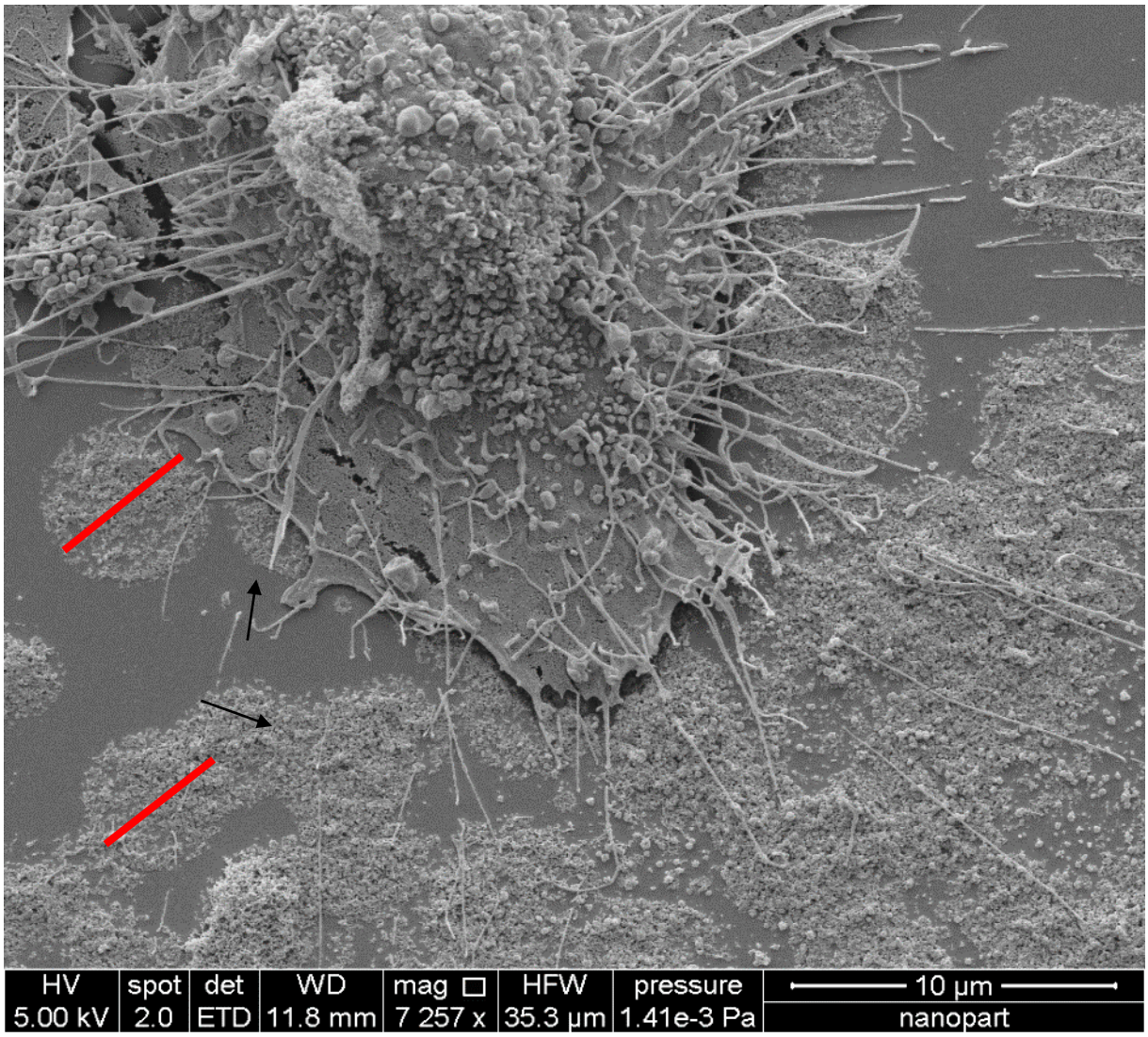

Figure 69 – An osteoblast spreading its filopodia onto nano-coated regions. The coated regions seem to be a combination of circular regions that make up the coated regions (black arrows and red lines). These regions are possibly encapsulated nanoparticulates inside each droplet formed by the EHDA process.

Selective attachment of osteoblasts onto nZnO coated regions

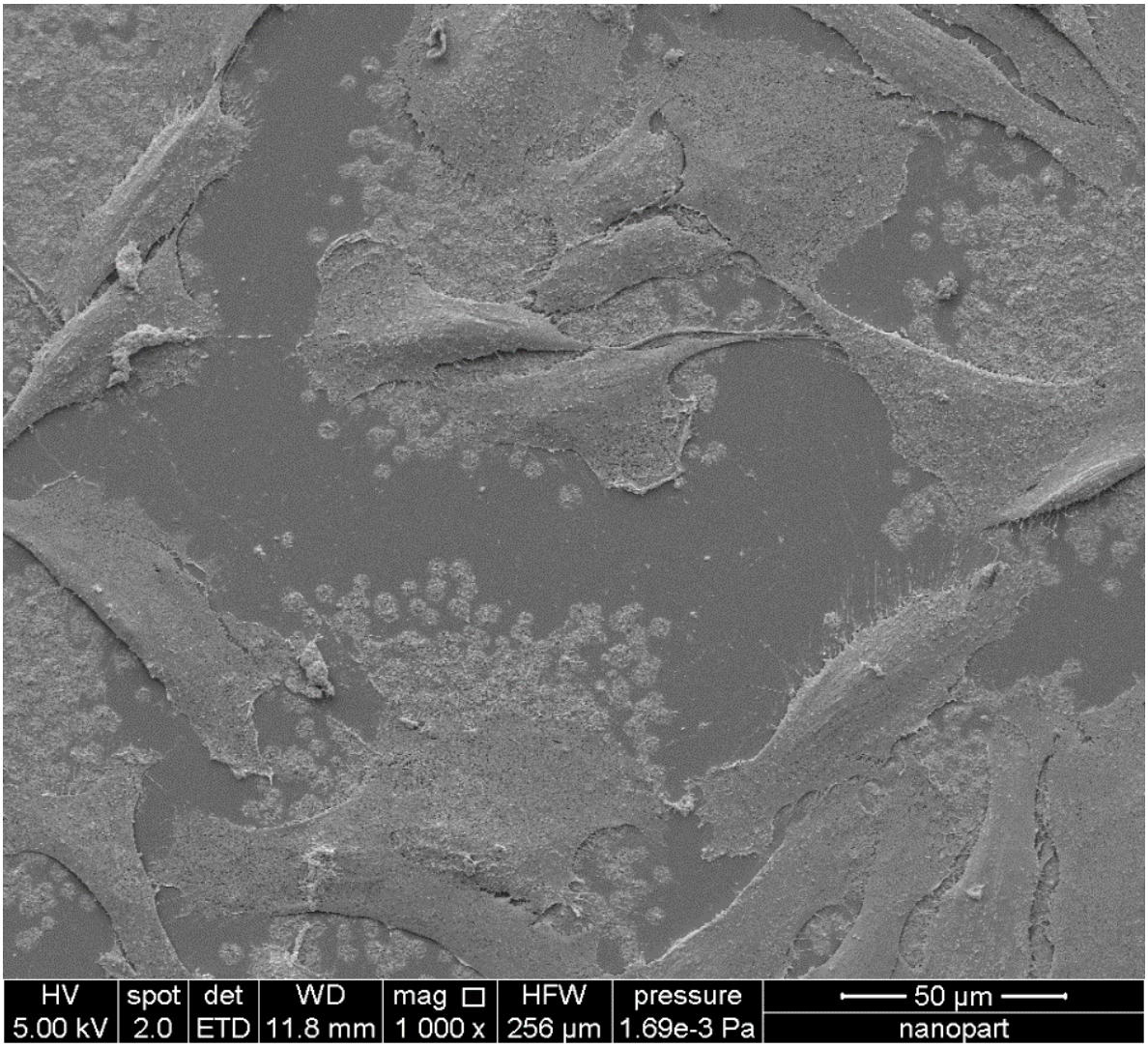

Figure 70 - Electron micrograph of osteoblasts attached onto the surface of a nZnO patterned structure. The arrangement of cellular attachment indicates that these cells prefer the patterned surfaces compared to the normal glass surface.

5.3 Discussion

The novel finding for osteoblast selectivity towards nZnO-patterned regions can provide insightful information as to how eukaryotic cells respond to different patterns of NPs in general. The underlying mechanisms that lead to such behaviour are currently unknown. However evidence presented in this thesis and other studies indicate that this is potentially related to zinc ions being present in the immediate environment of cells (Ito et al., 2002, Wang et al., 2010). However, within an aqueous medium, ions can potentially dissipate throughout the surface of the sample and therefore the nano-structured surface should not be the only region where cells generally prefer to adhere. It is thoroughly possible that the previous effect in combination with the hypothesis that nano-surfaces can promote cell growth (Pan et al., 2012) could contribute to this novel behaviour. The nanophase physical structure and the micro-patterns of these coatings maybe preferred by osteoblasts because of their increased surfaced area to volume ratio (Christenson et al., 2007, Jeon et al., 2010) as compared with the rather non-porous and smooth surface of glass or titanium.

5.4 Conclusion

Patterned systems can be a useful tool for future coating based implants. Selective attachment of osteoblasts to a specific area could help in the understanding of cellular behaviour in addition to helping the advancement of future goal directed biomaterials. Studies such as further migratory studies can be devised to analyse and establish a more efficient osteoconductive coating.

Chapter 5

1. General discussion

An ideal bone implant or prosthesis would allow bone growth on the coated surface of the implant, together with preventing the formation of a bacterial biofilm. The antimicrobial ability of an implant is highly relevant to the present study. A recent important report published by world health organisation (WHO - 2014) indicates that common infections by species such as *E. coli* and *S. aureus* are increasingly difficult to treat both within the public and medical sectors of society. This report points out that bacterial resistance is an "increasingly serious threat to global public health" and that if not controlled, the spread of infection can lead to prolonged hospital stays, major economic and social costs as well as a greater risk of death. The topic, presented in this thesis is therefore of upmost importance, not only because it provides the reader with an insight into a novel coating technique and material for future bone implants but because it involves a thorough examination of the effect of coated NPs on bacteria. The idea that coatings should be implemented onto surfaces to enhance their biological activity in order to make them multifunctional has existed for many years (de Groot et al., 1998). However, nanostructured coatings are a very recent phenomenon (Wagner et al., 2006). For bone related assignments, the porous structure of the coating is of outmost importance as it provides osteoblasts with regions to adhere to in order to proliferate and finally differentiate and generate a suitable ECM that allows healthy bone formation. However, many medical coatings used in the medical sector are either HA based or consist of other material that only allows better bone formation. The current projects, along with various others are changing this unidirectionality of nano-coatings. The evidence presented in the

current study suggests that there is room for improvement. Because bone does not have a natural tendency to combat different infections, coated NPs that are able to control the spread of biofilm formation are of great interest. Our investigations show that a nanoparticulate such as ZnO is capable of providing such advantages in addition to accommodating the additional role of being a surface that allows osteoblasts to adhere. This finding was based upon the employment of techniques designed in order to optimise observations. Of course, many methods employed in the present investigation are introductory and can be improved upon. At the end of each chapter, shortcomings that allow for these improvements have been included. While the bactericidal studies are performed with accuracy and precision, calculating values for MIC and MBC of a material that is not soluble in an aqueous environment can prove difficult. Some NPs may be soluble in liquid and this has an effect on their relative toxicity towards living organisms (Studer et al., 2010). Therefore suspension-based studies are only useful to observe and analyse the superficial antimicrobial activity of a nanoparticulate over time. In other words, utilising them is an initial step in determining their initial antimicrobial capability. Coating nZnO on glass samples provided much more insight as regards to their biocompatibility and antimicrobial activity. Studies showed that these coatings exhibit much antimicrobial potential as samples were submerged into a known concentration of bacteria suspended in PBS. This was encouraging and future studies on nZnO coated material led to investigations relating to their biocompatibility. In studies related to multifunctional devices, some functions need to take precedence over others. In the present investigation it is the biocompatibility that is of upmost importance. Some studies related to ZnO NP indicate its toxicity (Lin et al., 2008), therefore relevant studies were carried out to confirm these findings. At this phase, the intention was to

choose the correct concentration of nZnO that was not toxic to osteoblasts, or at least allowed for their adhesion to the coated surface, without further detachment. High concentrations (10,000 µg/mL) were deliberately used to establish if there were any detrimental effects towards cells. In addition, this chosen concentration of nZnO, would be made into a composite coating with the aid of nHA in order to potentially boost the osteoconductivity of the material while retaining the antimicrobial property. The surprising outcome was contradictory to the initial hypothesis. The implemented high concentrations of nZnO accommodated for attachment of osteoblasts.

2. Biocompatibility properties

There are various definitions for biocompatibility but this term is best explained by Williams, 2008 as "a system allowing for desired beneficial cellular or tissue response in relation to a medical related therapy" (Williams, 2008). This description can restfully be applied to findings explained in this thesis. The present data shows that utilisation of NPs as coatings can hinder material toxicity. These findings focused on cell morphology, mitochondrial activity and membrane integrity. An immediate cue for understanding cell health is an extreme change in morphology coupled with compromised adhesive properties (Nakayama et al., 2005, Shi et al., 2009). Present findings suggest that there is no change in morphology between cells adhered to an uncoated sample as compared to samples coated with nZnO. In addition, osteoblasts stained for paxillin showed no change in expression between uncoated, composite and nZnO coated samples, reinforcing the suitability of nano-coated surfaces as biocompatible materials. Furthermore, Our investigations (Memarzadeh et al., 2015) provide further evidence for increased proliferative and decreased cytotoxicity for osteoblasts adhered to the surface of nZnO coated

substrates. Recent findings also indicate that incorporating a specific concentration of nZnO particulates onto a nano-phased titanium sample results in enhanced cellular adhesion and reduced bacterial adhesion (Elizabeth et al., 2014). Further evidence for biocompatibility and osteoconductivity of nano-coatings were presented as patterned based coating systems. Findings suggest a novel observation where when low in numbers osteoblasts almost exclusively adhere to nano-coated regions. It is often claimed that cells can discriminate subtle topographical changes and are highly sensitive to both surface roughness and chemistry. The unique properties of a nano-coated surface may contribute to cellular affinity by attracting certain proteins onto its coating material (Oh et al., 2006) and hence may promote region specific osteoblast proliferation and differentiation.

3. Antimicrobial properties

It has been shown that the antimicrobial properties of nanoparticulates differ depending upon their size, method of synthesis and even their location (Allaker and Memarzadeh, 2014). The change in their application from in suspension to coated also affects their relative size and physical properties. Because of the continuous and constant nature of the coating process, NPs are built up layer upon layer. This in effect does not allow the easy exposure of individual nanoparticulates to the surface of microorganisms. If coated for a prolonged period, the lower layers of NPs will seldom have contact with an external environment, other than their immediate surroundings. Based upon the present findings, it can be stated that increasing coating time is inversely related to the antimicrobial activity of the coatings. Coating time also leads to the mechanical instability of coated regions, which can potentially lead to production of wear products if implemented into bone. Therefore, a thin coating is an ideal approach. The present findings indicate that nZnO alone (without

the aid of nHA) is a good candidate for potential future coatings. This is because it has both suitable antimicrobial as well osteoconductive properties. A brief discussion as regards the hypothetical mechanisms underlying both of these important properties is given below:

1) Ion release:

The results of the current study suggest that there is an element of ion related antibacterial activity. It is suggested that ion release is accountable for bactericidal effects in conjunction with ROS. Studies have confirmed that bacteria possess specific transmembrane proteins that are able to pump Zn^{+2} ions into the cell and cause toxicity. It has also been demonstrated that 500 µg/mL of ZnO nanoparticles can display significant antimicrobial activity (Li et al., 2011). In normal circumstances internal Zn^{+2} would not damage the bacteria. The mechanisms in which ZnO nanoparticles release their ions are as yet unknown, however the chemical reaction between ZnO nanoparticles and protons in suspension can potentially initiate the ion release. This is dependent on two main factors: the pH of the suspension and size of the NPs. Therefore, nZnO are able release ions when reacting with free protons available in solution. The reaction responsible can be depicted as: $ZnO + 2H^{+} \Rightarrow Zn^{2+} + H_2O$. A lower pH in a suspension seems to increase the ion release and a high pH results in a significant decrease (Yang and Xie, 2006). Findings in this study suggests that suspended nanoparticulates are able to release ions at very high concentrations, however nano-coated samples release trace levels of Zn^{2+} at the same concentration. Furthermore based upon other comparative studies performed and since PBS and ABS were used in the current studies (pH at approximately 7.2), it would be unlikely that the bactericidal effects are predominantly ion related (Raghupathi et al., 2011, Yang and Xie, 2006).

2) Contact killing:

Most bacteria have a negative charge on their membrane (Koprivnjak and Peschel, 2011) and this includes the species used in the current study. This property can be used to an advantage when undertaking antimicrobial studies. It has been shown that nZnO in a suspension are attracted to the membrane of *E.coli* due to possible electrostatic forces between the bacteria and the NPs (Zhang et al., 2008). This suggests that ZnO NPs can form strong dipole conditions when in aqueous environments. It is suggested that interaction between bacteria and the surface of these NPs can cause the destruction of the cell wall /membrane, instigating a forced introduction of foreign molecules (genetic material, proteins and possibly the nanoparticulates) into the cell, causing cell death. The effects caused by these NPs could be related to their physical structure as well as their surface area. The nZnO used in the current study possess many rod shaped structures as well as sharp edges that could contribute to bacterial damage. Furthermore other studies suggest that placing nZnO in a non-aqueous medium would result in an oxygen deficient surface that can interact strongly with the negatively charged cell membrane, leading to membrane damage. In the time based bactericidal studies, all NPs and bacteria were in suspension and in an aqueous environment. Although efforts were made to maximise nanoparticle-bacteria interaction, most bacteria would naturally remain in suspension longer than the NPs. This makes contact killing improbable. However, the direct contact studies as regards to coated NPs show an increase in the bactericidal properties as the percentage of nZnO is increased on the surface of the samples, indicating a possible contact related bactericidal activity when these NPs are fixed and stabilised on a surface.

3) Reactive oxygen species (ROS):

ROS are thought to be essential in the antimicrobial activity of nanoparticles. This is particularly applicable to metal oxides. These oxides are thought to release H_2O_2 (hydrogen peroxide) and other reactive oxygen species (Yamamoto, Xia et al., 2008, Premanathan et al., 2011) that are toxic to bacteria. It has been observed that hydrogen peroxide can interact with the membrane proteins of bacteria either by entering the cell via the surface proteins or by being created within bacteria and causing direct damage to DNA. A recent study (Zhang et al., 2008) suggests that the NPs with an average size of 93 nanometres, demonstrate their antimicrobial properties via the route of ROS release. They also show that compared to the "micron" size, the "nano-size" particles of ZnO have enhanced antimicrobial activity, indicating that the "nano-scaled" particles may play an important role in releasing more ROS and therefore an enhanced antimicrobial effect. Claims have been made that oxidative stress-related genes have been up-regulated in the presence of ZnO nanoparticles because of ROS release. This is evident in a study carried out on a gram negative bacterium (*Campylobacter jejuni)*. This study shows that certain oxidative and general stress-related genes have been up-regulated in the presence of ZnO nanoparticles (Xie et al., 2011). Moreover it is also claimed that ROS release from ZnO nanoparticles in a moist environment can lead to biofilm penetration (Shrestha et al., 2010).

The accumulation of similar scientific endeavours indicates a major shift from conventional methods (whereupon the utilisation of small molecules such as antibiotics were the suitable choice for infection prevention) to utilisation of innovative biomaterials that offer promising results which will potentially lead to addressing multiple clinical challenges that currently require bone prostheses.

4. Conclusions

The present study offers strong evidence in support of coated and stabilised nZnO as a potential antimicrobial agent for future medical device applications, particularly as a bone implant coating material. Further analysis of zinc oxide NPs would provide further confirmation as to its biocompatibility and provide mechanistic insight.

References

AARDEN, E. M., BURGER, E. H. & NIJWEIDE, P. J. 1994. Function of osteocytes in bone. ***J Cell Biochem,*** 55**,** 287-299.

ADAMCAKOVA-DODD, A., STEBOUNOVA, L. V., KIM, J. S., VORRINK, S. U., AULT, A. P., O'SHAUGHNESSY, P. T., GRASSIAN, V. H. & THORNE, P. S. 2014. Toxicity assessment of zinc oxide nanoparticles using sub-acute and sub-chronic murine inhalation models. ***Part Fibre Toxicol,*** 11**,** 15.

ALBERS, C. E., HOFSTETTER, W., SIEBENROCK, K. A., LANDMANN, R. & KLENKE, F. M. 2013. In vitro cytotoxicity of silver nanoparticles on osteoblasts and osteoclasts at antibacterial concentrations. ***Nanotoxicology,*** 7**,** 30-36.

ALCANTARA, E. H., LOMEDA, R. A., FELDMANN, J., NIXON, G. F., BEATTIE, J. H. & KWUN, I. S. 2011. Zinc deprivation inhibits extracellular matrix calcification through decreased synthesis of matrix proteins in osteoblasts. ***Mol Nutr Food Res,*** 55**,** 1552-1560.

ALCOFORADO, G. A., RAMS, T. E., FEIK, D. & SLOTS, J. 1991. Microbial aspects of failing osseointegrated dental implants in humans. ***J Parodontol,*** 10**,** 11-18.

ALLAKER, R. P. 2010. The use of nanoparticles to control oral biofilm formation. ***J Dent Res,*** 89**,** 1175-1186.

ALLAKER, R. P. & MEMARZADEH, K. 2014. Nanoparticles and the control of oral infections. ***Int J Antimicrob Agents,*** 43**,** 95-104.

ALLEN, H. K., DONATO, J., WANG, H. H., CLOUD-HANSEN, K. A., DAVIES, J. & HANDELSMAN, J. 2010. Call of the wild: antibiotic resistance genes in natural environments. ***Nat Rev Microbiol,*** 8**,** 251-259.

AVIV, M., BERDICEVSKY, I. & ZILBERMAN, M. 2007. Gentamicin-loaded bioresorbable films for prevention of bacterial infections associated with orthopedic implants. ***J Biomed Mater Res A,*** 83**,** 10-19.

AZAM, A., AHMED, A. S., OVES, M., KHAN, M. S. & MEMIC, A. 2012. Size-dependent antimicrobial properties of CuO nanoparticles against Gram-positive and -negative bacterial strains. ***Int J Nanomedicine,*** 7**,** 3527-3535.

BAEK, M., CHUNG, H. E., YU, J., LEE, J. A., KIM, T. H., OH, J. M., LEE, W. J., PAEK, S. M., LEE, J. K., JEONG, J., CHOY, J. H. & CHOI, S. J. 2012. Pharmacokinetics, tissue distribution, and excretion of zinc oxide nanoparticles. ***Int J Nanomedicine,*** 7**,** 3081-3097.

BAI, W., ZHANG, Z., TIAN, W., HE, X., MA, Y., ZHAO, Y. & CHAI, Z. 2010. Toxicity of zinc oxide nanoparticles to zebrafish embryo: a physicochemical study of toxicity mechanism. ***Journal of Nanoparticle Research,*** 12**,** 1645-1654.

BALASUBRAMANIAN, S. K., JITTIWAT, J., MANIKANDAN, J., ONG, C. N., YU, L. E. & ONG, W. Y. 2010. Biodistribution of gold nanoparticles and gene expression changes in the liver and spleen after intravenous administration in rats. ***Biomaterials,*** 31**,** 2034-2042.

BANCROFT, G. N., SIKAVITSAS, V. I. & MIKOS, A. G. 2003. Design of a flow perfusion bioreactor system for bone tissue-engineering applications. ***Tissue Eng,*** 9**,** 549-554.

BERNARD, L., HOFFMEYER, P., ASSAL, M., VAUDAUX, P., SCHRENZEL, J. & LEW, D. 2004. Trends in the treatment of orthopaedic prosthetic infections. ***J Antimicrob Chemother,*** 53**,** 127-129.

BINNIG, G., GARCIA, N. & ROHRER, H. 1985. Conductivity sensitivity of inelastic scanning tunneling microscopy. ***Phys Rev B Condens Matter,*** 32**,** 1336-1338.

BRUN, N. R., LENZ, M., WEHRLI, B. & FENT, K. 2014. Comparative effects of zinc oxide nanoparticles and dissolved zinc on zebrafish embryos and eleuthero-embryos: importance of zinc ions. ***Sci Total Environ,*** 476-477**,** 657-666.

BRUNET, L., LYON, D. Y., HOTZE, E. M., ALVAREZ, P. J. & WIESNER, M. R. 2009. Comparative photoactivity and antibacterial properties of C60 fullerenes and titanium dioxide nanoparticles. ***Environ Sci Technol,*** 43**,** 4355-4360.

BRUNNER, T. J., WICK, P., MANSER, P., SPOHN, P., GRASS, R. N., LIMBACH, L. K., BRUININK, A. & STARK, W. J. 2006. In vitro cytotoxicity of oxide nanoparticles: comparison to asbestos, silica, and the effect of particle solubility. ***Environ Sci Technol,*** 40**,** 4374-4381.

CAMPOCCIA, D., MONTANARO, L. & ARCIOLA, C. R. 2006. The significance of infection related to orthopedic devices and issues of antibiotic resistance. ***Biomaterials,*** 27**,** 2331-2339.

CANTON, R. 2009. Antibiotic resistance genes from the environment: a perspective through newly identified antibiotic resistance mechanisms in the clinical setting. ***Clin Microbiol Infect,*** 15 Suppl 1**,** 20-25.

CHEN, D., ZHANG, D., YU, J. C. & CHAN, K. M. 2011. Effects of Cu2O nanoparticle and CuCl2 on zebrafish larvae and a liver cell-line. ***Aquat Toxicol,*** 105**,** 344-354.

CHILLER, K., SELKIN, B. A. & MURAKAWA, G. J. 2001. Skin microflora and bacterial infections of the skin. ***J Investig Dermatol Symp Proc,*** 6**,** 170-174.

CHOI, O. & HU, Z. 2008. Size dependent and reactive oxygen species related nanosilver toxicity to nitrifying bacteria. ***Environ Sci Technol,*** 42**,** 4583-4588.

CHOPRA, I. 2007. The increasing use of silver-based products as antimicrobial agents: a useful development or a cause for concern? ***J Antimicrob Chemother,*** 59**,** 587-590.

CHRISTENSON, E. M., ANSETH, K. S., VAN DEN BEUCKEN, J. J., CHAN, C. K., ERCAN, B., JANSEN, J. A., LAURENCIN, C. T., LI, W. J., MURUGAN, R., NAIR, L. S., RAMAKRISHNA, S., TUAN, R. S., WEBSTER, T. J. & MIKOS, A. G. 2007. Nanobiomaterial applications in orthopedics. ***J Orthop Res,*** 25**,** 11-22.

CHU, T. M., ORTON, D. G., HOLLISTER, S. J., FEINBERG, S. E. & HALLORAN, J. W. 2002. Mechanical and in vivo performance of hydroxyapatite implants with controlled architectures. ***Biomaterials,*** 23**,** 1283-1293.

CLEMENTE, J. C., URSELL, L. K., PARFREY, L. W. & KNIGHT, R. 2012. The impact of the gut microbiota on human health: an integrative view. ***Cell,*** 148**,** 1258-1270.

CORCHERO, J. L., SERAS, J. & GARCÍA-FRUITÓS, E. 2010. Nanoparticle assisted tissue engineering. ***Nano Biotech,*** 13-16

COSTERTON, J. 2005. Biofilm theory can guide the treatment of device-related orthopaedic infections. ***Clinical orthopaedics and related research*****,** 7-18.

DANIËLLE, N., JOHANNES, G. E. H., JIM, R. V. H., HENNY, C. V. D. M. & HENK, J. B. 2005. Pseudomonas aeruginosa biofilm formation and slime excretion on antibiotic-loaded bone cement. ***Acta orthopaedica***, 76,109-14.

DARLEY, E. S. & MACGOWAN, A. P. 2004. Antibiotic treatment of gram-positive bone and joint infections. ***J Antimicrob Chemother,*** 53**,** 928-935.

DAROUICHE, R. O. 2004. Treatment of infections associated with surgical implants. ***N Engl J Med,*** 350**,** 1422-1429.

DAS, K., BOSE, S. & BANDYOPADHYAY, A. 2009. TiO2 nanotubes on Ti: Influence of nanoscale morphology on bone cell-materials interaction. ***J Biomed Mater Res A,*** 90**,** 225-237.

DAVIES, J. & DAVIES, D. 2010. Origins and evolution of antibiotic resistance. ***Microbiol Mol Biol Rev,*** 74**,** 417-433.

DE GROOT, K., WOLKE, J. G. & JANSEN, J. A. 1998. Calcium phosphate coatings for medical implants. ***Proc Inst Mech Eng H,*** 212**,** 137-147.

DEL CAMPO, A., SEN, T., LELLOUCHE, J.-P. & BRUCE, I. J. 2005. Multifunctional magnetite and silica–magnetite nanoparticles: Synthesis, surface activation and applications in life sciences. ***Journal of Magnetism and Magnetic Materials,*** 293**,** 33-40.

DEL POZO, J. L. & PATEL, R. 2009. Clinical practice. Infection associated with prosthetic joints. ***N Engl J Med,*** 361**,** 787-794.

DETHLEFSEN, L., MCFALL-NGAI, M. & RELMAN, D. A. 2007. An ecological and evolutionary perspective on human-microbe mutualism and disease. ***Nature,*** 449**,** 811-818.

DWIVEDI, S., WAHAB, R., KHAN, F., MISHRA, Y. K., MUSARRAT, J. & AL-KHEDHAIRY, A. A. 2014. Reactive oxygen species mediated bacterial biofilm inhibition via zinc oxide nanoparticles and their statistical determination. ***PLoS One,*** 9**,** e111289.

EDBERG, S. C., RICE, E. W., KARLIN, R. J. & ALLEN, M. J. 2000. Escherichia coli: the best biological drinking water indicator for public health protection. ***Symp Ser Soc Appl Microbiol*****,** 106S-116S.

EIGLER, D. M. & SCHWEIZER, E. K. 1990. Positioning single atoms with a scanning tunnelling microscope. ***Nature***, 4,803-10.

ELIZABETH, E., BARANWAL, G., KRISHNAN, A. G., MENON, D. & NAIR, M. 2014. ZnO nanoparticle incorporated nanostructured metallic titanium for increased mesenchymal stem cell response and antibacterial activity. ***Nanotechnology,*** 25**,** 115101.

FAHMY, B. & CORMIER, S. A. 2009. Copper oxide nanoparticles induce oxidative stress and cytotoxicity in airway epithelial cells. ***Toxicol In Vitro,*** 23**,** 1365-1371.

FERRARI, M. 2005. Cancer nanotechnology: opportunities and challenges. ***Nat Rev Cancer,*** 5**,** 161-171.

FEYNMAN, R. P. 1960. There's plenty of room at the bottom. ***Engineering and science,*** 23**,** 22-36.

FU, G., VARY, P. S. & LIN, C. T. 2005. Anatase TiO2 nanocomposites for antimicrobial coatings. ***J Phys Chem B,*** 109**,** 8889-8898.

GIANNOUDIS, P. V., DINOPOULOS, H. & TSIRIDIS, E. 2005. Bone substitutes: an update. ***Injury,*** 36 Suppl 3**,** S20-27.

GIORDANO, C., SANDRINI, E., DEL CURTO, B., SIGNORELLI, E., RONDELLI, G. & DI SILVIO, L. 2004. Titanium for osteointegration: Comparison between a novel biomimetic treatment and commercially exploited surfaces. ***J Appl Biomater Biomech,*** 2**,** 35-44.

GOODMAN, S. B., YAO, Z., KEENEY, M. & YANG, F. 2013. The future of biologic coatings for orthopaedic implants. ***Biomaterials,*** 34**,** 3174-3183.

GRICE, E. A. & SEGRE, J. A. 2011. The skin microbiome. ***Nat Rev Microbiol,*** 9**,** 244-253.

GRISTINA, A. G. 1987. Biomaterial-centered infection: microbial adhesion versus tissue integration. ***Science,*** 237**,** 1588-1595.

GU, Y., CHEN, X., LEE, J. H., MONTEIRO, D. A., WANG, H. & LEE, W. Y. 2012. Inkjet printed antibiotic-and calcium-eluting bioresorbable nanocomposite micropatterns for orthopedic implants. ***Acta biomaterialia***, 8,424-31.

GURKAN, U. A. & AKKUS, O. 2008. The mechanical environment of bone marrow: a review. ***Ann Biomed Eng,*** 36**,** 1978-1991.

HALAI, M., KER, A., MEEK, R. D., NADEEM, D., SJOSTROM, T., SU, B., MCNAMARA, L. E., DALBY, M. J. & YOUNG, P. S. 2014. Scanning electron microscopical observation of an osteoblast/osteoclast co-culture on micropatterned orthopaedic ceramics. ***J Tissue Eng,*** 5**,** 2041731414552114.

HANAGATA, N., ZHUANG, F., CONNOLLY, S., LI, J., OGAWA, N. & XU, M. 2011. Molecular responses of human lung epithelial cells to the toxicity of copper oxide nanoparticles inferred from whole genome expression analysis. ***ACS Nano,*** 5**,** 9326-9338.

HARADA, S. & RODAN, G. A. 2003. Control of osteoblast function and regulation of bone mass. ***Nature,*** 423**,** 349-355.

HARRIS, L. G. & RICHARDS, R. G. 2006. Staphylococci and implant surfaces: a review. ***Injury,*** 37 Suppl 2**,** 3-14.

HARRISON, B. S. & ATALA, A. 2007. Carbon nanotube applications for tissue engineering. ***Biomaterials,*** 28**,** 344-353.

HASAN, J., CRAWFORD, R. J. & IVANOVA, E. P. 2013. Antibacterial surfaces: the quest for a new generation of biomaterials. ***Trends Biotechnol,*** 31**,** 295-304.

HERNANDEZ-SIERRA, J. F., RUIZ, F., PENA, D. C., MARTINEZ-GUTIERREZ, F., MARTINEZ, A. E., GUILLEN ADE, J., TAPIA-PEREZ, H. & CASTANON, G. M. 2008. The antimicrobial sensitivity of Streptococcus mutans to nanoparticles of silver, zinc oxide, and gold. ***Nanomedicine,*** 4**,** 237-240.

HIE, M., IITSUKA, N., OTSUKA, T., NAKANISHI, A. & TSUKAMOTO, I. 2011. Zinc deficiency decreases osteoblasts and osteoclasts associated with the reduced expression of Runx2 and RANK. ***Bone,*** 49**,** 1152-1159.

HOFMANN, A. A., HEITHOFF, S. M. & CAMARGO, M. 2002. Cementless total knee arthroplasty in patients 50 years or younger. ***Clin Orthop Relat Res*****,** 102-107.

HUANG, C. C., ARONSTAM, R. S., CHEN, D. R. & HUANG, Y. W. 2010. Oxidative stress, calcium homeostasis, and altered gene expression in human lung epithelial cells exposed to ZnO nanoparticles. ***Toxicol In Vitro,*** 24**,** 45-55.

HUANG, J., LI, X., KOLLER, G. P., DI SILVIO, L., VARGAS-REUS, M. A. & ALLAKER, R. P. 2011. Electrohydrodynamic deposition of nanotitanium doped hydroxyapatite coating for medical and dental applications. ***J Mater Sci Mater Med,*** 22**,** 491-496.

HUNGERFORD, D. S. & JONES, L. C. 1988. The rationale of cementless revision of cemented arthroplasty failures. ***Clin Orthop Relat Res*****,** 12-24.

HUO, M. H. & OSIER, C. J. 2008. Is cement still a fixation option for total hip arthroplasty? ***J Arthroplasty,*** 23**,** 51-54.

ISIDOR, F. 2006. Influence of forces on peri-implant bone. ***Clin Oral Implants Res,*** 17 Suppl 2**,** 8-18.

ITO, A., KAWAMURA, H., OTSUKA, M., IKEUCHI, M., OHGUSHI, H., ISHIKAWA, K., ONUMA, K., KANZAKI, N., SOGO, Y. & ICHINOSE, N. 2002. Zinc-releasing calcium phosphate for stimulating bone formation. ***Materials Science and Engineering: C,*** 22**,** 21-25.

JACOBS, C. R., YELLOWLEY, C. E., DAVIS, B. R., ZHOU, Z., CIMBALA, J. M. & DONAHUE, H. J. 1998. Differential effect of steady versus oscillating flow on bone cells. ***J Biomech,*** 31**,** 969-976.

JAIN, P. K., EL-SAYED, I. H. & EL-SAYED, M. A. 2007. Au nanoparticles target cancer. ***nano today,*** 2**,** 18-47.

JEON, H., HIDAI, H., HWANG, D. J., HEALY, K. E. & GRIGOROPOULOS, C. P. 2010. The effect of micronscale anisotropic cross patterns on fibroblast migration. ***Biomaterials,*** 31**,** 4286-4295.

JORDAN, A., SCHOLZ, R., WUST, P., FÄHLING, H. & FELIX, R. 1999. Magnetic fluid hyperthermia (MFH): Cancer treatment with AC magnetic field induced excitation of biocompatible superparamagnetic nanoparticles. ***Journal of Magnetism and Magnetic Materials,*** 201**,** 413-832.

KARLSSON, H. L., CRONHOLM, P., GUSTAFSSON, J. & MOLLER, L. 2008. Copper oxide nanoparticles are highly toxic: a comparison between metal oxide nanoparticles and carbon nanotubes. ***Chem Res Toxicol,*** 21**,** 1726-1732.

KIM, H. W., KIM, H. E. & SALIH, V. 2005. Stimulation of osteoblast responses to biomimetic nanocomposites of gelatin-hydroxyapatite for tissue engineering scaffolds. ***Biomaterials,*** 26**,** 5221-5230.

KOPRIVNJAK, T. & PESCHEL, A. 2011. Bacterial resistance mechanisms against host defense peptides. ***Cell Mol Life Sci,*** 68**,** 2243-2254.

LEE, C. M., JEONG, H. J., KIM, D. W., SOHN, M. H. & LIM, S. T. 2012a. The effect of fluorination of zinc oxide nanoparticles on evaluation of their biodistribution after oral administration. ***Nanotechnology,*** 23**,** 205102.

LEE, C. M., JEONG, H. J., YUN, K. N., KIM, D. W., SOHN, M. H., LEE, J. K., JEONG, J. & LIM, S. T. 2012b. Optical imaging to trace near infrared fluorescent zinc oxide nanoparticles following oral exposure. ***Int J Nanomedicine,*** 7**,** 3203-3209.

LEE, D., COHEN, R. E. & RUBNER, M. F. 2005. Antibacterial properties of Ag nanoparticle loaded multilayers and formation of magnetically directed antibacterial microparticles. ***Langmuir,*** 21**,** 9651-9659.

LEONHARDT, Å., RENVERT, S. & DAHLÉN, G. 1999. Microbial findings at failing implants. ***Clinical Oral Implants Research,*** 10**,** 339-345.

LEW, D. P. & WALDVOGEL, F. A. 2004. Osteomyelitis. ***Lancet,*** 364**,** 369-379.

LI, M., ZHU, L. & LIN, D. 2011. Toxicity of ZnO nanoparticles to Escherichia coli: mechanism and the influence of medium components. ***Environ Sci Technol,*** 45**,** 1977-1983.

LI, P. 2003. Biomimetic nano-apatite coating capable of promoting bone ingrowth. ***J Biomed Mater Res A,*** 66**,** 79-85.

LI, Z., YUBAO, L., YI, Z., LAN, W. & JANSEN, J. A. 2010. In vitro and in vivo evaluation on the bioactivity of ZnO containing nano-hydroxyapatite/chitosan cement. ***J Biomed Mater Res A,*** 93**,** 269-279.

LIMA, A. L., OLIVEIRA, P. R., CARVALHO, V. C., SACONI, E. S., CABRITA, H. B. & RODRIGUES, M. B. 2013. Periprosthetic joint infections. ***Interdiscip Perspect Infect Dis,*** 2013**,** 542796.

LIN, W., XU, Y., HUANG, C.-C., MA, Y., SHANNON, K. B., CHEN, D.-R. & HUANG, Y.-W. 2008. Toxicity of nano- and micro-sized ZnO particles in human lung epithelial cells. ***Journal of Nanoparticle Research,*** 11**,** 25-39.

LIONG, M., LU, J., KOVOCHICH, M., XIA, T., RUEHM, S. G., NEL, A. E., TAMANOI, F. & ZINK, J. I. 2008. Multifunctional inorganic nanoparticles for imaging, targeting, and drug delivery. ***ACS Nano,*** 2**,** 889-896.

LOGOTHETIDIS, S. 2006b. Nanotechnology in medicine: the medicine of tomorrow and nanomedicine. ***Hippokratia***. 10, 7-21

LU, X., ZHAI, T., ZHANG, X., SHEN, Y., YUAN, L., HU, B., GONG, L., CHEN, J., GAO, Y., ZHOU, J., TONG, Y. & WANG, Z. L. 2012. WO3-x@Au@MnO2 core-shell nanowires on carbon fabric for high-performance flexible supercapacitors. ***Adv Mater,*** 24**,** 938-944.

MACK, D., ROHDE, H., HARRIS, L. G., DAVIES, A. P., HORSTKOTTE, M. A. & KNOBLOCH, J. K. 2006. Biofilm formation in medical device-related infection. ***Int J Artif Organs,*** 29**,** 343-359.

MAHAN, K. & CAREY, M. 1999. Hydroxyapatite as a bone substitute. ***Journal of the American Podiatric Medical Association,*** 89**,** 392-399.

MAKHLUF, S., DROR, R., NITZAN, Y., ABRAMOVICH, Y., JELINEK, R. & GEDANKEN, A. 2005. Microwave-Assisted Synthesis of Nanocrystalline MgO and Its Use as a Bacteriocide. ***Advanced Functional Materials,*** 15**,** 1708-1715.

MANDELL, G. L. 1975. Catalase, superoxide dismutase, and virulence of Staphylococcus aureus. In vitro and in vivo studies with emphasis on staphylococcal--leukocyte interaction. ***J Clin Invest,*** 55**,** 561-566.

MANN, E. E., RICE, K. C., BOLES, B. R., ENDRES, J. L., RANJIT, D., CHANDRAMOHAN, L., TSANG, L. H., SMELTZER, M. S., HORSWILL, A. R. & BAYLES, K. W. 2009. Modulation of eDNA release and degradation affects Staphylococcus aureus biofilm maturation. ***PLoS One,*** 4**,** e5822.

MARRIE, T. J. & COSTERTON, J. W. 1985. Mode of growth of bacterial pathogens in chronic polymicrobial human osteomyelitis. ***J Clin Microbiol,*** 22**,** 924-933.

MAY, R. M., HOFFMAN, M. G., SOGO, M. J., PARKER, A. E., O'TOOLE, G. A., BRENNAN, A. B. & REDDY, S. T. 2014. Micro-patterned surfaces reduce bacterial colonization and biofilm formation in vitro: Potential for enhancing endotracheal tube designs. ***Clin Transl Med,*** 3**,** 8.

MEIRELLES, L., ALBREKTSSON, T., KJELLIN, P., ARVIDSSON, A., FRANKE-STENPORT, V., ANDERSSON, M., CURRIE, F. & WENNERBERG, A. 2008. Bone reaction to nano hydroxyapatite modified titanium implants placed in a gap-healing model. ***J Biomed Mater Res A,*** 87**,** 624-631.

MEMARZADEH, K., SHARILI, A. S., HUANG, J., RAWLINSON, S. C. & ALLAKER, R. P. 2015. Nanoparticulate zinc oxide as a coating material for orthopedic and dental implants. ***J Biomed Mater Res A,*** 103**,** 981-989.

MEMARZADEH, K., VARGAS, M., HUANG, J. & FAN, J. 2012. Nano metallic-oxides as antimicrobials for implant coatings. ***Key Engineering Materials,*** 493-494**,** 489-494

MEYER, B. 2003. Approaches to prevention, removal and killing of biofilms. ***International Biodeterioration & Biodegradation***, 51, 249-253.

MIAO, A. J., ZHANG, X. Y., LUO, Z., CHEN, C. S., CHIN, W. C., SANTSCHI, P. H. & QUIGG, A. 2010. Zinc oxide-engineered nanoparticles: dissolution and toxicity to marine phytoplankton. ***Environ Toxicol Chem,*** 29**,** 2814-2822.

MIYAMOTO, T. & SUDA, T. 2003. Differentiation and function of osteoclasts. ***Keio J Med,*** 52**,** 1-7.

MOORE, M. N. 2006. Do nanoparticles present ecotoxicological risks for the health of the aquatic environment? ***Environ Int,*** 32**,** 967-976.

MORIARTY, T. F., SCHLEGEL, U., PERREN, S. & RICHARDS, R. G. 2010. Infection in fracture fixation: can we influence infection rates through implant design? ***J Mater Sci Mater Med,*** 21**,** 1031-1035.

MORONES-RAMIREZ, J. R., WINKLER, J. A., SPINA, C. S. & COLLINS, J. J. 2013. Silver enhances antibiotic activity against gram-negative bacteria. ***Sci Transl Med,*** 5**,** 190ra181.

MORONES, J. R., ELECHIGUERRA, J. L., CAMACHO, A., HOLT, K., KOURI, J. B., RAMIREZ, J. T. & YACAMAN, M. J. 2005. The bactericidal effect of silver nanoparticles. ***Nanotechnology,*** 16**,** 2346-2353.

MORSCHER, E. W. 1991. Hydroxyapatite coating of prostheses. ***J Bone Joint Surg Br,*** 73**,** 705-706.

MORTIMER, M., KASEMETS, K. & KAHRU, A. 2010. Toxicity of ZnO and CuO nanoparticles to ciliated protozoa Tetrahymena thermophila. ***Toxicology,*** 269**,** 182-189.

MORTIMER, M., KASEMETS, K., VODOVNIK, M., MARINSEK-LOGAR, R. & KAHRU, A. 2011. Exposure to CuO nanoparticles changes the fatty acid composition of protozoa Tetrahymena thermophila. ***Environ Sci Technol,*** 45**,** 6617-6624.

MUELLER, R., MÄDLER, L. & PRATSINIS, S. E. 2003. Nanoparticle synthesis at high production rates by flame spray pyrolysis. ***Chemical Engineering Science,*** 58**,** 1969-1976.

MUNIR, G., HUANG, J. I. E., EDIRISINGHE, M., NANGREJO, R. & BONFIELD, W. 2012. Electrohydrodynamic Processing of Calcium Phosphates: Coating and Patterning for Medical Implants. ***Nano Life,*** 02**,** 1250008.

NA, H. B., SONG, I. C. & HYEON, T. 2009. Inorganic Nanoparticles for MRI Contrast Agents. ***Advanced Materials,*** 21**,** 2133-2148.

NAKAYAMA, A., OGISO, B., TANABE, N., TAKEICHI, O., MATSUZAKA, K. & INOUE, T. 2005. Behaviour of bone marrow osteoblast-like cells on mineral trioxide aggregate: morphology and expression of type I collagen and bone-related protein mRNAs. ***Int Endod J,*** 38**,** 203-210.

NAVARRO, M., MICHIARDI, A., CASTANO, O. & PLANELL, J. A. 2008. Biomaterials in orthopaedics. ***J R Soc Interface,*** 5**,** 1137-1158.

NAYAB, S. N., JONES, F. H. & OLSEN, I. 2005. Effects of calcium ion implantation on human bone cell interaction with titanium. ***Biomaterials,*** 26**,** 4717-4727.

NEDELCU, A. M., DRISCOLL, W. W., DURAND, P. M., HERRON, M. D. & RASHIDI, A. 2011. On the paradigm of altruistic suicide in the unicellular world. ***Evolution,*** 65**,** 3-20.

NG, A. M., CHAN, C. M., GUO, M. Y., LEUNG, Y. H., DJURISIC, A. B., HU, X., CHAN, W. K., LEUNG, F. C. & TONG, S. Y. 2013. Antibacterial and photocatalytic activity of TiO2 and ZnO nanomaterials in phosphate buffer and saline solution. ***Appl Microbiol Biotechnol,*** 97**,** 5565-5573.

NISHIMURA, S., TSURUMOTO, T., YONEKURA, A., ADACHI, K. & SHINDO, H. 2006. Antimicrobial susceptibility of Staphylococcus aureus and Staphylococcus epidermidis biofilms isolated from infected total hip arthroplasty cases. ***J Orthop Sci,*** 11**,** 46-50.

NOOR, Z. 2013. Nanohydroxyapatite application to osteoporosis management. ***J Osteoporos,*** 2013**,** 679025.

NORMARK, B. H. & NORMARK, S. 2002. Evolution and spread of antibiotic resistance. ***J Intern Med,*** 252**,** 91-106.

OH, S., OH, N., APPLEFORD, M. & ONG, J. L. 2006. Bioceramics for tissue engineering applications-a review. ***Am. J. Biochem. Biotechnol,*** 2**,** 49-56.

OLSON, M. E., GARVIN, K. L., FEY, P. D. & RUPP, M. E. 2006. Adherence of Staphylococcus epidermidis to biomaterials is augmented by PIA. ***Clin Orthop Relat Res,*** 451**,** 21-24.

OSTROVSKY, S., KAZIMIRSKY, G., GEDANKEN, A. & BRODIE, C. 2009. Selective cytotoxic effect of ZnO nanoparticles on glioma cells. ***Nano Research,*** 2**,** 882-890.

OTTO, M. 2013. Staphylococcal infections: mechanisms of biofilm maturation and detachment as critical determinants of pathogenicity. ***Annu Rev Med,*** 64**,** 175-188.

PADHIARY, S. K., SRIVASTAVA, G., PANDA, S., SUBUDHI, S. & LENKA, S. 2013. E.coli Associated Extensive Bilateral Maxillary Osteomyelitis: A Rare Case Report. ***J Clin Diagn Res,*** 7**,** 2380-2382.

PADMAVATHY, N. & VIJAYARAGHAVAN, R. 2008. Enhanced bioactivity of ZnO nanoparticles—an antimicrobial study. ***Sci. Technol. Adv. Mater,*** 9, 035004.

PAN, H. A., HUNG, Y. C., CHIOU, J. C., TAI, S. M., CHEN, H. H. & HUANG, G. S. 2012. Nanosurface design of dental implants for improved cell growth and function. ***Nanotechnology,*** 23**,** 335703.

PARK, J. K., KIM, Y. J., YEOM, J., JEON, J. H., YI, G. C., JE, J. H. & HAHN, S. K. 2010. The topographic effect of zinc oxide nanoflowers on osteoblast growth and osseointegration. ***Adv Mater,*** 22**,** 4857-4861.

PARK, K., LEE, S., KANG, E., KIM, K., CHOI, K. & KWON, I. C. 2009. New Generation of Multifunctional Nanoparticles for Cancer Imaging and Therapy. ***Advanced Functional Materials,*** 19**,** 1553-1566.

PATTI, J. M., ALLEN, B. L., MCGAVIN, M. J. & HOOK, M. 1994. MSCRAMM-mediated adherence of microorganisms to host tissues. ***Annu Rev Microbiol,*** 48**,** 585-617.

PAUL, M. M., BENJAMIN, M. G. & THOMAS, J. W. 2014. Greater fibroblast proliferation on an ultrasonicated ZnO/PVC nanocomposite material. ***International journal of nanomedicine***.

PERCIVAL, S. L., BOWLER, P. G. & RUSSELL, D. 2005. Bacterial resistance to silver in wound care. ***J Hosp Infect,*** 60**,** 1-7.

PERSSON, R. G. & RENVERT, S. 2014. Cluster of Bacteria Associated with Peri Implantitis. ***Clinical implant dentistry and related research,*** 16**,** 783-793.

PETERSON, C. L. 2004. Nanotechnology: from Feynman to the grand challenge of molecular manufacturing. ***Technology and Society Magazine***.

POPAT, K. C., ELTGROTH, M., LATEMPA, T. J., GRIMES, C. A. & DESAI, T. A. 2007. Decreased Staphylococcus epidermis adhesion and increased osteoblast functionality on antibiotic-loaded titania nanotubes. ***Biomaterials,*** 28**,** 4880-4888.

PREMANATHAN, M., KARTHIKEYAN, K., JEYASUBRAMANIAN, K. & MANIVANNAN, G. 2011. Selective toxicity of ZnO nanoparticles toward Gram-positive bacteria and cancer cells by apoptosis through lipid peroxidation. ***Nanomedicine,*** 7**,** 184-192.

PYE, A. D., LOCKHART, D. E., DAWSON, M. P., MURRAY, C. A. & SMITH, A. J. 2009. A review of dental implants and infection. ***J Hosp Infect,*** 72**,** 104-110.

RAGHUPATHI, K. R., KOODALI, R. T. & MANNA, A. C. 2011. Size-dependent bacterial growth inhibition and mechanism of antibacterial activity of zinc oxide nanoparticles. ***Langmuir,*** 27**,** 4020-4028.

RAI, M., YADAV, A. & GADE, A. 2009. Silver nanoparticles as a new generation of antimicrobials. ***Biotechnol Adv,*** 27**,** 76-83.

REDDY, K. M., FERIS, K., BELL, J., WINGETT, D. G., HANLEY, C. & PUNNOOSE, A. 2007. Selective toxicity of zinc oxide nanoparticles to prokaryotic and eukaryotic systems. ***Appl Phys Lett,*** 90**,** 2139021-2139023.

REDDY, S. T., CHUNG, K. K., MCDANIEL, C. J., DAROUICHE, R. O., LANDMAN, J. & BRENNAN, A. B. 2011. Micropatterned surfaces for reducing the risk of catheter-associated urinary tract infection: an in vitro study on the effect of sharklet micropatterned surfaces to inhibit bacterial colonization and migration of uropathogenic Escherichia coli. ***J Endourol,*** 25**,** 1547-1552.

ROCO, M. C. 2004. Nanoscale Science and Engineering: Unifying and Transforming Tools. ***AIChE Journal,*** 50**,** 890-897.

SALATA, O. 2004. Applications of nanoparticles in biology and medicine. ***J Nanobiotechnology,*** 2**,** 3.

SAWAI, J. 2003. Quantitative evaluation of antibacterial activities of metallic oxide powders (ZnO, MgO and CaO) by conductimetric assay. ***J Microbiol Methods,*** 54**,** 177-182.

SAWAI, J., KAWADA, E., KANOU, F., IGARASHI, H., HASHIMOTO, A., KOKUGAN, T. & SHIMIZU, M. 1996. Detection of active oxygen generated from ceramic powders having antibacterial activity. ***JOURNAL OF CHEMICAL ENGINEERING OF JAPAN,*** 29**,** 627-633.

SEIL, J. T. & WEBSTER, T. J. 2008. Decreased astroglial cell adhesion and proliferation on zinc oxide nanoparticle polyurethane composites. ***Int J Nanomedicine,*** 3**,** 523-531.

SEIL, J. T. & WEBSTER, T. J. 2011. Reduced Staphylococcus aureus proliferation and biofilm formation on zinc oxide nanoparticle PVC composite surfaces. ***Acta Biomater,*** 7**,** 2579-2584.

SEO, H. J., CHO, Y. E., KIM, T., SHIN, H. I. & KWUN, I. S. 2010. Zinc may increase bone formation through stimulating cell proliferation, alkaline phosphatase activity and collagen synthesis in osteoblastic MC3T3-E1 cells. ***Nutr Res Pract,*** 4**,** 356-361.

SHAHVERDI, A. R., FAKHIMI, A., SHAHVERDI, H. R. & MINAIAN, S. 2007. Synthesis and effect of silver nanoparticles on the antibacterial activity of different antibiotics against Staphylococcus aureus and Escherichia coli. ***Nanomedicine,*** 3**,** 168-171.

SHARMA, V., SHUKLA, R. K., SAXENA, N., PARMAR, D., DAS, M. & DHAWAN, A. 2009a. DNA damaging potential of zinc oxide nanoparticles in human epidermal cells. ***Toxicology Letters,*** 185**,** 211-218.

SHARMA, V., SHUKLA, R. K., SAXENA, N., PARMAR, D., DAS, M. & DHAWAN, A. 2009b. DNA damaging potential of zinc oxide nanoparticles in human epidermal cells. ***Toxicol Lett,*** 185**,** 211-218.

SHI, J., DONG, L. L., HE, F., ZHAO, S. & YANG, G. L. 2013. Osteoblast responses to thin nanohydroxyapatite coated on roughened titanium surfaces deposited by an electrochemical process. ***Oral Surg Oral Med Oral Pathol Oral Radiol,*** 116**,** e311-316.

SHI, Z., HUANG, X., CAI, Y., TANG, R. & YANG, D. 2009. Size effect of hydroxyapatite nanoparticles on proliferation and apoptosis of osteoblast-like cells. ***Acta Biomater,*** 5**,** 338-345.

SHRESTHA, A., SHI, Z., NEOH, K. G. & KISHEN, A. 2010. Nanoparticulates for antibiofilm treatment and effect of aging on its antibacterial activity. ***J Endod,*** 36**,** 1030-1035.

SILVER, S. 2003. Bacterial silver resistance: molecular biology and uses and misuses of silver compounds. ***FEMS Microbiol Rev,*** 27**,** 341-353.
SINGH, M. & MANIKANDAN, S. 2011. Nanoparticles: A new technology with wide applications. ***Nanoparticles: A new technology with wide applications***.
SITTKA, A. & VOGEL, J. 2008. A glimpse at the evolution of virulence control. ***Cell host & microbe,*** 4**,** 310-312.
SONDI, I. & SALOPEK-SONDI, B. 2004. Silver nanoparticles as antimicrobial agent: a case study on E. coli as a model for Gram-negative bacteria. ***J Colloid Interface Sci,*** 275**,** 177-182.
SOTIRIOU, G. A. & PRATSINIS, S. E. 2010. Antibacterial activity of nanosilver ions and particles. ***Environ Sci Technol,*** 44**,** 5649-5654.
SOTOME, S., UEMURA, T., KIKUCHI, M., CHEN, J., ITOH, S., TANAKA, J., TATEISHI, T. & SHINOMIYA, K. 2004. Synthesis and in vivo evaluation of a novel hydroxyapatite/collagen–alginate as a bone filler and a drug delivery carrier of bone morphogenetic protein. ***Materials Science and Engineering: C,*** 24**,** 341-347.
STEWART, P. S. & COSTERTON, J. W. 2001. Antibiotic resistance of bacteria in biofilms. ***Lancet,*** 358**,** 135-138.
STOODLEY, P., EHRLICH, G. D., SEDGHIZADEH, P. P., HALL-STOODLEY, L., BARATZ, M. E., ALTMAN, D. T., SOTEREANOS, N. G., COSTERTON, J. W. & DEMEO, P. 2011. Orthopaedic biofilm infections. ***Curr Orthop Pract,*** 22**,** 558-563.
STUDER, A. M., LIMBACH, L. K., VAN DUC, L., KRUMEICH, F., ATHANASSIOU, E. K., GERBER, L. C., MOCH, H. & STARK, W. J. 2010. Nanoparticle cytotoxicity depends on intracellular solubility: comparison of stabilized copper metal and degradable copper oxide nanoparticles. ***Toxicol Lett,*** 197**,** 169-174.
SUN, B. & LYNN, D. M. 2010. Release of DNA from polyelectrolyte multilayers fabricated using 'charge-shifting' cationic polymers: tunable temporal control and sequential, multi-agent release. ***J Control Release,*** 148**,** 91-100.
SUN, L., BERNDT, C. C., GROSS, K. A. & KUCUK, A. 2001. Material fundamentals and clinical performance of plasma-sprayed hydroxyapatite coatings: a review. ***J Biomed Mater Res,*** 58**,** 570-592.
TAM, K. H., DJURIŠIĆ, A. B., CHAN, C. M. N., XI, Y. Y. & TSE, C. W. 2008. Antibacterial activity of ZnO nanorods prepared by a hydrothermal method. ***Thin solid films***.
TANG, J., XIONG, L., WANG, S., WANG, J., LIU, L., LI, J., YUAN, F. & XI, T. 2009. Distribution, translocation and accumulation of silver nanoparticles in rats. ***J Nanosci Nanotechnol,*** 9**,** 4924-4932.
TORCHILIN, V. P. 2005. Recent advances with liposomes as pharmaceutical carriers. ***Nat Rev Drug Discov,*** 4**,** 145-160.
TURNER, C. E. 2000. Paxillin and focal adhesion signalling. ***Nat Cell Biol,*** 2**,** E231-236.
VARGAS-REUS, M. A., MEMARZADEH, K., HUANG, J., REN, G. G. & ALLAKER, R. P. 2012. Antimicrobial activity of nanoparticulate metal oxides against peri-implantitis pathogens. ***Int J Antimicrob Agents,*** 40**,** 135-139.
VIGUET-CARRIN, S., GARNERO, P. & DELMAS, P. D. 2006. The role of collagen in bone strength. ***Osteoporos Int,*** 17**,** 319-336.
WAGNER, V., DULLAART, A., BOCK, A. K. & ZWECK, A. 2006. The emerging nanomedicine landscape. ***Nat Biotechnol,*** 24**,** 1211-1217.
WANG, E. E., KELLNER, J. D. & ARNOLD, S. 1998. Antibiotic-resistant Streptococcus pneumoniae. Implications for medical practice. ***Can Fam Physician,*** 44**,** 1881-1888.
WANG, H., WICK, R. L. & XING, B. 2009. Toxicity of nanoparticulate and bulk ZnO, Al2O3 and TiO2 to the nematode Caenorhabditis elegans. ***Environ Pollut,*** 157**,** 1171-1177.
WANG, K. 1996. The use of titanium for medical applications in the USA. ***Materials Science and Engineering: A,*** 213**,** 134-271.

WANG, X., ITO, A., SOGO, Y., LI, X. & OYANE, A. 2010. Zinc-containing apatite layers on external fixation rods promoting cell activity. ***Acta Biomater,*** 6**,** 962-968.
WENNERBERG, A. & ALBREKTSSON, T. 2009. Effects of titanium surface topography on bone integration: a systematic review. ***Clin Oral Implants Res,*** 20 Suppl 4**,** 172-184.
WHITCHURCH, C. B., TOLKER-NIELSEN, T., RAGAS, P. C. & MATTICK, J. S. 2002. Extracellular DNA required for bacterial biofilm formation. ***Science,*** 295**,** 1487.
WIDAA, A., CLARO, T., FOSTER, T. J., O'BRIEN, F. J. & KERRIGAN, S. W. 2012. Staphylococcus aureus protein A plays a critical role in mediating bone destruction and bone loss in osteomyelitis. ***PLoS One,*** 7**,** e40586.
WILHELMI, V., FISCHER, U., WEIGHARDT, H., SCHULZE-OSTHOFF, K., NICKEL, C., STAHLMECKE, B., KUHLBUSCH, T. A., SCHERBART, A. M., ESSER, C., SCHINS, R. P. & ALBRECHT, C. 2013. Zinc oxide nanoparticles induce necrosis and apoptosis in macrophages in a p47phox- and Nrf2-independent manner. ***PLoS One,*** 8**,** e65704.
WILLIAMS, D. F. 2008. On the mechanisms of biocompatibility. ***Biomaterials,*** 29**,** 2941-2953.
WOZNIAK, M. A., MODZELEWSKA, K., KWONG, L. & KEELY, P. J. 2004. Focal adhesion regulation of cell behavior. ***Biochim Biophys Acta,*** 1692**,** 103-119.
WU, X., LIU, X., WEI, J., MA, J., DENG, F. & WEI, S. 2012. Nano-TiO2/PEEK bioactive composite as a bone substitute material: in vitro and in vivo studies. ***Int J Nanomedicine,*** 7**,** 1215-1225.
XIA, T., KOVOCHICH, M., LIONG, M., MADLER, L., GILBERT, B., SHI, H., YEH, J. I., ZINK, J. I. & NEL, A. E. 2008. Comparison of the mechanism of toxicity of zinc oxide and cerium oxide nanoparticles based on dissolution and oxidative stress properties. ***ACS Nano,*** 2**,** 2121-2134.
XIE, Y., HE, Y., IRWIN, P. L., JIN, T. & SHI, X. 2011. Antibacterial activity and mechanism of action of zinc oxide nanoparticles against Campylobacter jejuni. ***Appl Environ Microbiol,*** 77**,** 2325-2331.
XU, J., HU, M., TAN, X. Y. & LIU, C. K. 2013. Zinc ion implantation-deposition modification of titanium for enhanced adhesion of focal plaques of osteoblast-like cells. ***Chin Med J (Engl),*** 126**,** 3557-3560.
XU, J., MAHOWALD, M. A., LEY, R. E., LOZUPONE, C. A., HAMADY, M., MARTENS, E. C., HENRISSAT, B., COUTINHO, P. M., MINX, P., LATREILLE, P., CORDUM, H., VAN BRUNT, A., KIM, K., FULTON, R. S., FULTON, L. A., CLIFTON, S. W., WILSON, R. K., KNIGHT, R. D. & GORDON, J. I. 2007. Evolution of symbiotic bacteria in the distal human intestine. ***PLoS Biol,*** 5**,** e156.
YAMAMOTO, O. Influence of particle size on the antibacterial activity of zinc oxide. ***International Journal of Inorganic Materials,*** 3**,** 643-1289.
YANG, S. C., LU, L. F., CAI, Y., ZHU, J. B., LIANG, B. W. & YANG, C. Z. 1999. Body distribution in mice of intravenously injected camptothecin solid lipid nanoparticles and targeting effect on brain. ***J Control Release,*** 59**,** 299-307.
YANG, Z. & XIE, C. 2006. Zn2+ release from zinc and zinc oxide particles in simulated uterine solution. ***Colloids Surf B Biointerfaces,*** 47**,** 140-145.
YANO, H., MAZAKI, Y., KUROKAWA, K., HANKS, S. K., MATSUDA, M. & SABE, H. 2004. Roles played by a subset of integrin signaling molecules in cadherin-based cell-cell adhesion. ***J Cell Biol,*** 166**,** 283-295.
YARWOOD, J. M., BARTELS, D. J., VOLPER, E. M. & GREENBERG, E. P. 2004. Quorum sensing in Staphylococcus aureus biofilms. ***J Bacteriol,*** 186**,** 1838-1850.
ZAAT, J. H. 1983. A quarter of a century of plasma spraying. ***Annual Review of Materials Science***, 13, 9-42.

ZAKARIA, S. M., SHARIF ZEIN, S. H., OTHMAN, M. R., YANG, F. & JANSEN, J. A. 2013. Nanophase hydroxyapatite as a biomaterial in advanced hard tissue engineering: a review. ***Tissue Eng Part B Rev,*** 19**,** 431-441.

ZAVERI, T. D., DOLGOVA, N. V., CHU, B. H., LEE, J., WONG, J., LELE, T. P., REN, F. & KESELOWSKY, B. G. 2010. Contributions of surface topography and cytotoxicity to the macrophage response to zinc oxide nanorods. ***Biomaterials,*** 31**,** 2999-3007.

ZHANG, L., DING, Y., POVEY, M. & YORK, D. 2008. ZnO nanofluids–A potential antibacterial agent. ***Progress in Natural Science***, 18, 939-944.

ZHAO, S. F., DONG, W. J., JIANG, Q. H., HE, F. M., WANG, X. X. & YANG, G. L. 2013. Effects of zinc-substituted nano-hydroxyapatite coatings on bone integration with implant surfaces. ***J Zhejiang Univ Sci B,*** 14**,** 518-525.